university of groningen

faculty of mathematics and natural sciences

MSc Thesis Mathematics & Physics

Exceptional points and $\mathcal{PT}$ symmetric systems in adiabatic quantum theory

Eric J. Pap

Supervisor Mathematics: prof. dr. H. Waalkens

Supervisor Physics: prof. dr. D. Boer

August 27, 2018

Abstract

We investigate the theory of exceptional points (EPs); degeneracies of non-hermitian systems famous for the swaps of eigenstates that arise when encircling the EP according to the adiabatic approximation. We review various characterizations of EPs that are used in the literature. We observe that they are not equivalent and consequently a unanimous definition is lacking. The theory of $\mathcal{PT}$ symmetric systems is studied as an aid in the study of EPs. In particular, we deal explicitly with a three-channel waveguide system originating from $\mathcal{PT}$ theory and supporting various EPs. We show how one can properly compose the eigenvalue permutations arising from EPs and how this generates a non-abelian group which we call the Λ-group. We finish with the needed geometry as induced by the adiabatic approximation. The adiabatic change as measured in experiment can be modelled naturally on a principal $\mathbb{C}^\times \wr S_n$-bundle consisting of the eigenframes of the operator family. To the best of our knowledge this bundle is not found in the literature to date. The adiabatic approximation induces a canonical connection on this bundle. The special shape of the holonomy group induces three groups, one of which is the Λ-group, that fit together in a short exact sequence (SES). This SES can be used to describe and distinguish degeneracy structures. In particular, the Λ-group allows one to phrase a new definition of exceptional point that specializes existing definitions. Explicitly, one can define an EP by demanding that swaps of eigenvalues occur arbitrarily close to the EP. This definition is widely applicable, yet guarantees that the eigenvalue and eigenstates sheets are connected in a non-trivial way.

Contents

1 Introduction

In this thesis we explore the theory of exceptional points (EPs). These degeneracies appearing in finite-dimensional hamiltonian systems are famous as many interesting effects occur at and around these points.

We start with an exposition of EP characteristics in section 2. Various properties of EPs are listed in the literature, most of them focusing on a property of the eigenstates of the system. Amongst these are swaps of eigenstates & eigenvalues upon adiabatically encircling the EP, complex analytic branch structure, coalescence and self-orthogonality. We investigate if these properties can be used to define an EP according to physical intuition.

As the existence of EPs requires the system to be non-hermitian, we also look at non-hermitian theory. A particularly interesting subfield is that of $\mathcal{PT}$, parity-time, symmetric systems, which we treat in section 3. The connection with EP theory primarily lies in the fact that $\mathcal{PT}$ symmetry can break spontaneously when one adjusts the system parameters. The point of breaking, also known as the $\mathcal{PT}$ symmetry phase transition, is indeed an EP in generic cases. We will look into this EP-$\mathcal{PT}$ phase transition correspondence, as well as the equivalence of exact $\mathcal{PT}$ symmetric theory with hermitian theory.

With the knowledge of these two sections, we move on to real experiments and applications of the theory in section 4. We start with some examples of EP experiments in which different techniques are used, both experimental and theoretical. We likewise go over some $\mathcal{PT}$ symmetric systems to illustate their applications.

One of the treated experimental set-ups uses a $\mathcal{PT}$ symmetric waveguide system with two coupled channels. The $\mathcal{PT}$ symmetry imposes that the channels have opposite gain and loss of intensity along the propagation direction. In section 5 we consider a system with an additional (neutral) channel in the middle. This not only supports EPs with 2 or 3 connected eigenstates, but also provides a setting in which the effects of multiple EPs can be mixed. In particular, we see that the group of adiabatic eigenstates changes is non-abelian. This work was recently published in Physical Review A.

The theory needed to explore more complex systems like the three-channel waveguide is treated in section 6. At the basis is the adiabatic approximation from quantum mechanics, which defines a parallel transport equation on a principal fiber bundle (PFB). After comparing with PFBs from the literature, we find that a PFB naturally suited for EP theory is missing and we introduce one to this end. The section continues by studying various properties of the obtained holonomy theory and how this can be applied to EP theory. This includes a new definition of EP that does not have the disadvantage of allowing trivial cases, yet is applicable to any smooth family of operators.

2 Definitions of exceptional points

Degeneracies appear in the context of (finite-dimensional) operator families that depend on some parameters; any point in parameter space for which the corresponding operator has a double eigenvalue is called a degeneracy. A physical context is given by systems modelled by matrix equations, as appearing in e.g. quantum physics and optics.

Degeneracies are extensively studied in physics, even near- or avoided degeneracies have their own terminology, as words as anti-crossing, level repulsion and quasi-degenerate illustrate. Some degeneracies have special names; a well-known example is the diabolic point (DP, also known as hermitian degeneracy) where the eigenvalues coincide, yet the eigenvectors remain linearly independent. Another property of DPs is the state acquiring a phase of π upon adiabatic encircling, regardless of the precise path. The topological properties of these points have attracted considerable interest in the fields of quantum mechanics and optics. A variety of confirmations and applications of these points exists in the literature.

This sets the stage for exceptional points (EPs), which tend to go a step further in the 'degree of degeneracy'. In addition, at an EP the eigenvectors are also required to coincide, also phrased as coalescence of the eigenvectors. In many physical systems, this is induced as the degeneracy is a branch point singularity. The branch structure also implies that encircling the EP swaps the eigenstates of the system. A well established exact definition is lacking in literature, but these are frequently occurring features; complex branch structure, coalescence of the eigenvectors and exchange of eigenvectors upon adiabatic encirclement. We will see that any of these definitions requires the system to be non-hermitian, hence EPs are also called non-hermitian degeneracies. Nevertheless, similar to the DP case, this name is easily seen to be too general for a definition and we do not use it. In the next subsection we review various characteristics of EPs and investigate if they provide a definition that respects physical settings yet discards the uninteresting.

2.1 First appearance

Let us start with the earliest definition of an exceptional point, as found in a book by Kato on perturbation theory of linear operators [1]. We will see some confusion already at this point appearing as nowadays this definition is not used, despite the fact that many recent papers still cite this book when referring to the concept 'EP'.

The setting in which Kato places EPs is that of finite-dimensional operators $T(x)$ depending analytically on a complex parameter x. It is argued that the eigenvalues of $T(x)$ then depend on x in an analytic way up to algebraic singularities. Consequently the matrix $T(x)$ is non-degenerate for generic x, up to some degeneracies which appear as isolated points in the complex x plane. Because of this property, such points were called *exceptional points.*

Definition 2.1 (Exceptional Point; Def. 1 (Kato))**.** Let V be a complex vector space of finite dimension n. Given a linear operator $T(x)$ on V dimensional space depending analytically on $x \in \mathbb{C}$, the exceptional points are the points $x_k \in \mathbb{C}$ at which the number of different eigenvalues is less than n.

According to Kato, then any degeneracy of such a system is an EP. He provides several elementary examples, some we show here for future reference.

Example 2.1. Let

$$T(x) = \begin{pmatrix} 1 & x \\ x & -1 \end{pmatrix}$$

so that the eigenvalues are $\pm\sqrt{1+x^2}$. The eigenvectors are given by

$$\begin{pmatrix} 1 \pm \sqrt{1+x^2} \\ x \end{pmatrix}.$$

We see that $\lambda_{1,2} = \pm i$ are the two exceptional points.

In the example above we see a non-trivial dependence of both eigenvalues and eigenvectors on the parameter x; the dependence follows a branch structure on which more in the next section. However, this definition also includes more trivial cases like the one in the example below.

Example 2.2. Let

$$T(x) = \begin{pmatrix} 0 & x \\ x & 0 \end{pmatrix}$$

so that the eigenvalues are $\pm x$ and hence $\lambda_0 = 0$ is the only exceptional point according to definition 2.1. We note that the eigenvectors are given by

$$\begin{pmatrix} \pm 1 \\ 1 \end{pmatrix}.$$

The book continues with group theoretical aspects of EPs. Although this has not attracted nearly as much attention as the degeneracy aspect, nevertheless we want to treat it as a generalization of this theory is treated in section 6.

The idea is to track the permutations of the eigenvalues at some point x_0 close to the EP. Fix a simply connected subdomain D containing x_0 but not containing any EP. On D, the eigenvalues $\lambda_1(x), \ldots, \lambda_k(x)$ of $T(x)$ are holomorphic functions without intersecting graphs. Now, let us move the domain D continuously around the EP. By analytic continuation all $\lambda_i(x)$ can be continued following this movement. When D returns to its initial position after a full turn and in particular if we trace the $\lambda_i(x)$ back to x_0, the $\lambda_i(x)$ will be permuted as the set they constitute is fixed. Hence one obtains a permutation σ of the set $\{\lambda_1(x_0), \ldots, \lambda_k(x_0)\}$ from encircling the EP once, where σ is allowed to be trivial. One observes that slight deformations of the loop still give σ, imposing that we keep the point x_0 fixed. The group generated by this permutation was defined to be the λ-group of the EP.

Definition 2.2 (λ-group)**.** Given an EP, x_0, D and $\lambda_i(x)$ as above. The λ-*group* (at x_0) is the group of permutations of the $\lambda_i(x)$ corresponding to analytic continuation around the EP. Decomposing a generator of this group in disjoint cycles, each cycle permutes certain $\lambda_i(x)$; each such a set is also called a *cycle*. The number of elements of such a cycle is called its *period*.

Example 2.3. In example 2.1 the eigenvalues can be permuted, so the λ-group is $\mathbb{Z}/2\mathbb{Z}$. In other words, there is 1 cycle of period 2 consisting of both eigenvalues.

On the other hand, in example 2.2 the eigenvalues can not be permuted and the λ-group is trivial. Hence both eigenvalues constitute their own cycle, both with period 1.

As the above example illustrates, Kato's definition may include systems where the encircling behavior is trivial as measured by the λ-group. More precisely, each eigenvalue makes up its own cycle with period 1. Such cases are mathematically trivial and physically uninteresting. Hence people did not want the term 'exceptional point' to include these, although this is usually not mentioned in papers. Different definitions of EPs have appeared instead, and we review the most prominent below.

2.2 Branches

One of the two most popular EP definitions in literature is to define an EP to be branch point singularity of the eigenvalues. The other popular definition uses the coalescence of eigenvectors and we want to discuss this in the next section. We will see that the branch point definition will imply the other used EP characteristics and ensures non-triviality. The main disadvantage is the assumption of analytic dependence; the parameter is complex, where in practice many parameters are real.

Let us motivate the branch point picture with a simple example, passing over the introduction provided in [2]. The system we consider is

$$H(k) = \begin{pmatrix} E_1 + i\Gamma_1 & k \\ k & E_2 + i\Gamma_2 \end{pmatrix}$$

where k is a complex parameter modelling the coupling between two levels with complex energy $E_j + i\Gamma_j$ for $j = 1, 2$. Systems of the above form reappear in section 3 on $\mathcal{PT}$ symmetry. The eigenvalues of the system are given by

$$\begin{aligned} \lambda_\pm &= \left(\frac{E_1 + E_2}{2} + i\frac{\Gamma_1 + \Gamma_2}{2}\right) \pm \sqrt{k^2 + \left(\frac{E_1 - E_2}{2} + i\frac{\Gamma_1 - \Gamma_2}{2}\right)^2} \\ &= \lambda_0 \pm \sqrt{k - k_0}\sqrt{k + k_0} \end{aligned}$$

where we introduced

$$\begin{aligned} \lambda_0 &= \left(\frac{E_1 + E_2}{2} + i\frac{\Gamma_1 + \Gamma_2}{2}\right) \\ k_0 &= i\left(\frac{E_1 - E_2}{2} + i\frac{\Gamma_1 - \Gamma_2}{2}\right) = i\left(\frac{\Delta E}{2} + i\frac{\Delta\Gamma}{2}\right). \end{aligned}$$

The degeneracies of the system are given by $k = k_0$ and $k = -k_0$, and according to Kato both are EPs. However, in case $k_0 = 0$ the two points coincide and the square roots merge into a linear term. Hence the eigenvalues only follow a square root branch structure if $k_0 \neq 0$, and this case is illustrated in fig. 2.1. As seen in this figure it is the connected branch structure that allows one to go from one energy to the other simply by walking around.

The branch structure is also present in the eigenvectors, and this has serious consequences. The eigenvectors can be written as

$$|\psi_{1,2}\rangle = \begin{pmatrix} \frac{1}{2}\Delta E + \frac{i}{2}\Delta\Gamma \pm \sqrt{k - k_0}\sqrt{k + k_0} \\ -k \end{pmatrix} \tag{2.1}$$

where indeed the same square root term as in the eigenvalues appears. That is, the eigenvectors follows a branch structure similar to that of the eigenvalues. In particular, the eigenvectors *coalesce* at the branch points given by the degeneracies $k = k_0$ and $k = -k_0$.

At this point we note that hermitian systems can not support connected sheets without becoming trivial. As they have real eigenvalues the right part of fig. 2.1 showing the imaginary part becomes a flat surface at height 0. By analyticity the real part must be constant, so the picture would consist of some disconnected surfaces situated above each other[1]. Hence hermitian system only support trivial sheet structure. The eigenvectors provide a second argument; the coalescence of the eigenvectors at the degeneracy contradicts the existence of a complete set of eigenstates for the system.

[1] In section 6 we show that smooth dependence instead of analyticity is already sufficient for this argument.

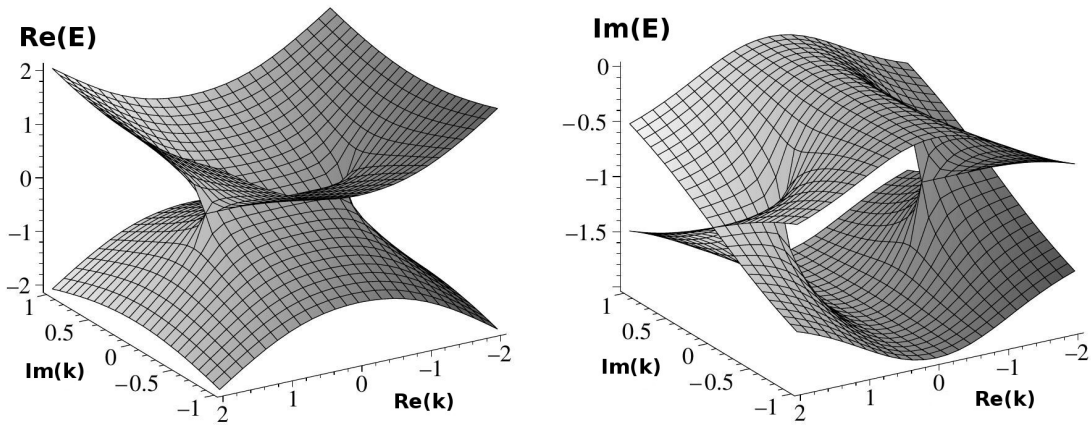

Figure 2.1: Adapted from [3]; example of real (left) and imaginary (right) part of eigenvalues. We see that a single turn around an EP causes both real and imaginary parts to move to the other sheet, meaning that the eigenvalues are swapped. A second turn moves points back to the initial sheet.

Consequently, one must use techniques that are suited for a non-hermitian setting. Using an inner product from the state space poses a problem as the bra of an eigenstate not need be a left-eigenstate. Hence one uses bi-orthogonal normalization which directly uses left-eigenstates $\langle\chi_i|$, see also appendix C. Normalizing the eigenstates introduces a fourth root. As usual we walk around one EP at a time, and if we pick the EP at $k = k_0$ the relevant factor is

$$|\psi_i\rangle \sim \frac{1}{\sqrt[4]{k-k_0}}.$$

It is easily seen that the normalized eigenstate blows up at the EP. This is a consequence of the fact that the eigenstates coalesce at the EP; bi-orthogonality can not be extended continuously to the EP as the equations become contradictory at the EP.

A crucial observation is that the normalization factor effects the phases of the eigenstates. Let us give a heuristic argument. As a fourth root is involved each counterclockwise turn around the EP shifts the phase by a factor of $1/i = -i$. Let us pick eigenstate $|\psi_1\rangle$ to have phase zero, i.e. with no extra phase. The second eigenstate has then relative phase i due to the minus in eq. (2.1). As visualized in fig. 2.2 the $-i$ phase shift moves $|\psi_2\rangle$ to $|\psi_1\rangle$. The state $|\psi_1\rangle$ in turn gets opposite of $|\psi_2\rangle$, so becomes $-|\psi_2\rangle$. That is, encircling the EP multiple times gives the pattern

$$|\psi_1\rangle \to -|\psi_2\rangle \to -|\psi_1\rangle \to |\psi_2\rangle \to |\psi_1\rangle. \tag{2.2}$$

This operation is linear, so in the basis $(|\psi_1\rangle, |\psi_2\rangle)$ it is given by the matrix

$$\begin{pmatrix} 0 & 1 \\ -1 & 0 \end{pmatrix}. \tag{2.3}$$

To finish the example, another implication of the branch structure that is referred in the literature is the blowing up of the derivative near an EP. Indeed, as the eigenvalues are proportional to $\sqrt{k-k_0}$, or an even higher root, one has

$$\frac{\mathrm{d}\,E}{\mathrm{d}\,k} \propto \frac{1}{\sqrt{k-k_0}}.$$

It was thought that this could be used for high-precision sensors [4]. However, recently it has been shown that such sensors will effectively have a modest signal-to-noise ratio

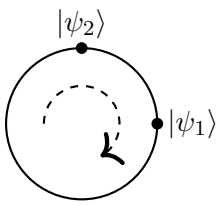

Figure 2.2: Schematic illustration of the phases of the eigenstates. The loop around the EP causes the states to move a quarter turn in clockwise direction. Hence $|\psi_2\rangle$ moves to $|\psi_1\rangle$ and $|\psi_1\rangle$ moves to $-|\psi_2\rangle$.

[5]. Indeed, the steep slope of the complex energy splitting need not imply a better signal field, and in fact DPs turn out to have higher precision.

Until now we have only seen 2-dimensional operators where the EPs involved two connected eigenvalues. In higher dimensional systems one can have general EPNs in which N levels are connected. Observe that if the operator has dimension n necessarily $N \leq n$. For a long time most EPs studied were EP2s, but recently these higher order EPs have become of interest, notably EP3s. The theoretical classification of EPs in 3-dimensional systems had already been done in [6]; one either has a genuine EP3 with a cyclic permutation of eigenstates or an EP2 with a disconnect third state. Explicitly, in the EP3 case write $|\phi_1\rangle$, $|\phi_2\rangle$ and $|\phi_3\rangle$ for the three connected eigenstates. Encircling the EP gives the behavior

$$|\phi_1\rangle \to |\phi_2\rangle \to |\phi_3\rangle \to |\phi_1\rangle$$

or in matrix notation

$$\begin{pmatrix} 0 & 0 & 1 \\ 1 & 0 & 0 \\ 0 & 1 & 0 \end{pmatrix}.$$

In the other case of the EP2, let $|\psi_1\rangle$ and $|\psi_2\rangle$ be the two connected states and $|\psi_0\rangle$ the remaining unconnected state. Encircling the EP now induces the pattern

$$\begin{aligned} |\psi_1\rangle &\to |\psi_2\rangle \to |\psi_1\rangle \\ |\psi_0\rangle &\to -|\psi_0\rangle \to |\psi_0\rangle \end{aligned}$$

with associated matrix

$$\begin{pmatrix} 0 & 1 & 0 \\ 1 & 0 & 0 \\ 0 & 0 & -1 \end{pmatrix}.$$

In other words, we obtain the usual rule for $|\psi_1\rangle$ and $|\psi_2\rangle$ but the only phase now appears in front of $|\psi_0\rangle$. This shows that the eigenvector sheets of this EP2 are significantly different from the standard planar EP2.

Figure 2.3 illustrates the eigenvalue sheets corresponding to two classes. The permutations can already be deduced from this picture, one needs to calculate the eigenstates in order to see the phase changes. We remark that the used technique in [6] is that of Puiseux series; instead of usual expansion in z^k one expands in $z^{k/N}$ where N is the order of the EP. This in combination with perturbation theory around the EP allows one to find the phases and swaps of the eigenstates.

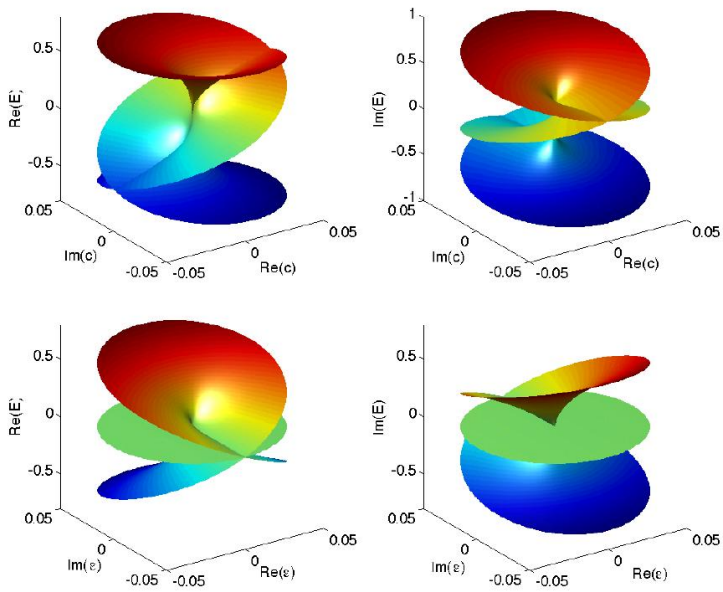

Figure 2.3: Eigenvalue sheets of the normal forms of EPs occuring in 3D systems [6]. Shown above is the EP3 case where all three eigenvalues are involved in a third-root singularity. Depicted below is the case with only two connected eigenvalues; like a standard EP2 but with an extra (constant) eigenvalue.

Given the most interesting consequences and the frequent occurrences in physical system of branch structure it is not surprising that it is commonly used as the mathematical backbone behind an EP. Hence we include a rigorous definition based on this idea. This indeed excludes the uninteresting case of example 2.2, but keeps example 2.1.

Definition 2.3 (Exceptional point; Def. 2)**.** Given a linear finite-dimensional operator family $T(x)$ depending analytically on $x \in U$ where U is an open subset of $\mathbb{C}$. The exceptional points are the points $x_k \in U$ at which some of the eigenvalues coalesce in a branch point singularity. If the branch structure is like that of the Nth root, the EP is called an EPN.

Nevertheless, this definition has a problem due to the requirement of analytic dependence. In experiments, system parameters are usually real and complexified parameters may not be feasible in experiment. Even if two parameters constitute real and imaginary part of a complex parameter, one may need to use complex conjugates (and we will), breaking the analytic dependence requirement. We conclude that the above definition is too restrictive by requiring the analytic dependence.

2.3 Coalescence & self-orthogonality

In the previous section we saw that if one defines an EP as a branch point of the eigenvalue, then many interesting consequences are immediate but one restricts oneself too severely. Hence we continue with the less severe requirement of the coalescence of eigenvectors, one of the consequences of the branch point definition. We also treat the closely related concept of self-orthogonality as it will for 2-dimensional systems be equivalent to coalescence.

Coalescence

The coalescence of eigenvectors at a degeneracy is often used as the EP definition in mathematically oriented EP papers (e.g. [7]). In other words, at an EP the operator

should obtain a non-trivial Jordan block; this is an equivalent phrasing one frequently encounters. It has the advantage that one only needs continuous dependence on system parameters. One can phrase this as shown below. We note that this coalescence is not part of Kato's definition 2.1, but as said is a consequence of the branch point definition 2.3.

Definition 2.4 (Exceptional point; Def. 3)**.** Given a finite-dimensional operator family $T(x)$ which depends continuously on $x \in U$ where U is open in $\mathbb{R}^k \times \mathbb{C}^l$. A point $y \in U$ is an EP $\iff$ some eigenvectors coalesce at y, which is equivalent to a non-trivial Jordan block at y.

The coalescence is understood to be non-trivial; arbitrarily close to the point y one can find a point where the relevant eigenvectors are linearly independent.

We note right away that the fact that y must be a degeneracy is implicit an coinciding eigenvectors imply coinciding eigenvalues. Also, the requirement of non-trivial coalescence is needed to discard system as in the example below.

Example 2.4. Consider

$$T(x) = \begin{pmatrix} 0 & x \\ 0 & 0 \end{pmatrix}$$

which has double (constant) eigenvalue 0 and a single (constant) eigenvector.

However, this definition 2.4 does not ensure us that the geometry of the eigenvector sheets is non-trivial, in the sense that these are connected and encircling may produce non-trivial results.

Example 2.5. We consider an example seen in [8] given by

$$T(x) = \begin{pmatrix} x & 1 \\ 0 & -x \end{pmatrix}$$

where x is a complex parameter. For $x = 0$ this system has a single eigenvector, but also independent eigenvectors arbitrarily close to $x = 0$. However, the eigenvector corresponding to $\lambda_2 = -x$ (for $x \neq 0$) is

$$v_2 = \begin{pmatrix} -\frac{1}{2x} \\ 1 \end{pmatrix} \propto \begin{pmatrix} 1 \\ -2x \end{pmatrix}$$

where the other eigenvector is identically $(1, 0)^T$. We warn the reader; in the first form v_2 blows up, but we do have coalescence as shown by the second. Normalizing the eigenvector will not create non-trivial branch structure around $x = 0$ as well. The eigenvectors and so eigenvalues live on separate sheets, whence encircling of $x = 0$ will always yield trivial outcomes.

Self-orthogonality

We move on to another property that is used to characterize EPs, the self-orthogonality of the eigenstate at the EP (compare [9]). This of course assumes some agreement on an inner product on the state space or at least a pairing between vectors. Indeed, no hermitian inner product is used here which is not a big surprise given the non-hermitian nature of EPs. Instead, there is a replacement known as the c-product [9] which is equivalent to the bi-orthogonality of left- and righteigenvectors as treated in appendix C. For the matrix systems that we consider this product coincides with the usual pairing of left- and righteigenvectors, that is the standard multiplication of row vector and column vector.

The reason that we treat self-orthogonality here is the following: coalescence and self-orthogonality are equivalent descriptions for all practical purposes. It always holds that

the coalescence requirement, hence also the branch point picture, implies self-orthogonality of the single remaining eigenstate at the EP [10]. Conversely, self-orthogonality implies the non-existence of an eigenframe which in generic cases implies coalescence. Technically, we want to have distinct eigenvectors arbitrarily close to a point of self-orthogonality to assure that the coalescence is non-trivial. Formally, the statements are as follows.

Lemma 2.1. Let $T(x)$ be a family of operators depending continuously on x in some open set U in $\mathbb{R}^k \times \mathbb{C}^l$. If some eigenstates coalesce at y, then the resulting eigenstate $|\psi_{\mathrm{EP}}\rangle$ is self-orthogonal. If degeneracies have codimension at least 1, the converse holds as well.

Proof. Let $|\psi_j\rangle$ be the (right-)eigenvectors and $\langle\chi_j|$ the corresponding left-eigenvectors. We may assume the normalization

$$\langle\chi_{j'}|\psi_j\rangle = \delta_{j'j}$$

which we can do away from degeneracies (see appendix C). This identity holds identically in the system parameters. Pick distinct labels j, j' of two (out of possibly many) coalescing levels. The product away from the EP is then identically zero, and taking the limit to the EP gives

$$\langle\chi_{\mathrm{EP}}|\psi_{\mathrm{EP}}\rangle = 0$$

where the $\langle\chi_j|\psi_j\rangle = 1$ identity implies that the normalization factor blows up. We thus conclude self-orthogonality of $|\psi_{\mathrm{EP}}\rangle$.

Conversely, assume an eigenvector v is self-orthogonal. Then there is no eigenframe that contains v; if so there would be an eigencoframe contradicting self-orthogonality. Hence the eigenspaces do not span the entire state space, and so some eigenvectors must have coalesced as by assumption they can be chosen distinct arbitrarily closeby.

□

It follows that we do not need to formulate and inspect a definition for EPs based on self-orthogonality arguments. We an also conclude that self-orthogonality is not sufficient for non-trivial sheet structure.

We finish this subsection with an explicit 2-dimensional system to explore the eigenvector obtained at the EP. The motivation is the frequent appearance of such systems and the physical interest in the coalesced eigenvector which is also self-orthogonal; in the symmetric case the modes will differ only by a phase of $\pi/2$ exactly. This reappears in the $\mathcal{PT}$ experiments of section 3.

Let us write a general 2D system as

$$A = \begin{pmatrix} z_1 & s_2 \\ s_1 & z_2 \end{pmatrix}$$

which has eigenvalues (defining $v = (z_1 - z_2)/2$)

$$\lambda_\pm = \frac{z_1 + z_2}{2} \pm \sqrt{v^2 + s_1 s_2}$$

with corresponding right-eigenvectors

$$v_\pm = \begin{pmatrix} s_2 \\ -v \pm \sqrt{v^2 + s_1 s_2} \end{pmatrix} = \begin{pmatrix} s_2 \\ -z_1 + \lambda_\pm \end{pmatrix}.$$

The corresponding left-eigenvectors are

$$w_\pm = \begin{pmatrix} s_1 & -v \pm \sqrt{v^2 + s_1 s_2} \end{pmatrix} = \begin{pmatrix} s_1 & -z_1 + \lambda_\pm \end{pmatrix}$$

so that

$$w_\pm v_\pm = s_1 s_2 + \left(v \mp \sqrt{v^2 + s_1 s_2}\right)^2 = s_1 s_2 + (-z_1 + \lambda_\pm)^2 .$$

This allows us to check when the system has the eigenstates $(1, \pm i)$ at the EPs.

Lemma 2.2. A 2D system A can have one of the states $(1, \pm i)$ at coalescence if and only if A is symmetric. In particular, a $\pi/2$ phase difference at coalescence only appears for symmetric systems.

Proof. By a density argument we may assume that both s_1 and s_2 are non-zero. At coalescence, we must have $v^2 + s_1 s_2 = 0$, and the eigenvectors reduce to

$$v_0 = \begin{pmatrix} s_2 \\ -v \end{pmatrix} = \begin{pmatrix} s_2 \\ \mp\sqrt{-s_1 s_2} \end{pmatrix} \sim \begin{pmatrix} 1 \\ \mp i\sqrt{s_1/s_2} \end{pmatrix}.$$

We conclude that the special eigenstates $(1, \pm i)$ occur only when $s_1 = s_2$, i.e. when the matrix is symmetric. The converse holds as well as the above argument can be reversed (observe that then $s_1 = 0$ if and only if $s_2 = 0$ and in this case coalescence means that A is proportional to identity). □

If one starts with a symmetric system already, the special eigenstates can be found in another nice way. As $A = A^T$, one has

$$Av = \lambda v \implies v^T A = v^T \lambda$$

so that the left-eigenvectors are right-eigenvectors transposed. This forces the shape of the eigenstate in the symmetric case; if $|\psi_{\mathrm{EP}}\rangle = (a, b)^T$, then by the above $\langle \chi_{\mathrm{EP}}| = (a, b)$ and

$$0 = \langle \chi_{\mathrm{EP}} | \psi_{\mathrm{EP}} \rangle = a^2 + b^2$$

meaning that

$$b = \pm i a$$

and scaling a away yields the desired chiral eigenstates. As shown in [11] the relative $\pi/2$ phase differences also appear in 3-dimensional systems, and we find similar results in section 5.

2.4 Higher order zeros

In this subsection we look at another way to investigate EPs, namely EPs as higher order zeros of the characteristic polynomial. This will be foremost a practical way of finding EP candidates. Also in the literature, this concept is considered primarily for practical applications.

To start, note that higher order zeroes are a directly connected to general degeneracies and not to EPs exclusively. To illustrate, let us fix an operator family $T(x)$ acting on an n-dimensional vector space V that is differentiable in x, where x is taken in some open set of $\mathbb{R}^k \times \mathbb{C}^l$. The eigenvalues also depend on x and can be found by solving the characteristic equation

$$p_T(\lambda, x) := \det(\lambda I - T)(x) = 0. \tag{2.4}$$

If we fix $x = x_0$, the above is a degree n polynomial in λ. From algebra we know that

$$p_T(\lambda, x_0) := \prod_{i=1}^{n} (\lambda - \lambda_i(x_0)) \tag{2.5}$$

where the $\lambda_i(x_0)$ are the eigenvalues at x_0. A degeneracy means that two solutions are equal, say $\lambda_i(x_0)$ appears twice, and hence the polynomial has a factor $(\lambda - \lambda_i(x_0))^2$. A similar story holds for zeros of degree at least 3.

A convenient function that detects degeneracies is the discriminant of a polynomial. Assuming the polynomial is monic (i.e. the term with highest degree has coefficient 1), like the characteristic polynomial, it is defined in terms of the zeros as

$$\Delta(x) = \prod_{i<j} (\lambda_i(x) - \lambda_j(x))^2. \tag{2.6}$$

Indeed, x is a degeneracy if and only if $\Delta(x) = 0$. The function $\Delta(x)$ can also be expressed in the coefficients of the characteristic polynomial, hence the function can be calculated explicitly. We observe that the order of the degeneracy is not given immediately.

Alternatively, one can detect higher order zeros of the characteristic polynomial using its derivatives, which directly puts constraints on the order of the degeneracy. This is particularly interesting in the search for EPs of some given order N. The needed observation is that $p_T(\lambda, x_0)$ has a factor $(\lambda - \lambda_i(x_0))^2$ if and only if $\lambda_i(x_0)$ is a degeneracy and

$$\frac{\partial}{\partial \lambda} p_T(\lambda_i(x_0), x_0) = 0. \tag{2.7}$$

Hence, second order degeneracies can be found be solving the system.

$$\begin{aligned} p_T(\lambda, x) &= 0 \\ \frac{\partial}{\partial \lambda} p_T(\lambda, x) &= 0 \end{aligned} \tag{2.8}$$

This generalizes in a straightforward way: degree N degeneracies should satisfy

$$\left(\frac{\partial}{\partial \lambda}\right)^k p_T(\lambda, x) = 0 \tag{2.9}$$

for $k = 0, 1, \ldots, N-1$. Let us give an example.

Example 2.6. Let the characteristic polynomial be $\lambda^2 - a\lambda + b$. The second equation of zero derivative implies

$$2\lambda - a = 0 \implies \lambda = \frac{a}{2}.$$

Hence, if we also demand that the characteristic polynomial vanishes we obtain

$$\frac{a^2}{4} - \frac{a^2}{2} + b = 0$$

which can be rewritten as

$$a^2 - 4b = 0.$$

We recognize in the lefthandside the discriminant of the characteristic polynomial, which must indeed equal 0 at an degeneracy.

At this point, we remark that every EPN is a degree N degeneracy, so they can be found using equations 2.9. Although they are called 'exceptional' points, a generic solution of these equations will be an EP independent of the precise definition that one uses. Indeed, trivial cases may still appear but are unlikely to occur in practice. Again example 2.5 can be used for illustration, for one has

$$\begin{aligned} p_A(\lambda, x) &= (\lambda - x)(\lambda + x) = \lambda^2 - x^2 \\ \frac{\partial}{\partial \lambda} p_A(\lambda, x) &= 2\lambda \end{aligned}$$

showing that an EP can only occur at $x = 0$ with $\lambda = 0$. As we saw earlier, we still want to reject this point as EP, so one needs more than higher order zeros in order to exclude this case.

2.5 Swaps of eigenstates

The final property we consider is the appearance of swaps of eigenstates that occur upon encircling an EP. Although this is not commonly used to define an EP, it is one of the clearest concepts that can be verified experimentally (see section 4) and it excludes trivial cases.

The first issue we want to deal with is the availability of the degeneracy. Namely, in some papers it is not required that the EP lies in the allowed parameter space. Instead it is allowed to be in the complexified parameter space as illustrated in the below example.

Example 2.7. We consider the system with single real parameter z;

$$\begin{pmatrix} 2i & z-3i \\ z+3i & -2i \end{pmatrix}$$

with eigenvalues

$$\lambda_\pm = \pm\sqrt{z^2+3^3-2^2} = \pm\sqrt{z^2+5}.$$

As stated, we have $z \in \mathbb{R}$, which corresponds to the $\mathcal{PT}$ symmetric regime as seen in section 3. Although a non-trivial square root appears, hence also coalescence of eigenstates and self-orthogonality, the degeneracy can not be reached as none of the points $z = \pm i\sqrt{5}$ is in the parameter space.

In what follows, once a parameter space has been chosen we stick to it. Another motivation for this is that we want to allow non-analytic systems for which a generalization of the illustrated procedure is technically involved.

We can now consider the main point of this subsection; how to define an EP by means of the induced swaps. As this turns out to be our favorite way of defining an EP we check the needed geometry in section 6. However, we can still phrase a simple argument where we leave the technical details for this later section. Indeed the idea itself is straightforward; the connected eigenvalues sheets as seen before can be detected using swaps, and conversely swaps indicate connected sheet structure. The EPs are then the points where connected sheets intersect. So, arbitrarily close to an EP one can find a loop around it such that a swap occurs. Of course, we do not want the loop to pass over a degeneracy in the process of encircling as then the swap becomes ill-defined. The definition is then the following, which we label as 'experimental EP' as it is inspired by the properties measured in experiment (cf. section 4).

Definition 2.5 (Experimental EP)**.** Let $T(x)$ be an operator family with x in parameter space P. An EP $x_0 \in P$ is called experimental $\iff$ for every neighborhood $U \subset P$ of x_0, there exists a loop $\gamma\colon S^1 \to U$ so that along γ the eigenvalues are exchanged without becoming degenerate in the process.

A few remarks are in order. First, the swaps of the eigenvalues imply that the eigenvalues are multi-valued. Looking at the equation

$$T(x)v_i(x) = \lambda_i(x)v_i(x)$$

one concludes that the eigenvectors must be multi-valued as well; otherwise the lefthand-side is single-valued while the righthandside is not. The arbitrarily small neighborhood U is used to single out the point x_0. If P has dimension 3, then degeneracies form lines in P as they have codimension 2. It is a well-defined notion if a given loop γ encircles this line, but a precise point on the line is not apparent. In fact, one may choose to take away the EPs from the parameter space P and retain the swaps as the below (artificial) example illustrates. We see that for the swap definition it is not necessary to know the data *at* the EP.

Example 2.8. Consider

$$T(x,y) = \begin{pmatrix} c & x+iy \\ 1 & c \end{pmatrix}$$

where c is any (complex) constant and the real parameters x and y are such that $x+iy \in P = S^1$. The eigenvalues are

$$\lambda_\pm = \pm\sqrt{x+iy}$$

which can be swapped by paths in P, e.g. by traversing the circle one. Nevertheless, the EP supposedly at 0 does not exist in parameter space.

It is not hard to see that such problems only arise when P is not simply connected. In this case, swaps can be attributed to some degeneracy structure; if no such structure would be present then there are no swaps as we see in section 6. One can even show that then coalescence occurs at the EPs.

Proposition 2.1 (Experimental implies coalescence)**.** Let $T(x)$ be a operator family depending continuously on $x \in P$, assume that the parameter space P is simply connected. If $x_0 \in P$ is an experimental EP, then the relevant eigenvectors coincide at x_0 (up to a scalar).

Proof. Suppose coalescence does not appear. Then there is a neighborhood U of x_0 on which one has n eigenvectors $v_i(x)$ depending continuously on $x \in U$ and the $v_i(x_0)$ are linearly independent. Let us consider the cones

$$C_i = \left\{ cv_i(x) \mid x \in U, c \in \mathbb{C}^\times \right\},$$

then U may be taken small enough such that the cones do not intersect. However, then no curve γ in U can swap the eigenstates. By contradiction then coalescence must appear. □

2.6 Discussion

As we have treated the most commonly used characteristics of EPs, we can investigate which one is well-suited to form the definition of an EP.

The first definition 2.1 as found in Kato's book is no longer used. Not only does it restrict to complex analytic systems, it also allows trivial case. The similar definition 2.3 using complex analytic branch structure rules out the non-trivial cases but again is too restrictive due to the analyticity requirement.

On the other side are the coalescence definition 2.4 and the self-orthogonality condition. These only need continuous dependence on system parameters, which is a significant advantage with respect to the previous ones. However, also here trivial cases concerning the eigenvalue structure are allowed. The experimental EP of definition 2.5 works similarly but does discard the trivial cases. However, we see that the coalescence defines special points in its own right.

All in all we consider definition 2.5 to be the best suited definition, and we investigate the mathematical framework behind it in section 6. This involves primarily the technical details that one needs to check. Until we discuss the swap definition in more detail we take the coalescence definition 2.4 for an EP in order to be in line with the literature that is treated.

3 $\mathcal{PT}$ symmetry

Describing a quantum system usually begins with specifying a (complex) state space V with inner product such that the structure of a Hilbert space is obtained. We note that there is a canonical identification of V with its dual V^*; there is a bijection between vectors/kets $|\psi\rangle$ and functionals/bras $\langle\psi|$. Here the functional $\langle\psi|$ is given by taking the inner product $\langle\psi|-\rangle$ as the notation already suggests.

The dynamics is fully determined by a linear operator $H\colon V \to V$ called the hamiltonian. A priori, this need not have any special relation involving the inner product on V. Such relation however is usually imposed (immediately) by declaring that H must yield unitary time-evolution. The dynamics is given by

$$i\hbar\frac{\partial}{\partial t}|\psi(t)\rangle = H|\psi(t)\rangle$$

and if H is time-independent, as we will assume throughout this text, it follows that

$$|\psi(t)\rangle = e^{-itH/\hbar}|\psi(0)\rangle.$$

Usually, the time-evolution operator $e^{-itH/\hbar}$ is denoted $U(t)$, signifying the unitarity in usual quantum mechanics. Unitarity is imposed as

$$\langle\psi(t)|\psi(t)\rangle = \langle U\psi(0)|U\psi(0)\rangle = \langle\psi(0)|U^\dagger(t)U|\psi(0)\rangle = \langle\psi(0)|\psi(0)\rangle$$

where we must require $U^\dagger(t)U(t) = I$ for all t, and as $U(t)$ is invertible ($(U(t))^{-1} = U(-t)$) also $U(t)U^\dagger(t) = I$. Functional analysis tells us that H must be self-adjoint (plus details we ignore, which is OK if the space has finite dimension), that is $H^\dagger = H$ or with explicit reference to the inner product

$$\langle\chi|H\psi\rangle = \langle H\chi|\psi\rangle$$

for any two states χ, ψ. Indeed, if we require $U(t)^{-1} = U^\dagger(t)$, we find

$$e^{itH/\hbar} = e^{itH^\dagger/\hbar}$$

and so $H = H^\dagger$, as found by differentiation at $t = 0$. As the argument can be reversed, we see that time-evolution is unitary if and only if H is self-adjoint.

The unitary time-evolution is a fundamental axiom in quantum mechanics for closed systems; probability should be conserved in time. The self-adjointness of the hamiltonian has some further consequences which may be considered standard facts of quantum mechanics. We list a few;

- the hamiltonian has a complete set of orthonormal eigenstates. This follows from the fact that H is normal, or $HH^\dagger = H^\dagger H$, as both sides equal H^2.
- the spectrum of H is real, for if E is an eigenvalue of H with normalized eigenvector $|\psi\rangle$;

  $$E = \langle\psi|E\psi\rangle = \langle\psi|H\psi\rangle = \langle H^\dagger\psi|\psi\rangle = \langle H\psi|\psi\rangle = \langle E\psi|\psi\rangle = E^*\langle\psi|\psi\rangle = E^*$$

  and E must be real. That is, an eigenstate of a quantum system has a well-defined real energy. This in turn means that time-evolution (of eigenstates and so of any state by the previous) is oscillatory.
- there is conservation of energy, expressible as $[U(t), H] = 0$, which follows from the fact that $U(t)$ is an exponential of H.

The above depends crucially on the fact that H is self-adjoint, which we can also phrase as the 'dagger-symmetry' of H. Yet, there is considerable physical motivation to consider cases where H is not self-adjoint, but satisfies another symmetry. Hamiltonians describing open systems (as found in e.g. optics) may lose energy into the environment which leads to complex energies. The imaginary part then gives the decay rate. As we will see, such systems can be realized by time-independent hamiltonians and we keep restricting ourselves to this case. Also EPs form strong motivation as they can't appear at points where the operator is self-adjoint; if multiple eigenvectors coincide, the dimension of the eigenspace drops, meaning one can't have a complete set of eigenstates.

The question was if other frameworks for quantum theory existed that maintained unitary time-evolution and real eigenvalues. The answer is yes, one remarkable theory being that of $\mathcal{PT}$ symmetry. Instead of $H = H^\dagger$, one requires invariance under combined parity and time reversal, $[H, \mathcal{PT}] = 0$ in symbols, where such H are called $\mathcal{PT}$-symmetric. We will investigate $\mathcal{PT}$ theory in this chapter. Indeed, unitarity and real spectrum follow from $\mathcal{PT}$ symmetry if there is no spontaneous breaking of the symmetry.

Initially, people investigated if $\mathcal{PT}$ symmetric quantum mechanics defined a new elementary quantum theory. Indeed, $\mathcal{PT}$ symmetric theory allows for phenomena that are not available in standard hermitian theory (see e.g. [12, 13]). However, in [14] it was shown that if the $\mathcal{PT}$ symmetry is not spontaneously broken, then the system is quasi-hermitian, i.e. there is a unitary equivalence between the $\mathcal{PT}$ system and a hermitian system. We will consider this equivalence in more detail in section 3.5.

3.1 Basic properties of $\mathcal{PT}$ theory

In this section we first consider the basics of $\mathcal{PT}$ symmetry. We follow the introduction by Bender as given in [15]. At the end of the 1990s, $\mathcal{PT}$ symmetry was hinted at by complex non-Hermitian Hamiltonians that did have a real spectrum, but so did not fit in the contemporary view on quantum mechanics. In a dynamical setting, the operators $\mathcal{P}$ and $\mathcal{T}$ are defined by their action on $\hat{x}, \hat{p}$ and i. Explicitly:

$$\begin{aligned} \mathcal{P}: \ \hat{x} \mapsto -\hat{x}, \quad \hat{p} \mapsto -\hat{p}, \quad i \mapsto i \\ \mathcal{T}: \ \hat{x} \mapsto \hat{x}, \quad \hat{p} \mapsto -\hat{p}, \quad i \mapsto -i \end{aligned} \tag{3.1}$$

so that their combined operation is

$$\mathcal{PT}: \ \hat{x} \mapsto -\hat{x}, \quad \hat{p} \mapsto \hat{p}, \quad i \mapsto -i. \tag{3.2}$$

The action on $\hat{x}$ and $\hat{p}$ is well-known, the action of $\mathcal{T}$ on i is picked to conserve the canonical commutation relation

$$[\hat{x}, \hat{p}] = i. \tag{3.3}$$

This means that $\mathcal{T}$ and $\mathcal{PT}$ are anti- or conjugate linear. In a finite-dimensional hamiltonian setting the definitions of $\mathcal{P}$ and $\mathcal{T}$ are similar. In such systems $\mathcal{P}$ flips states while $\mathcal{T}$ can be chosen as only complex conjugation as we assume a that the hamiltonian is constant in time.

The most famous example of a $\mathcal{PT}$ symmetric operator family is

$$H = \hat{p}^2 - (i\hat{x})^N \tag{3.4}$$

where one fixes appropriate boundary conditions. This was presented in [16], where numerical calculations indicated that for $N > 2$ the spectrum was real, which was proven in [17]. As $\hat{p}$ and $i\hat{x}$ are invariant under $\mathcal{PT}$, indeed every operator of the family in eq. (3.4) in $\mathcal{PT}$ symmetric. This includes interesting cases like $H = \hat{p}^2 - \hat{x}^4$ for $N = 4$. A plot showing various eigenvalues is shown in fig. 3.1.

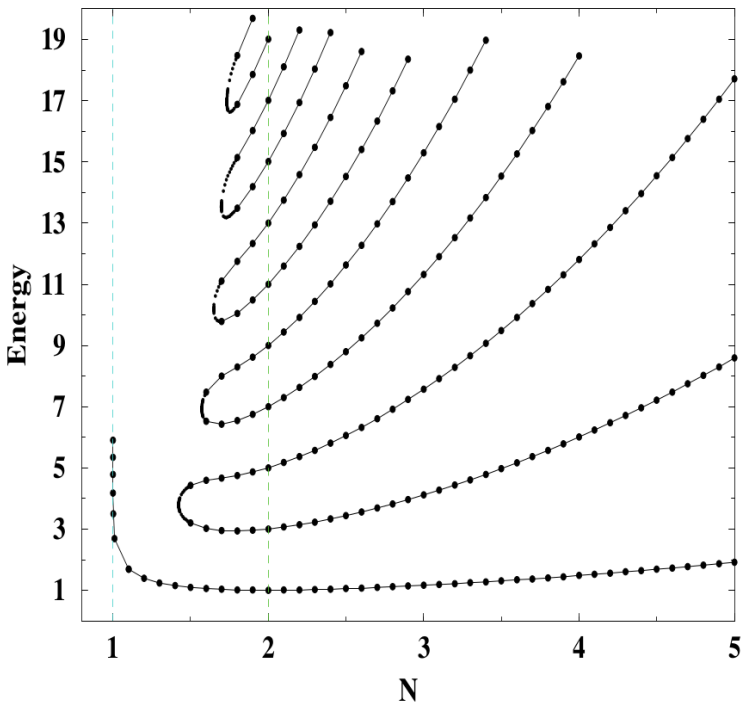

Figure 3.1: Illustration showing real eigenvalues of $H = \hat{p}^2 - (i\hat{x})^N$, taken from [16]. For $N = 2$ one obtains real equidistant levels. The diagram separates into two regimes, which correspond to spontaneously broken symmetry for $N < 2$ and unbroken symmetry for $N > 2$. The only real eigenvalue for small N blows up as $N \to 1$.

As can be seen in the figure, for $N = 2$ gives the harmonic oscillator with the equidistant real energies. For $N > 2$ the energies are still real, but for $N < 2$ we see more and more annihilating pairs. Indeed, these are real-to-complex singularities and the spectrum contains complex numbers for $N < 2$. Hence the spectrum of a $\mathcal{PT}$ symmetric operator may be real, but may also not be.

It turns out that $\mathcal{PT}$ symmetric systems fall into one of two separate classes. The question is whether or not the $\mathcal{PT}$ symmetry is spontaneously broken, that is whether or not all H-eigenstates are $\mathcal{PT}$-eigenstates. This is a non-trivial question due to the fact that $\mathcal{PT}$ is conjugate linear instead of linear. It thus makes sense to introduce the following definition.

Definition 3.1. Given a system defined by a $\mathcal{PT}$ symmetric hamiltonian H. In case the $\mathcal{PT}$ symmetry is spontaneously broken we say that the system is in *broken* $\mathcal{PT}$ phase, that is if and only if there is an eigenvector of H that is not an eigenvector of $\mathcal{PT}$. Otherwise the $\mathcal{PT}$ symmetry is said to be *exact* and the system is in unbroken or exact phase. An point separating unbroken and broken phase is called a $\mathcal{PT}$ phase transition.

At this point we warn the reader for potential confusion; symmetries can be broken either spontaneously (SSB) or explicitly (ESB). The latter would mean that H is changed in such a way that it no longer satisfies $\mathcal{PT}$ symmetry. In the context of $\mathcal{PT}$ symmetry we always refer to spontaneous breaking unless we clearly state otherwise. The table below summarizes the discussion.

This definition opens the way for one of the most famous results in $\mathcal{PT}$ theory: if the system has unbroken $\mathcal{PT}$ symmetry, then the spectrum is real. One can show that H as in eq. (3.4) has unbroken symmetry for $N \geq 2$, hence the spectrum in fig. 3.1 illustrates the following proposition.

Symmetry	H is $\mathcal{PT}$ symmetric?	Eigenvector H is eigenvector $\mathcal{PT}$?
Unbroken/Exact	Yes	Yes
Broken	Yes	No (at least for one)
Explicitly broken	No	Irrelevant

Table 1: Explanation of symmetry names

Proposition 3.1. If H is $\mathcal{PT}$ symmetric and $\mathcal{PT}$ symmetry is unbroken, then the spectrum is real and the eigenstates ϕ can be chosen so that $\mathcal{PT}\phi = \phi$.

Proof. In the described situation, we may write

$$H\phi = E\phi, \quad \mathcal{PT}\phi = \lambda\phi$$

for some complex numbers E and λ. If we multiply the second equation by $\mathcal{PT}$, we obtain

$$(\mathcal{PT})^2\phi = \mathcal{PT}(\lambda\phi).$$

As $\mathcal{P}$ and $\mathcal{T}$ commute and are there own inverse by definition, the lefthandside equals ϕ. On the right, we may take λ out to get λ^* as $\mathcal{PT}$ is conjugate linear. That is,

$$\phi = \lambda^*\mathcal{PT}\phi = \lambda^*\lambda\phi$$

so that $|\lambda|^2 = 1$. Hence $\lambda = e^{i\theta}$ is a phase, and we may choose the convention to rescale $\phi \to e^{-i\theta/2}\phi$ so that $\mathcal{PT}\phi = \phi$, proving the last claim.
Multiplying the first equation by $\mathcal{PT}$ results in

$$E^*\phi = \mathcal{PT}H\phi = H\mathcal{PT}\phi = H\phi = E\phi$$

using the convention we just had. Hence $E = E^*$, meaning that the spectrum of H is real. □

Conversely, when $\mathcal{PT}$ symmetry is broken the spectrum is usually complex as in fig. 3.1 for $N < 2$. Rephrasing the proposition; the fact that the eigenvalue under $\mathcal{PT}$ can be chosen 1 means we may pick wave-functions satisfying $\psi(x) = \psi^*(-x)$.

It has been shown that $\mathcal{PT}$ symmetry really defines a quantum theory. However, the steps are quite different from the usual set-up. Originally, instead of first finding the inner product and then looking for the eigenstates, one would first find the eigenstates to then define the inner product to be used.

3.2 Original set-up

We briefly review the original set-up of $\mathcal{PT}$ theory as discussed in [15]. That is, we consider a finite-dimensional complex vector space that is *a priori* not endowed with an inner product. We only consider symmetric matrix hamiltonians H; in [13] it is argued that asymmetric H lead to non-unitary behavior, which we discard for the moment. In the integrals that follow o, special integration paths in the complex plane need to be chosen, in accordance with the boundary conditions.

The process starts by defining the ($\mathcal{PT}$ symmetric) hamiltonian and finding its eigenstates $\phi_n(x)$. A natural guess for the inner product would be

$$(f, g) = \int (\mathcal{PT}f)g \,\mathrm{d}\,x = \int f^*(-x)g(x) \,\mathrm{d}\,x,$$

but numerical results indicate that instead of the usual orthonormality one would find

$$(\phi_m, \phi_n) = (-1)^n \delta_{mn} \tag{3.5}$$

implying that this inner product is indefinite. On the other hand, (f, f) is independent of added phase and constant in time. The next step is to 'fix' the indefiniteness.

To this end we need the modified completeness relation

$$\sum_{n=0}^{\infty} (-1)^n \phi_n(x)\phi_n(y) = \delta(x-y). \tag{3.6}$$

which was also found by numerical calculations. Now define

$$\mathcal{C}(x,y) = \sum_{n=0}^{\infty} \phi_n(x)\phi_n(y) \tag{3.7}$$

and the corresponding operator, also denoted $\mathcal{C}$, which acts on a function f as

$$(\mathcal{C}f)(x) = \int \mathcal{C}(x,y) f(y)\,\mathrm{d}\,y.$$

One has $\mathcal{C}^2 = 1$ so that $\mathcal{C}$ has eigenvalues ± 1. Also, $\mathcal{C}$ is linear and commutes with H, meaning every energy eigenstate has a well-defined $\mathcal{C}$ eigenvalue as well. In fact,

$$\mathcal{C}\phi_n(x) = \int \mathcal{C}(x,y)\phi_n(y)\,\mathrm{d}\,y = \sum_{m=0}^{\infty} \phi_m(x) \int \phi_m(y)\phi_n(y)\,\mathrm{d}\,y = (-1)^n \phi_n(x). \tag{3.8}$$

Hence $\mathcal{C}$ gives the sign of the $\mathcal{PT}$ norm of an eigenstate. It follows that $\mathcal{C}$ can be used to fix the $\mathcal{PT}$ pairing. Explictily, one has the inner product

$$\langle \psi | \chi \rangle^{\mathcal{CPT}} = \int \psi^{\mathcal{CPT}}(x)\chi(x)\,\mathrm{d}\,x \tag{3.9}$$

where

$$\psi^{\mathcal{CPT}}(x) = \int \mathcal{C}(x,y)(\mathcal{PT}\psi)(y)\,\mathrm{d}\,y = \int \mathcal{C}(x,y)\psi^*(-y)\,\mathrm{d}\,y. \tag{3.10}$$

It follows that this inner product is phase independent and conserved in time (as the time-evolution is still given by e^{-iHt}).

The completeness relation now has the desired form

$$\sum_{n=0}^{\infty} \phi_n(x)[\mathcal{CPT}\phi_n(y)] = \delta(x-y). \tag{3.11}$$

In [15], it is furthermore noted that in general $\mathcal{P}^2 = \mathcal{C}^2 = 1$, yet $\mathcal{P} \neq \mathcal{C}$ and $[\mathcal{P}, \mathcal{C}] \neq 0$. Where $\mathcal{P}$ was real, $\mathcal{C}$ may be complex. On the other hand, $\mathcal{C}$ commutes with $\mathcal{PT}$. The above construction can be done explicitly for finite-dimensional systems, and a 2×2 matrix example is also found in [15]. We will do a similar example later involving both EPs and $\mathcal{PT}$ symmetry.

We want to add a small note on the $\mathcal{C}$ operator. Although it has largely disappeared, still the term c-product survives as a name for the bi-orthogonal product, see e.g. [9]. That is, one has right-eigenstates and left-eigenstates that together form a bi-orthogonal system, see appendix C. Details on existence can be found in Mostafazadehs paper series on this subject, see [14].

The complexity of the above theory in comparison with standard quantum mechanics is striking. However, it turns out that one the level of the Schrödinger equation any $\mathcal{PT}$ symmetric system can be described in a hermitian setting if the $\mathcal{PT}$ symmetry is exact [14], which is the case usually considered. Or, as [12] puts it, any $\mathcal{PT}$ symmetric system with real eigenvalues is unitarily equivalent to hermitian system. We will look into this in section 3.5, first we want to do investigate explicit 2×2 $\mathcal{PT}$ symmetric hamiltonians.

3.3 Explicit 2-dimensional $\mathcal{PT}$ symmetric systems

To get more intuition concerning $\mathcal{PT}$ symmetric systems we deal with the 2-dimensional case explicitly. Therefore, let us pick the most general 2-dimensional H;

$$H = \begin{pmatrix} a & b \\ c & d \end{pmatrix}$$

where a, b, c, d are a priori independent complex parameters. We may take $\mathcal{P}$ equal to the exchange operator as

$$\mathcal{P} = \begin{pmatrix} 0 & 1 \\ 1 & 0 \end{pmatrix}$$

and $\mathcal{T}$ to be complex conjugation. Hence H is $\mathcal{PT}$ symmetric if and only if $H = \mathcal{P}H^*\mathcal{P}$ which explicitly means

$$\begin{pmatrix} a & b \\ c & d \end{pmatrix} = \begin{pmatrix} 0 & 1 \\ 1 & 0 \end{pmatrix} \begin{pmatrix} a^* & b^* \\ c^* & d^* \end{pmatrix} \begin{pmatrix} 0 & 1 \\ 1 & 0 \end{pmatrix} = \begin{pmatrix} d^* & c^* \\ b^* & a^* \end{pmatrix}$$

so that $a = d^*$ and $b = c^*$. We may thus set $a = x + iy$ and $b = z - iw$ where x, y, z, w are real. Hence, the most general 2×2 $\mathcal{PT}$ symmetric H is

$$H = \begin{pmatrix} x + iy & z - iw \\ z + iw & x - iy \end{pmatrix} \tag{3.12}$$

as also encountered in some EP examples previously. We note that theoretically we may limit ourselves to the symmetric case $w = 0$, but this may not be in the chosen basis. Nevertheless, the formula for purely real coupling is easily recovered and indeed keeps the qualitative behavior.

If $w = 0$, we see that the matrix models a set-up with two levels with specific properties. Their base energy is the same but the decay rates differ by a minus sign. Physically, one would encounter a system like

$$\begin{pmatrix} E + i\Gamma & k \\ k & E - i\Gamma \end{pmatrix}$$

where E is the common energy of the basis states, k the coupling between these states. The $\pm\Gamma$ indicates that one states experience gain while the other has the same amount of loss. The change in energy supplied externally, hence this is an example of an open system with time-independent hamiltonian. The parameter k should be $|z+iw|$ for general system. The absolute value give the coupling strength, whereas the argument indicates a phase. One may guess correctly that the system behaves differently for high or low coupling relative to the gain/loss. This will reappear below in the two phases of the system.

The characteristic polynomial is (put $\omega^2 = z^2 + w^2 - y^2$)

$$\lambda^2 - 2x\lambda + (x^2 + y^2 - z^2 - w^2) = (\lambda - x)^2 - \omega^2.$$

Let us introduce the notation $ke^{i\alpha}$ for the polar form of $z + iw$. As $\omega^2 = k^2 - y^2$ we can write the eigenvalues as

$$\lambda_\pm = x \pm \sqrt{k^2 - y^2} = x \pm \sqrt{k - y}\sqrt{k + y} = x \pm \omega.$$

For convenience, in case $k \neq 0$, let us also introduce $t = y/k$ and put $\cos(s) = t$. The eigenvectors can then be written as

$$v_\pm = \begin{pmatrix} iy \pm \omega \\ z + iw \end{pmatrix} \sim \begin{pmatrix} it \pm \sqrt{1 - t^2} \\ e^{i\alpha} \end{pmatrix} = \begin{pmatrix} ie^{\mp is} \\ e^{i\alpha} \end{pmatrix}.$$

The sign of ω^2, and so the question of ω being real or (purely) imaginary, is the key property to classify symmetry regimes. We see that ω carries a square root and so EPs may occur for $\omega = 0$, that is when a $\mathcal{PT}$ phase transition occurs. We go over the separate regions next.

When $\omega^2 > 0$, i.e. $|y| < k$ or in words the coupling is stronger than the gain/loss the quantity ω is real. Alternatively, the parameter s is real, and we may write

$$\mathcal{PT}v_\pm = \begin{pmatrix} z - iw \\ -iy \pm \omega \end{pmatrix} = \frac{-iy \pm \omega}{z + iw} v_\pm, \quad \text{or } \mathcal{PT}v_\pm = \begin{pmatrix} e^{-i\alpha} \\ -ie^{\pm is} \end{pmatrix} = e^{i(\pm s - \alpha - \pi/2)} v_\pm$$

which shows that this is a region of unbroken $\mathcal{PT}$ symmetry. Note that the factor arising from the $\mathcal{PT}$ operator is indeed a pure phase.

When $\omega^2 < 0$, that is $|y| > k$ or the coupling is weaker than the gain/loss, then ω is imaginary. Hence $s = i\tilde{s}$ is imaginary, and we have

$$\mathcal{PT}v_\pm = \begin{pmatrix} z - iw \\ -iy \mp \omega \end{pmatrix} = \frac{-iy \mp \omega}{z + iw} v_\mp, \quad \text{or } \mathcal{PT}v_\pm = \begin{pmatrix} e^{-i\alpha} \\ -ie^{\mp \tilde{s}} \end{pmatrix} = e^{\mp \tilde{s} + i(-\alpha - \pi/2)} v_\mp$$

where one observes that the eigendirections are permuted. This implies that $\omega^2 < 0$ is a region of broken $\mathcal{PT}$ symmetry.

When $\omega^2 = 0$, i.e. $y = \pm k$ or the coupling (in absolute value) is exactly the gain/loss, the eigenvalues both equal x. There is also one eigenvector at a point given by

$$\phi_{\text{EP}} = \begin{pmatrix} \pm ik \\ z + iw \end{pmatrix} \sim \begin{pmatrix} \pm i \\ e^{i\alpha} \end{pmatrix} = \begin{pmatrix} e^{\pm i\pi/2} \\ e^{i\alpha} \end{pmatrix}$$

where the $\pm$ corresponds to $y = \pm k$. The relative phase between the components equals

$$\theta = \pm \frac{\pi}{2} - \alpha$$

so that the $\pi/2$ relative phase applies iff $w = 0$. Note that this is a consequence of lemma 2.2. As there is a only 1 eigenvector and $\mathcal{PT}$ permutes the eigenvectors, the $\mathcal{PT}$ symmetry is unbroken.

We conclude that this general two-dimensional $\mathcal{PT}$ symmetric H has a cone of phase transitions, as illustrated by a segment in fig. 3.2. The phase is broken inside the cone and unbroken outside. As expected, the value of x is irrelevant in the phase diagram as this would only give a real shift to the eigenvalues and preserve eigenvectors. The cone consists of EPs, hence the $\mathcal{PT}$ phase transitions and EPs coincide. In case $y = 0$, the hermitian case, we are in the plane through the apex of the cone, which itself marks a system proportional to identity (equivalent to the zero matrix).

We end this subsection by looking at the bi-orthogonal system. One has (unnormalized) left-eigenvectors

$$\tilde{v}_\pm = \begin{pmatrix} iy \pm \omega & z - iw \end{pmatrix} \tag{3.13}$$

satisfying

$$\tilde{v}_\pm \cdot v_\pm = \pm 2iy\omega$$

$$\tilde{v}_\pm \cdot v_\mp = 0.$$

Hence, proper normalization would scale the vectors with a factor $\propto \omega^{-1/2}$, implying fourth root behavior (neglecting y for a moment). As $\omega \to 0$ when one approaches an EP indeed the normalization factor blows up at the EP.

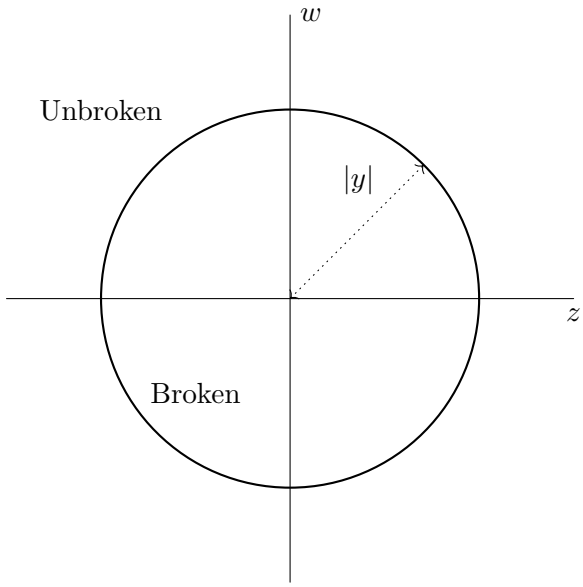

Figure 3.2: Phase diagram of $\mathcal{PT}$ symmetry for the system in eq. (3.12), which is a cone in full z, w, y-space. The separating circle itself corresponds to EPs. Note that the gain/loss sets the radius in this complex coupling plane.

3.4 Finite dimensional $\mathcal{PT}$ symmetric systems

A first step is to generalize the $\mathcal{PT}$ operator. We only need that it is anti-linear and involutive. For the generalization we introduce the abbreviation ALIS. We introduce the needed definitions below.

Definition 3.2. An operator T on a complex vector space V is *anti-linear* iff for all $x, y \in V$ and $a, b \in \mathbb{C}$

$$T(ax + by) = a^* Tx + b^* Ty.$$

Definition 3.3. An operator P is an *involution* iff $P^2 = 1$, so iff $P^{-1} = P$.

Definition 3.4. Given a system defined by a hamiltonian H. An operator X is called an anti-linear involution symmetry (ALIS) of H if and only if X is an anti-linear involution commuting with H. We omit "of H" whenever the precise system is clear or irrelevant. On the other hand, if we say "X symmetric H", we mean that X is an ALIS of H.

Given an anti-linear involution one can obtain a linear involution by composition with complex conjugation, that is composition with $\mathcal{T}$. Indeed, $(\mathcal{PT})\mathcal{T} = \mathcal{T}(\mathcal{PT}) = \mathcal{P}$. More precisely, the following result holds. We will denote a general linear real involution by P and view it as a generalization of $\mathcal{P}$.

Proposition 3.2 ([14])**.** Set $P = X\mathcal{T}$ where X is anti-linear. Then

- P is linear.
- if X is an involution, P is a real involution.

Proof. Linearity follows as $\mathcal{T}$ takes another conjugate and P is clearly involutive. To see P is real, the requirement $(P\mathcal{T})^2 = (X\mathcal{TT})^2 = X^2 = 1$ implies $P(\mathcal{T}P\mathcal{T}) = PP^* = 1$. Acting with P on the left yields $P = P^*$. □

Note that if one demands the obtained involution P to be unitary, i.e. $P^\dagger P = 1$, then $P^\dagger = P$ and as P is real $P^T = P$. The most general P in two dimensions is then

$$P_\phi = \begin{pmatrix} \cos(\phi) & \sin(\phi) \\ \sin(\phi) & -\cos(\phi) \end{pmatrix}$$

which is a rotation times $\mathrm{diag}(1, -1)$, which in turn is similar to

$$\begin{pmatrix} 0 & 1 \\ 1 & 0 \end{pmatrix}.$$

This is the only non-trivial building block for an operator P. To see this, we observe that the involution property induces a partition of the eigenvectors in sets of 1 or 2 elements.

Proposition 3.3. If X is an ALIS of H, then X permutes the eigenvectors of H, sending eigenvalues to their complex conjugate. The operator X so partitions the set of eigenvectors into cycles of length 1 or 2;

- in case of length 1, the eigenvector is part of unbroken symmetry and has real eigenvalue under H.
- in case of length 2, the eigenvector and X times the eigenvector contribute to the broken symmetry and have complex conjugate eigenvalues.

Proof. If v is an eigenvector H then

$$H(Xv) = XHv = XE_v v = E_v^*(Xv)$$

so $w := Xv$ is again an eigenvector with complex conjugate eigenvalue. As $X^2 = 1$, for any vector v only v and Xv may be distinct, so cycle length is at most 2.

In case of length 1, w is proportional to v, so v is an eigenvector of X. Proposition 3.1, which holds for a general ALIS, then guarantees we may scale v so that $w = Xv = v$. Also $E_v = E_w^* = E_v^*$, hence the eigenvalue E_v is real.

In case of length 2, w is not proportional to v, in particular we can't scale w to v. Hence v is not an eigenvector of X, implying broken symmetry by definition. □

Corollary 3.1. Let X be an ALIS of H, assume H is diagonalizable. Then there exists a basis in which H is diagonal and $P = X\mathcal{T}$ is block diagonal with blocks being

$$(1)\,, \quad \text{or} \quad \begin{pmatrix} 0 & 1 \\ 1 & 0 \end{pmatrix}.$$

Proof. Start with a complete set S of eigenvectors of H. If $v \in S$ is also an eigenvector of X, it gives a trivial block. Otherwise the above provides an H-eigenvector w (linearly dependent on S) such that P is the non-trivial block when restricted to the span of v and w. □

Although in the broken regime we have $X(v \pm w) = \pm(v \pm w)$, this new eigenvector of X need not be an eigenvector of H. In fact, this holds iff $E_v = E_w$, implying degeneracy. Such a question is also relevant when we want to investigate a converse to unbroken symmetry implying real eigenvalues. Explicitly, under what condition does a real spectrum imply unbroken symmetry for a $\mathcal{PT}$ symmetric system? We see that non-degeneracy is sufficient.

Proposition 3.4. Given an X symmetric non-degenerate H;

- if the X symmetry is broken, the complex conjugate pairs have strictly non-zero imaginary part

- X symmetry is unbroken $\iff$ the spectrum is real

Proof. The broken symmetry supplies eigenvectors v and $w = Xv \neq v$. Assume the eigenvalue of H is real, i.e. the conjugate pair degenerates to $E_v = E_v^* = E$ real. However, then H is degenerate in E, contradicting the assumption. Thus, broken symmetry implies strictly complex spectrum in this case.
In general, unbroken symmetry implies a real spectrum, and with the previous the equivalence follows. □

Non-degeneracy was explicitly assumed in the above. However, it may also be a consequence as shown in the next result.

Lemma 3.1. (The spectrum of) an unbroken X symmetric system H is non-degenerate. This may not hold when the X symmetry is broken.

Proof. Suppose E is an eigenvalue of H and $v_1 \neq v_2$ are associated eigenvectors, by assumption also of X and where we normalized $Xv_i = v_i$. Then $av_1 + bv_2$ with complex coefficients is again an eigenvector of H. Now

$$X(av_1 + bv_2) = a^* X v_1 + b^* X v_2 = a^* v_1 + b^* v_2 \not\propto av_1 + bv_2$$

for suitable a and b (e.g. pick different phases). So, $av_1 + bv_2$ can be an eigenvector of H which is not an eigenvector of X, contradicting unbroken symmetry. Hence no v_2 can be chosen, implying the first claim.
A counterexample in a broken system is to take H proportional to the identity in 2D; 1 eigenvalue but a 2 dimensional eigenspace. □

Hence unbroken ALIS symmetry allows one to use all kinds of results based on non-degeneracy like the ones in appendix C. An notable example is that the hamiltonian is diagonalizable.

EP-$\mathcal{PT}$ transition correspondence

We can now show that in any generic case an EP will be situated at the $\mathcal{PT}$ phase transition, and that conversely $\mathcal{PT}$ transitions will happen at EPs. We need little theory if we agree to consider only generic non-pathological cases, e.g. not having an EP at the edge of parameter space. The connecting notion is that of higher order zero. We immediately note that limiting to $\mathcal{PT}$ symmetric systems is a serious limitation in EP theory. However, as seen more clearly in section 5.2, one may still use $\mathcal{PT}$ theory is a subregion of parameter space where $\mathcal{PT}$ symmetry holds.

We already saw that EPs correspond to higher order zeroes, more precisely, that EPNs are (at least) N^{th} order zeroes. In generic case a zero of order N is an EPN.

Lemma 3.2. Let $T(x)$ be a differentiable $\mathcal{PT}$ symmetric operator. Then in generic cases; $p_T(\lambda, x)$ has a double zero (in λ) $\iff$ x is at a $\mathcal{PT}$ phase transition.

Proof. Suppose $p_T(\lambda, x)$ has a double zero, then $\frac{d}{d\lambda} p_T(\lambda, x) = 0$ and in generic cases the eigenvalues form a non-differentiable structure. In a $\mathcal{PT}$ symmetric system this means that there is a real-to-complex singularity, hence a $\mathcal{PT}$ phase transition by proposition 3.4.

Conversely, a $\mathcal{PT}$ phase transition is also real-to-complex singularity. In particular, two eigenvalues degenerate so that $p_T(\lambda, x)$ has a double zero.

□

We can now state the desired correspondence.

Theorem 3.1. Let $T(x)$ be a differentiable $\mathcal{PT}$ symmetric operator, then the set of EPs and the region of $\mathcal{PT}$ phase transition coincide (up to pathologies).

Proof. We observe that generically; x is EP $\iff$ x provides higher order zero of the characteristic polynomial $\iff$ x marks a $\mathcal{PT}$ phase transition. We note that the $\iff$ symbols hold up to issues like perfect squares, strange matrix elements and other things that do not happen in a generic physical system. □

EPs and $\mathcal{PT}$ symmetry breaking

When reviewing the experiments done with EPs, something peculiar appears. Usually, one starts with a parameter dependent hamiltonian that is $\mathcal{PT}$ symmetric for all (real) parameters. However, in order to measure/encircle the EP, one moves to a region where the hamiltonian is *not* $\mathcal{PT}$ symmetric (often by complexifying parameters, where the imaginary part comes from a physically real parameter). That is, $\mathcal{PT}$ symmetry is broken explicitly, not spontaneously.

Let us introduce a convenient function for further study. First, if we put

$$A = \begin{pmatrix} a & b \\ c & d \end{pmatrix}$$

then its eigenvalues are given by

$$\lambda_\pm = \frac{a+d}{2} \pm \sqrt{\left(\frac{a-d}{2}\right)^2 + bc}.$$

The relevant information for us is encoded in the argument of the square root. For an operator family $T(x)$, the above quantities depend on x and we can write $\lambda_\pm(x) = f(x) \pm \sqrt{g(x)}$ for some complex functions f, g defined on parameter space. We define the g-function of a 2×2 operator family to be the argument of the square root. Note that EPs are given by the zeros of the g-function in non-pathological cases.

If $T(x)$ is $\mathcal{PT}$ symmetric for all x, the g-function has some special property. As $T(x)$ is $\mathcal{PT}$ symmetric, by proposition 3.3 the eigenvalues appear in complex conjugates. Hence the characteristic polynomial has real coefficients, and the g-function is real valued. This means that the eigenvalues only differ in real or imaginary part, but not in both. Experimentally, this means that real-to-complex singularities can occur. On the other hand, swaps are ruled out as the g-function needs to complex for that.

We can now use the above in the generic example of

$$H = \begin{pmatrix} E_1 + i\Gamma_1 & k \\ k & E_2 + i\Gamma_2 \end{pmatrix}.$$

This system has g-function

$$g = k^2 + \left(\frac{E_1 - E_2}{2} + i\frac{\Gamma_1 - \Gamma_2}{2}\right)^2$$

which gives many EPs. It is $\mathcal{PT}$ symmetric if and only if $E_1 = E_2 = E$ and $\Gamma_1 = -\Gamma_2 = \Gamma$, in which case

$$g = k^2 - \Gamma^2.$$

We can introduce the symmetry breaking parameters

$$\delta = 1 - \frac{E_2}{E_1}, \quad \epsilon = 1 + \frac{\Gamma_2}{\Gamma_1}$$

meaning that H is $\mathcal{PT}$ symmetric if and only if $\delta = \epsilon = 0$, where we neglect division by zero issues. Notice that paths in parameter space that explicitly break $\mathcal{PT}$ symmetry correspond to paths with non-zero δ and/or ϵ. Also, using suitable substitutions, allowing such paths corresponds to complexifying parameter space.

We may write g as

$$g = k^2 + \frac{1}{4}\left(\delta E_1 + i(2-\epsilon)\Gamma_1\right)^2,$$

and we observe that g is real iff $\delta = 0$ or $\epsilon = 2$

If $\delta = 0$, then $g = s^2 - ((2-\epsilon)\Gamma_1/2)^2$, implying a real root and so implying that the EP is accessible. In this case, the precise value of ϵ is not important, up to $\epsilon = 2$ causing a double zero.

In the case $\epsilon = 2$, accessibility of the EP is not there. Note that $\epsilon = 2$ corresponds to a self-adjoint H, meaning $(2-\epsilon)$ measures the breaking of this symmetry.

For all other values of δ, ϵ, the function is complex and experimental EPs may appear. In fact, any real zero of g then corresponds to an experimental EP.

We note that $\epsilon = 0$ was not treated separately. Without $\delta = 0$ as well we can say not that much, but if this is the case then

$$g = k^2 - \Gamma_1^2 = k^2 - \Gamma_2^2$$

meaning we once again obtain the EPs at the phase transition.

3.5 Equivalence unbroken symmetry and Hermitian case

We zoom in on the remarkable fact that unbroken $\mathcal{PT}$ symmetry is, to large extend, equivalent to standard Hermitian theory. Only the main argument is reproduced here, for the full details we refer to Mostafazadehs papers such as [14] and preceding papers.

A key point is to define notions as pseudo-Hermicity to encorporate a larger class of operators with favorable properties like a real spectrum and unitary evolution. As made precise in the below definition, we extend hermicity to system where hermicity holds up to a basis transformation.

Definition 3.5. An operator H is called *η-pseudo Hermitian* iff $H^\dagger$ is equivalent to H via a similarity (basis) transformation η, explicitly

$$H^\dagger = \eta^{-1} H \eta$$

If such η exists, the operator is called pseudo Hermitian.
If in addition the operator η can be chosen positive definite, we say H is *η-quasi-Hermitian.*

The pseudo part guarantees e.g. the transfer of real spectrum, the quasi part is needed to keep positive-definite inner products.

For physical equivalence, we want to leave the Schrödinger equation invariant, and adopt a definition from [18].

Definition 3.6. A *pseudo-canonical* transformation is a linear automorphism that leaves the Schrodinger equation form-invariant.

In [14], we first restrict the space and operators in a certain way to get a diagonalizable $H\colon \mathcal{H} \to \mathcal{H}$ and exact symmetry (note: including real spectrum); for convenience we take this plus the assumption of a discrete spectrum as our starting point and follow the argument presented in the paper.

We start the argument with the following equivalence as stated in [18]. Part of it is an infinite dimensional extension of results in appendix C.

Proposition 3.5. Given H a diagonalizable Hamiltonian, the following are equivalent;

1. the spectrum of H is real
2. there is a positive-definite inner-product on the Hilbert space with respect to which H is Hermitian
3. there is a pseudo-canonical transformation of the Hilbert space that maps H into a Hermitian operator.

Let $\ll -, - \gg$ be the inner product in which a given H is Hermitian, then it is related to the given inner product $\langle -, - \rangle$ as

$$\ll \phi, \psi \gg = \langle \phi, \eta_+ \psi \rangle$$

for some (standard) Hermitian invertible linear operator η_+. We note

$$\ll \phi, H\psi \gg = \ll H\phi, \psi \gg$$

reads

$$\langle \phi, \eta_+ H\psi \rangle = \langle H\phi, \eta_+ \psi \rangle$$

and so is equivalent to

$$\eta_+ H = H^\dagger \eta_+$$

which says H is η_+-pseudo Hermitian.

The unitary equivalence with the original inner product is closely related to η_+. As $\ll -, - \gg$ is positive-definite, so is η_+, and so there is a positive operator ρ_+ such that $\rho_+^2 = \eta_+$. Let $\tilde{\mathcal{H}}$ denote the same space, but with the new inner product. Also, ρ_+ is invertible, and even

$$\ll \rho_+^{-1}\phi, \rho_+^{-1}\psi \gg = \langle \rho_+^{-1}\phi, \eta_+ \rho_+^{-1}\psi \rangle = \langle \phi, \psi \rangle$$

or equivalently

$$\ll \phi, \rho_+^{-1}\psi \gg = \langle \rho_+ \phi, \psi \rangle.$$

The defining relation for $(\rho_+^{-1})^\dagger$ is

$$\ll \phi, \rho_+^{-1}\psi \gg = \langle (\rho_+^{-1})^\dagger \phi, \psi \rangle$$

and so

$$(\rho_+^{-1})^\dagger = \rho_+ = (\rho_+^{-1})^{-1}$$

implying that $\rho_+^{-1} : \mathcal{H} \to \tilde{\mathcal{H}}$ is unitary. Hence, the space with standard inner product and the same space with new inner product are related via a unitary operator.

The unitary equivalence extends to operators on the space. Let h be any Hamiltonian acting in $\mathcal{H}$ defining time-evolution, then define

$$\tilde{h} = \rho_+^{-1} h \rho_+$$

so that ρ_+^{-1} maps solutions $\psi(t)$ to solutions $\tilde{\psi}(t)$.
Similarly, observables $O : \mathcal{H} \to \tilde{\mathcal{H}}$ are mapped to observables

$$\tilde{O} = \rho_+^{-1} O \rho_+$$

where in both cases a unitary similarity transformation is used.

Set $\tilde{h} = H$, then

$$h = \rho_+ H \rho_+^{-1}$$

is an Hermitian (in $\mathcal{H}$) Hamiltonian which we can check directly;

$$\begin{aligned}\langle \phi, h\psi \rangle &= \langle \phi, \rho_+ H \rho_+^{-1} \psi \rangle = \ll \rho_+^{-1}\phi, H\rho_+^{-1}\psi \gg = \ll H\rho_+^{-1}\phi, \rho_+^{-1}\psi \gg \\ &= \langle \rho_+ H \rho_+^{-1}\phi, \psi \rangle = \langle h\phi, \psi \rangle.\end{aligned}$$

Now H and h are related by a unitary transformation between spaces with the same underlying vector space structure. Hence, they are related by a pseudo-canonical transformation, and so physically equivalent.

In summary, a diagonalizable Hamiltonian with discrete real spectrum is physically equivalent to a Hermitian system. Lemma 3.1 guarantees that unbroken (exact) symmetry implies not only a real but also a non-degenerate spectrum. The discrete spectrum assumption holds for many quantum systems and implies together with the previous that the Hamiltonian is diagonalizable. Hence, exact symmetry is equivalent to Hermitian theory. We finish with a concluding theorem from [18].

Theorem 3.2. Let $H\colon \mathcal{H} \to \mathcal{H}$ be a diagonalizable linear operator with a discrete spectrum. Then the following are equivalent:

1. The eigenvalues of H are real or come in complex-conjugate pairs
2. H is pseudo-Hermitian
3. H has an antilinear symmetry

Comments on equivalence

We note that the equivalence described above relates many concepts of $\mathcal{PT}$ symmetric theory to standard Hermitian theory. We do note that not all characteristics carry over, not even in the unbroken case where this could seem trivial.

One problem is the quantum brachistochrone problem; if you vary H but fix the difference between its largest and smallest eigenvalue, what is the smallest time in which a state $|0\rangle$ becomes a given $|1\rangle$ under time-evolution? We see in [12] that the Hermitian theory gives an elliptic constraint on system parameters, where $\mathcal{PT}$ symmetric theory gives a hyperbolic one. Hence, the Hermitian case has a bound on 'driving force' and so transition time, whereas the $\mathcal{PT}$ symmetric has not and so transition time may be arbitrarily small. In [19], a quantum computer was simulated, where indeed the evolution time of $\mathcal{PT}$ symmetric systems could be decreased beyond the Hermitian set-up.

Another problem is the assumption that H is diagonalizable, especially if one is interested in EPs. Namely, coalescence of eigenvectors implies that the relevant Jordan block still has a off-diagonal 1, meaning that H is not diagonalizable.

Then, we note that broken symmetry will in general not be equivalent to Hermitian theory. Usually, broken symmetry implies complex eigenvalues, and although a similarity transformation exists, this may not respect the inner product structure. Yet this broken symmetry is crucial for phase transitions and EPs.

A final note is that the invertible antilinear symmetries are treated. This includes the involutions, which on the other hand have some special properties. For instance, the fact

that an ALIS permutes some chosen eigenvectors of H needs more than invertibility; the operator $2\mathcal{PT}$ for example is invertible but will introduce extra numerical factors. On one hand, restricting to involution may be to restrictive, but on the other hand convenient to start with.

4 Applications of EP and $\mathcal{PT}$ theory

In this section we like to see how measurements concerning EPs and $\mathcal{PT}$ symmetric systems can be done. We start with selected EP experiments that show various practical aspects of EPs. The second part looks into $\mathcal{PT}$ symmetry in both linear and non-linear settings.

4.1 EP experiments

In this section we will discuss some EP experiments that involve key aspects of EP theory. We start with the first experiment in which an EP was found and demonstrating both swap and phase change. As this experiment is quasi-static, i.e. the parameters are changed in steps, we move on to a dynamical measurement. This experiment also utilized the breakdown of the adiabatic approximation to achieve orientation dependent mode selection. We finish with the 'merging loop method' which is an alternative way of measuring EPs, and treat an experiment where this was used.

First EP experiment

The first article reporting experimental evidence of EPs used a microwave cavity [20]. The cavity was like a disk cut in two by a slit of variable width s, which controls the coupling between the two sectors. On one side of the slit, a Teflon semicircle was attached, with the center a variable distance δ from the center of the cavity. This controls the asymmetry between the sectors. We adopt an overview of the set-up in fig. 4.1.

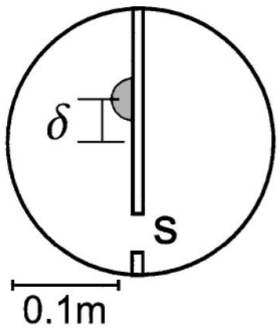

Figure 4.1: The set-up used in [20], illustrating also the system parameters.

The cavity supports various eigenmodes, but in the theory we limit ourselves to two selected ones. Indeed, for certain values of s and δ these modes coalesce. More precisely, the corresponding (simplified) operator is

$$H(s,\delta) = \begin{pmatrix} \delta f_1 + i\Gamma_1 & s \\ s & f_2 + i\Gamma_2 \end{pmatrix} \tag{4.1}$$

with δf_1 and f_2 the frequencies and Γ_1 and Γ_2 the widths of the uncoupled resonances.

The g function of the system, i.e. the expression that enters the square root in the eigenvalues of eq. (4.1), is given by

$$g(s,\delta) = s^2 + \left(\frac{\delta f_1 - f_2}{2} + i\frac{\Gamma_1 - \Gamma_2}{2}\right)^2$$

which is clearly complex. We see a general rule appearing; with only real parameters at our disposal, the factors of i are 'put in', usually with gain/decay or coupling. Otherwise, only real-to-complex transitions and no swaps are available.

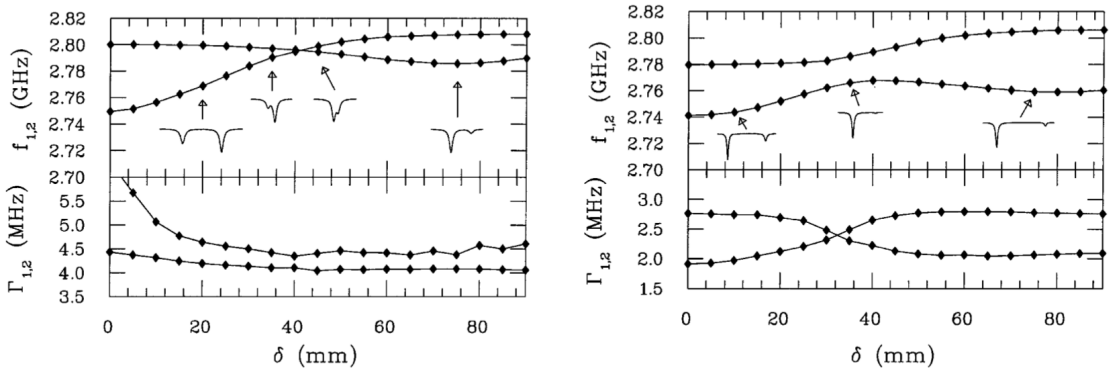

Figure 4.2: The avoided level crossings in the experiment[20] for $s = 58$mm resp. $s = 66$mm, note that these are observed quantities and not the system parameters as they appear in eq. (4.1). One observes that either frequencies or linewidths cross, where the roles are exchanged when s passes s_{EP}.

The EPs appear in the zero set of g, and letting $\tilde{s}$ denote s complexified (as is done in [20]), the EPs appear at

$$\tilde{s}_{\mathrm{EP}} = \pm\left(\frac{\Gamma_1 - \Gamma_2}{2} - i\frac{\delta f_1 - f_2}{2}\right). \tag{4.2}$$

Of course, only real s values are accessible in the laboratory. The detection of the branch structure must then be achieved by varying both s and δ to encircle an isolated EP in the δs-plane.

In our formalism it is convenient to work with real equations. Hence we split g in its real and imaginary part;

$$\begin{aligned} \mathrm{Re}(g) &= s^2 + \left(\frac{\delta f_1 - f_2}{2}\right)^2 - \left(\frac{\Gamma_1 - \Gamma_2}{2}\right)^2 \\ \mathrm{Im}(g) &= 2\frac{\delta f_1 - f_2}{2}\frac{\Gamma_1 - \Gamma_2}{2}. \end{aligned} \tag{4.3}$$

Assuming no special relation on the frequencies and linewidths, equating to 0 yields

$$\begin{aligned} s_{\mathrm{EP}} &= \pm\frac{\Gamma_1 - \Gamma_2}{2} \\ \delta_{\mathrm{EP}} &= \frac{f_2}{f_1}. \end{aligned} \tag{4.4}$$

This gives two isolated points in the δs-plane. We note that these are both EPs, in fact they are what we called experimental EPs in section 2.5. Indeed, measurements like this were the main motivation for us to introduce this concept.

In the experiment δ and s were adjusted individually so that the loop has the shape of a rectangle, where the loop encloses the positive s_{EP} solution. At each step the frequencies and linewidths were measured, and following these already showed two characteristics of an EP. One is the avoided level crossing in energy or linewidth. That is, either the real and imaginary part must differ, or both. This is showed in fig. 4.2, where on the other side of the EP the role of becoming degenerate is played by the other party.

The swap can thus be detected by measuring the eigenvalues only. However, to detect the acquired phase one really needs to track the eigenstates. In the experiment the state

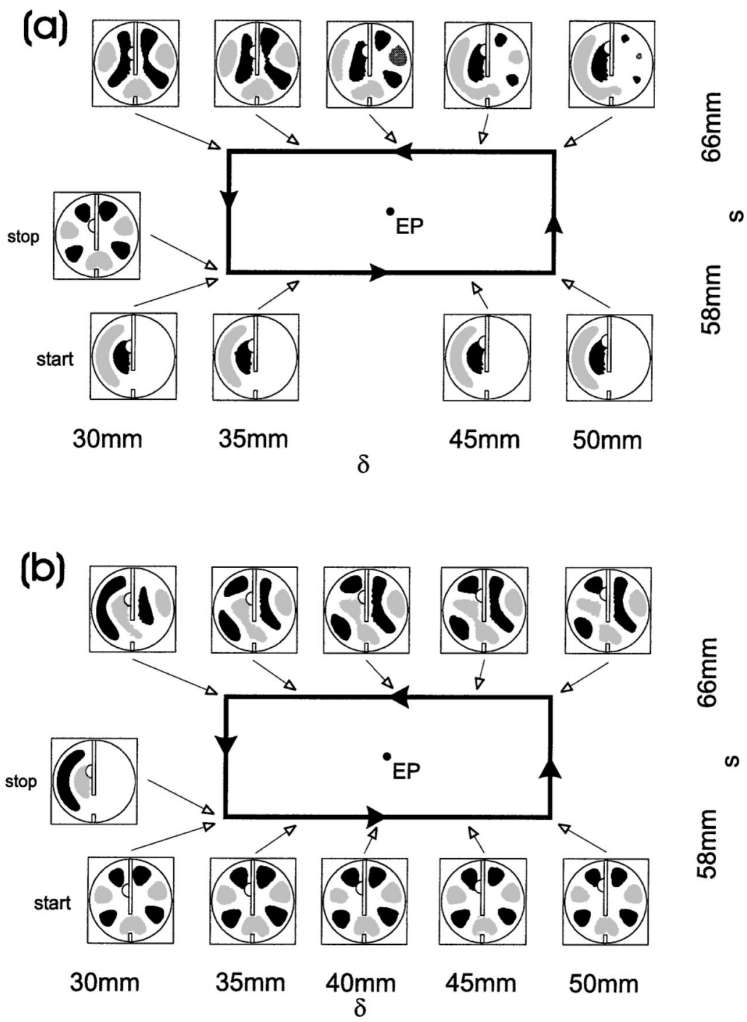

Figure 4.3: The change of the fields in [20]. Drawn in the traversed path in δs space, along with the field configurations at various times. The intensity in the cavity is shown, including the phase using gray scale. In (a) one finds the change $|\psi_1\rangle \to |\psi_2\rangle$, whereas (b) reveals the change $|\psi_2\rangle \to -|\psi_1\rangle$.

in terms of intensity and relative phases was measured at each step, as summarized in fig. 4.3. One observes that the phase change has been confirmed. Moreover, it was found that depending on the orientation of the measurement loop either one or the other eigenstate acquires the minus sign.

Dynamically encircling an EP

The previous experiment was a quasi-static experiment: the measurement consists of repeatedly fixing a point in parameter space and measuring the instantaneous eigenvalues/eigenstates there. Effectively, the measurement takes place with $\dot{H} = 0$. In this way one can accurately measure the eigenstates and/or eigenvalues without having to worry about the adiabatic approximation.

One could also try a dynamical EP experiment: one traverses a loop in parameter space continuously (not point by point) and directly drags the eigenstate along to measure the final state upon return, hence one explicitly sets $\dot{H} \neq 0$. However, one may ask if it is possible to perform such an experiment in such a way that the adiabatic approximation indeed dominates the dynamics. It was previously believed that slowly encircling an

EP would not significantly violate the adiabatic approximation as we will investigate in section 6. Nevertheless, as argued in [21] there is a catch due to the complex energies of the non-hermitian hamiltonian. These complex energies induce an extra decay factor via the dynamical phase which is proportional to $\exp(\int \mathrm{Im}(E)\,\mathrm{d}\,t)$. Hence there are two competing time-scales; on one hand one should work slowly to approach the adiabatic limit, on the other hand one must be fast in order to have a small contribution from the dynamical phase factor. On top of this is the problem that deviations from the idealized adiabatic situation are magnified in time. It is thus an experimental challenge to measure adiabatic encircling around an EP.

Instead of trying to avoid the appearing decay one can also try to use it. This was succesfully done in [22] using a waveguide setting. This allows for another trick; the system is formally equivalent to a Schrödinger equation, but the role of time is played by the propagation direction x. Hence the decay happens in space and not in time.

One starts with a waveguide and selects two modes to which we restrict the model. A general mode is then obtained by superposition of the two basis modes, hence defined by coefficients $c_1(x)$ and $c_2(x)$ depending on position. The evolution of these coefficients could be written as

$$i\partial_x \begin{pmatrix} c_1(x) \\ c_2(x) \end{pmatrix} = \begin{pmatrix} \delta(x) - i\gamma_1/2 & g(x) \\ g(x) & -i\gamma_2/2 \end{pmatrix} \begin{pmatrix} c_1(x) \\ c_2(x) \end{pmatrix} \tag{4.5}$$

where one has $\delta(x)$ the detuning, $g(x)$ the coupling between the levels and γ_i the gain/loss of mode i. The variation in x could be achieved using for instance a curved wobbly layout of the waveguide. In this way, a wave travelling through the waveguide experiences a varying hamiltonian, and can so encircle an EP in parameter space. The non-adiabatic effects induces a difference in amplitude between the basis modes, depending on the chirality of the wave. Effectively, the waveguide selects one of the two basis modes depending on whether the wave comes from the left or the right, see fig. 4.4. This is related to the asymmetry of the wobbling of the waveguide. Although both modes undergo significant losses, the ratio of the modal transmission rates was measured to be about 450, meaning that one of the modes practically disappears.

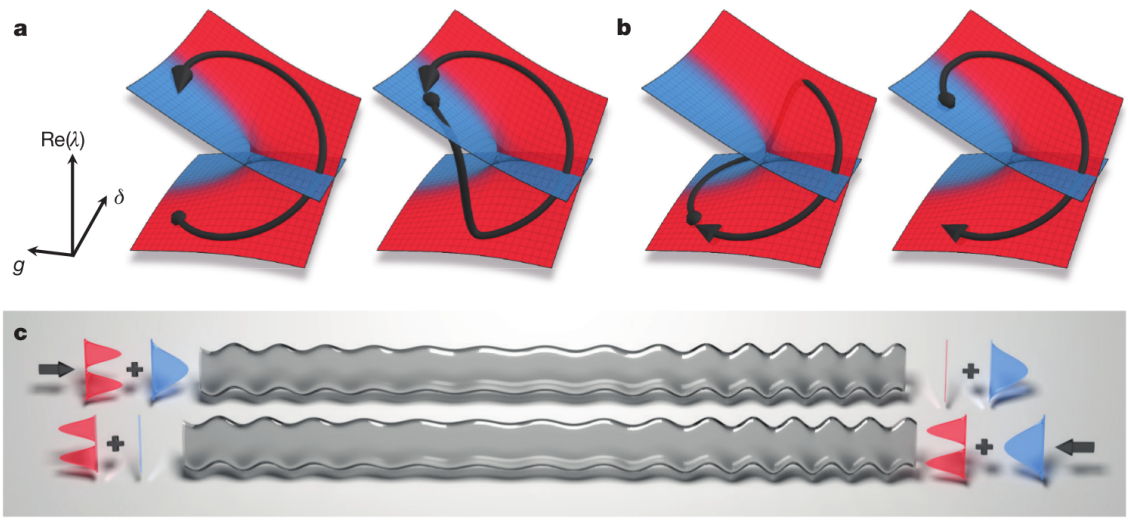

Figure 4.4: Illustration of the non-adiabatic behavior of the system, taken from [22]. In **a** and **b** the evolution of the modes for positive resp. negative encircling direction is depicted. In **c** the implied selection of the eigenmodes is illustrated.

Merging loop method

We finish this section on EP experiments with an experiment to illustrate how one can detect an EP without measuring, or even deducing, the eigenstates. Indeed, measuring the eigenvalues alone is sufficient and this method was already explained in [23]. We will refer to it as the *merging loop method*.

The idea is as follows. If there is no degeneracy present, then traversing a loop in parameter space will cause the eigenvalues to return to themselves individually [2]. Hence, each eigenvalue traces out its own loop in complex energy space. This radically changes if an EP is encircled. Say the path in parameter space runs from $t = 0$ to $t = 1$. If $\lambda_i(1) = \lambda_j(0)$ we say that eigenvalue λ_i goes to eigenvalue λ_j. If $j \neq i$ the locus of $\lambda_i(t)$ ends not at its initial value $\lambda_i(0)$ but instead ends at $\lambda_j(0)$. In particular, the locus of $\lambda_i(t)$ is no longer a loop. What does happen is that the loci of λ_i, λ_j and possibly more eigenvalues together form one big loop. Indeed, given that λ_i goes to λ_j, also λ_j must attain another index than j as its original place is already taken. After tracing the indices far enough one must return to index i by finite-dimensionality.

The case of an EP2 is illustrated in fig. 4.5. As often in such pictures, the energy corresponding to the EP is marked. This is not the EP itself according to our standards, but some refer to it as EP nevertheless. Regardless of this issue, marking the corresponding energy provides a visual aid indicating whether or not the EP in parameter space is encircled. The principle behind this is that the eigenvalues are locally bijective with parameter values in the case of 2 system parameters.

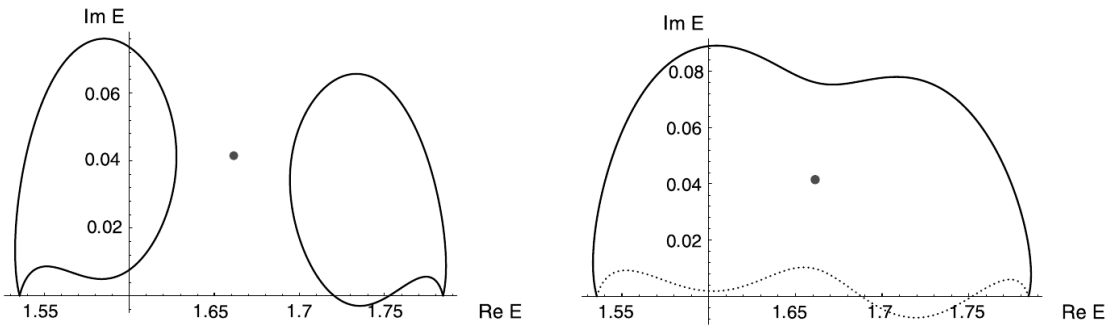

(a) No EP is encircled and both eigenvalues return to their original values.

(b) An EP is encircled and the eigenvalues are both part of one big loop. One of the eigenvalues is now indicated with dots to emphasize the merging.

Figure 4.5: Schematic view of possible paths of the eigenvalues, taken from [23]. The black dot marks the energy corresponding to the EP, not the EP itself.

The argument works also the other way around; if one finds that an eigenvalue does not return to itself, then there is non-trivial topology. Indeed, there is a non-trivial permutation of eigenvalues, indicating that an EP is present. Of course, one needs to check if really a single degeneracy is encircled to conclude on the order of the EP.

Now that we explained the method, let us review the experiment in [24] which used it to show the presence of an EP2. In [24], a nanometer thin membrane in a microcavity was excited with a laser. The radiation pressure then drives vibrations of the membrane. System parameters where the power P of the driving laser and Δ the mean detuning between the laser and the cavity. This was modelled with a 2×2 effective hamiltonian system, having an exceptional point for appropriate parameter values. The energy of the system is then given by the mechanical frequency (corresponding to $\mathrm{Re}(E)$) and mechanical linewidth (corresponding to $\mathrm{Im}(E)$) of the membrane. Figure 4.6 shows their results, and

[2] One can see that this happens at least locally. A proof for the global case can be found in section 6.

we recognize the shape of fig. 4.5.

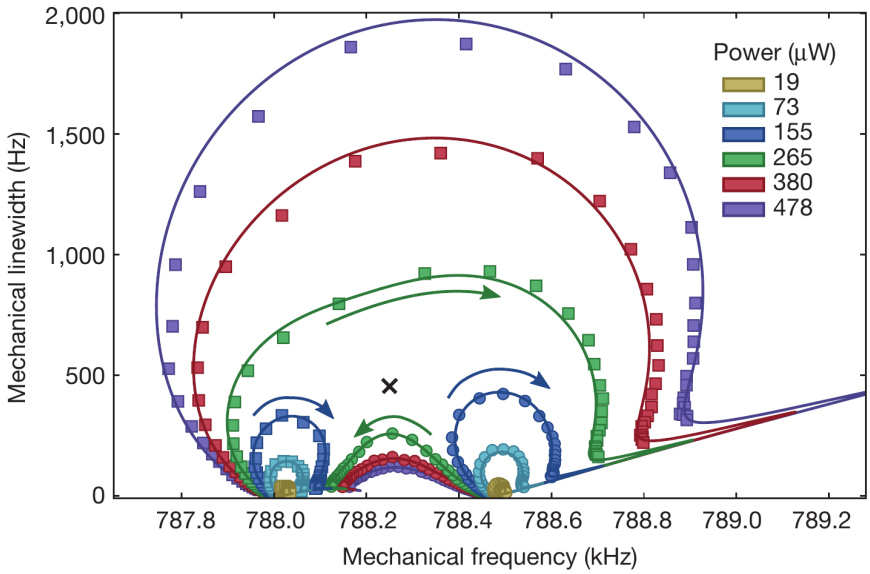

Figure 4.6: EP topology as measured in [24]. Blocks and circles mark the two different eigenvalues, which are given by frequency and linewidth. Varying the laser power allowed to measure different loci, which in turn are traversed using detuning. The energy corresponding to the EP is indicated with a cross, and the lines are the fitted model.

In the experiment even the sheets themselves were measured, going a step beyond what was necessary for finding an EP. As shown in fig. 4.7 the expected sheets were found in reasonable agreement with the model.

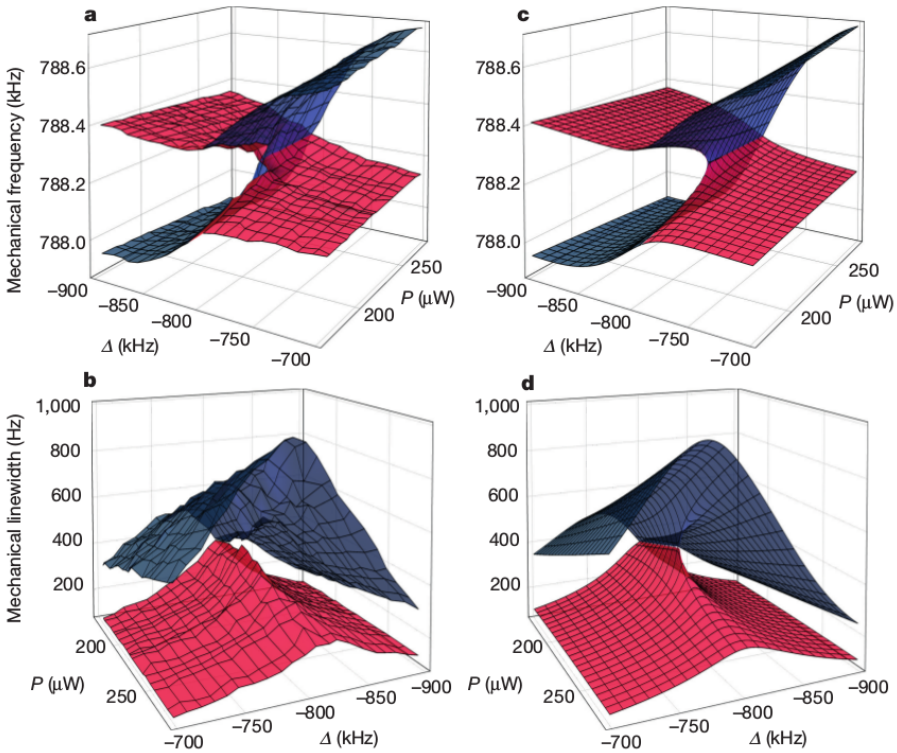

Figure 4.7: Eigenvalue/energy sheets measured in [24]. The two real system parameters P and Δ appear as input, the output is $\mathrm{Re}(E)$ on the upper line (**a** and **c**) and $\mathrm{Im}(E)$ at the lower line (**b** and **d**). The left column shows the measurement, the right one the theoretical expectation. Note that the viewing angles between upper and lower line differ.

4.2 $\mathcal{PT}$ phenomenology

We now turn to some $\mathcal{PT}$ phenomena. A recent overview of non-hermitian / $\mathcal{PT}$ symmetric experiments can be found in [25], and some will be treated here as well. We first focus on a $\mathcal{PT}$ symmetric waveguide experiment. This will confirm various $\mathcal{PT}$ symmetry effects and will set the stage for an extended set-up used in a later section of this thesis. After that we treat some $\mathcal{PT}$ symmetric systems of differential equations. This will e.g. place $\mathcal{PT}$ symmetry in a non-linear setting, but one can extend the ideas in a straight-forward way and so use $\mathcal{PT}$ symmetry to study these systems. As $\mathcal{PT}$ experiments have not yet been done with genuine quantum mechanics, we finish with a recent proposal using circuit-QED.

$\mathcal{PT}$ symmetric optical channels

One of the fields in which $\mathcal{PT}$ symmetry occurs is optics; many hamiltonians are $\mathcal{PT}$ symmetric but not hermitian. The general idea we can get by treating theory and experiment as given in [26].

To start, consider

$$H = \hat{p}^2 + V_R(\hat{x}) + iV_I(\hat{x}) \tag{4.6}$$

with V_R and V_I the real resp. imaginary parts of the potential. This H is $\mathcal{PT}$ symmetric if and only if V_R, V_I satisfy

$$\begin{aligned} V_R(\hat{x}) &= V_R(-\hat{x}) \\ V_I(\hat{x}) &= -V_I(-\hat{x}) \end{aligned} \tag{4.7}$$

that is, V_R is an even and V_I an odd function of $\hat{x}$. In optics, V is usually given by the refractive index $n(x) = n_R(x) + in_I(x)$, hence we demand similar equations for n_R and n_I. The analogy with quantum mechanics is for instance shown by the equation for the electric field of an optical beam travelling paraxially;

$$i\frac{\partial E}{\partial z} + \frac{1}{2k}\frac{\partial^2 E}{\partial x^2} + k_0[n_R(x) + in_I(x)]E = 0 \tag{4.8}$$

where k_0 is the vacuum wavenumber and $k = k_0 n_0$ with n_0 the substrate index. Indeed, this is a Schrödinger type equation where z plays the role of time.

A $\mathcal{PT}$ symmetric system is obtained by coupling a waveguide channel with gain to its $\mathcal{PT}$ symmetry partner; a channel with an equal amount of loss. The experimental realization of such a setup as done in [26] is depicted in fig. 4.8. The main part is the 2 channel waveguide on which a pump laser is directed. Using an amplitude mask, one of the channels will not be optically pumped and a wave in this channel experiences a natural loss γ_{L}. The pumped channel will experience an effective gain $\gamma_{\mathrm{Geff}} = \gamma_{\mathrm{G}} - \gamma_{\mathrm{L}}$. Note that this makes the imaginary part of the potential an odd function as desired. The real part of the potential, given by the real refractive index, is obtained by appropriately doping the used substrate material and follows an even function. The resulting potential is depicted in fig. 4.9a. The coupling is achieved by placing the channels sufficiently close together. The evanescent waves of the channels may then overlap and there arises a coupling $\kappa = \pi/(2L_c)$ with L_c the coupling length. The measurement is done by sending a signal beam into one of the two channels. The resulting beam is directed to a CCD camera to measure both intensity and phase.

The corresponding modelling equations are

$$\begin{aligned} i\frac{\partial E_1}{\partial z} - i\frac{\gamma_{\mathrm{Geff}}}{2}E_1 + \kappa E_2 &= 0 \\ i\frac{\partial E_2}{\partial z} + i\frac{\gamma_{\mathrm{L}}}{2}E_2 + \kappa E_1 &= 0 \end{aligned} \tag{4.9}$$

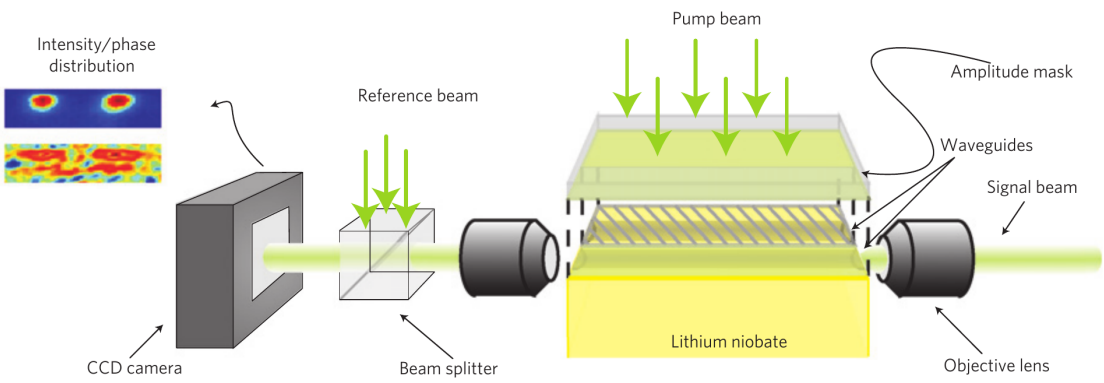

Figure 4.8: Setup used in [26]. A light beam hits a waveguide with 2 channels, one of which is pumped.

or in matrix form

$$i\frac{\partial}{\partial z}\begin{pmatrix}E_1\\E_2\end{pmatrix}=\begin{pmatrix}\frac{i}{2}\gamma_{\text{Geff}} & -\kappa\\ -\kappa & -\frac{i}{2}\gamma_{\text{L}}\end{pmatrix}\begin{pmatrix}E_1\\E_2\end{pmatrix} \tag{4.10}$$

with E_1 and E_2 the fields in the channels. Hence we are in the setting of 2×2 matrix hamiltonian systems. This system is $\mathcal{PT}$ symmetric iff $\gamma_{\text{Geff}}=\gamma_{\text{L}}=\gamma$, that is when the gain and loss are in balance. The g-function of this system is

$$g=\kappa^2-\frac{1}{16}(\gamma_{\text{Geff}}+\gamma_{\text{L}})^2$$

which in the $\mathcal{PT}$ symmetric region simplifies to

$$g=\kappa^2-\frac{1}{4}\gamma^2.$$

The phase transition occurs at $\gamma=2\kappa$. At the same point an EP is present, where EPs also exist in the non-$\mathcal{PT}$ symmetric region.

The behavior of the system can be divided into three parts, corresponding to the 2 $\mathcal{PT}$ phases and the transition:

- unbroken phase region where we are below threshold; $\gamma<2\kappa$. Indeed, $g>0$ and $\mathcal{PT}$ symmetry is exact. One can define $\sin\theta=\gamma/2\kappa$, and find supermodes (superpositions of modes of the individual channels) given by

  $$|1,2\rangle=\begin{pmatrix}1\\ \pm\exp(\pm i\theta)\end{pmatrix}$$

  with corresponding (real) eigenvalues $\pm\cos\theta$. We observe that the relative phase can vary, but the relative intensities are fixed.

- broken phase region where we are above threshold; $\gamma>2\kappa$. Here $g<0$ and $\mathcal{PT}$ symmetry is spontaneously broken. Setting $\cosh\theta=\gamma/2k$, we have

  $$|1,2\rangle=\begin{pmatrix}1\\ i\exp(\mp\theta)\end{pmatrix}$$

  with (imaginary) eigenvalues $\mp i\sinh\theta$. In this case the relative phase is fixed while the relative intensity varies with the gain.

- phase transition region $\gamma = 2\kappa$. Here $g = 0$, and one is at an EP. The modes coalesce to
$$|\mathrm{EP}\rangle = \begin{pmatrix} 1 \\ i \end{pmatrix},$$
meaning that both channels have equal intensity and have a relative phase of $\pi/2$.

One can check that the eigenmode basis $(|1\rangle, |2\rangle)$ is not orthogonal w.r.t. the standard hermitian inner product. This is illustrated in fig. 4.9b.

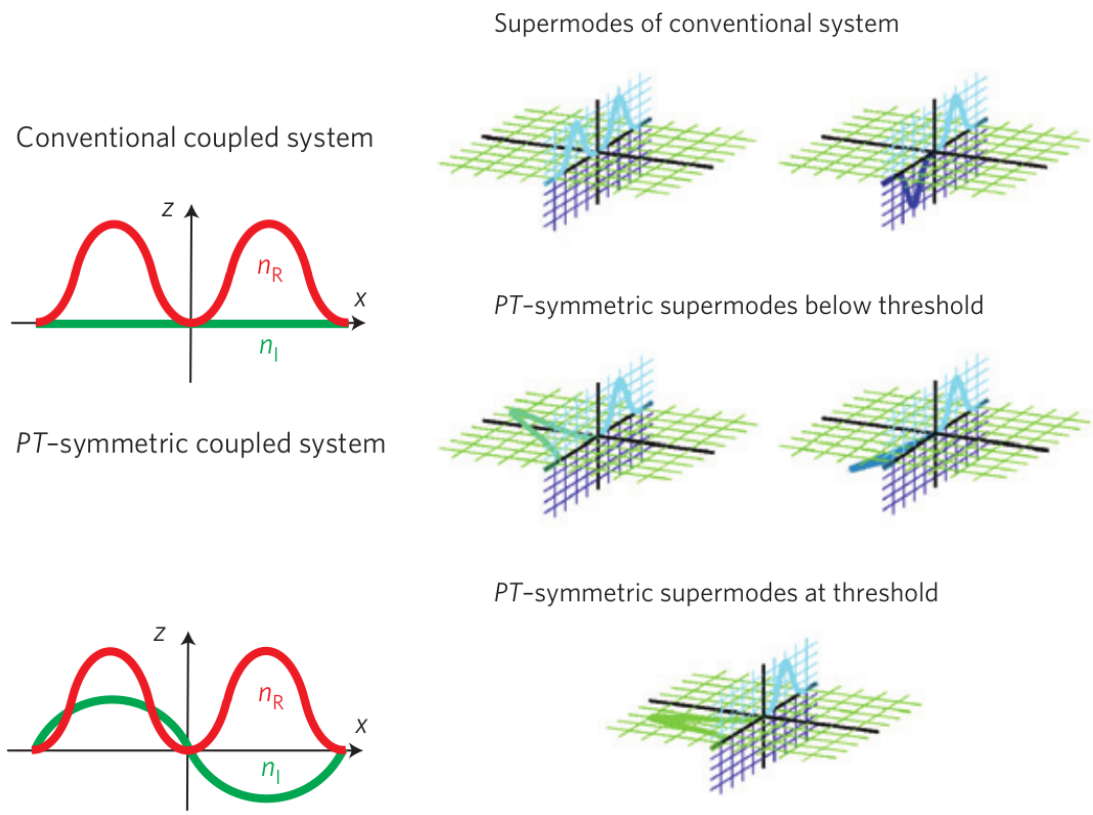

(a) Potentials in a conventional/hermitian system and a $\mathcal{PT}$ symmetric system. Here z is the propagation direction of the signal beam and x is the direction perpendicular to both z and the direction of the pump laser.

(b) Schematic overview of supermodes in different system classes. The upper row depicts even resp. odd modes in a conventional/hermitian system. Similarly the second row depicts the modes for a $\mathcal{PT}$ symmetric system with unbroken symmetry. The modes have coalesced at the threshold as seen in the final row.

Figure 4.9: Potentials and supermodes for both conventional/hermitian and $\mathcal{PT}$ symmetric systems [26].

The different forms of the eigenmodes depending on the type of hamiltonian induce different intensity patterns in the channels, as is shown in fig. 4.10. Conventional hermitian systems, i.e. systems with no gain or equivalently n_0 being identically zero, have the well-known $\sin(\omega t)$ unitary time-evolution. This case has multiple symmetries; left-right symmetric (i.e. the wave is the same when viewed from the front or from the back) and is reciprocal (if the other channel is excited the pattern is swapped accordingly). In the unbroken $\mathcal{PT}$ symmetric case, fig. 4.10 shows that one recovers a pattern much like the conventional case, and the equivalence between unbroken $\mathcal{PT}$ symmetry and hermicity from the previous section this is not surprising. Two major differences do appear, both consequences of the skew eigenmode basis: the left-right symmetry is gone and now the behavior is non-reciprocal. For the latter, observe that on the left the signal moves away

slowly, while on the right the signal is gone rather quickly. Finally, the case of broken $\mathcal{PT}$ symmetry is very different. If the gain channel is excited the beam 'stays there', whereas if the loss channel is excited everything goes to the gain channel.

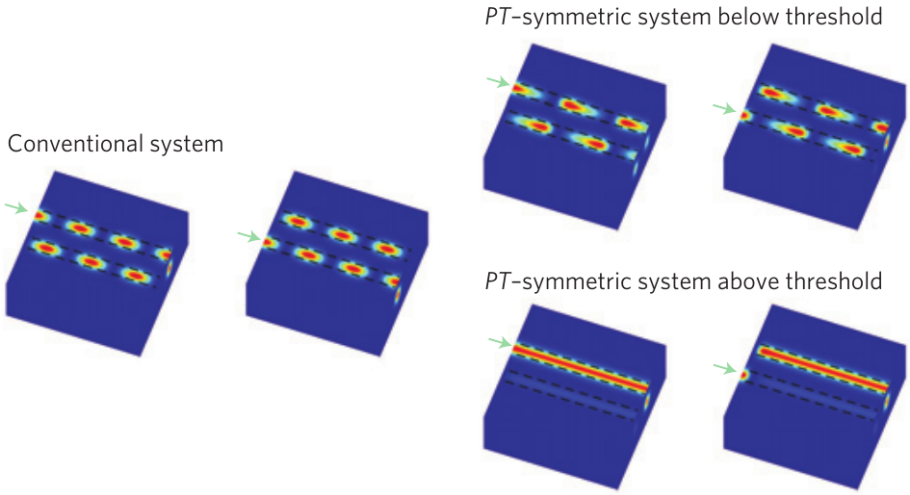

Figure 4.10: Field solutions as presented in [26], an arrow marking which channel is excited. The threshold refers to 2κ, where the gain γ is increased from left to top right to bottom right. In conventional (hermitian) systems the pattern is reciprocal, while in $\mathcal{PT}$ symmetric systems this fails irrespective of being above threshold (exact symmetry with real eigenvalues) or below (spontaneously broken symmetry with imaginary eigenvalues).

Some of the phase measurements are shown in fig. 4.11. The first two pictures show the situation without gain. In **c** we have gain below the threshold 2κ and unbroken $\mathcal{PT}$ symmetry. The phase can be any value in $[0, \pi]$, depending on $\gamma/2\kappa$. In **d**, the gain has increased just beyond the EP. Indeed, the relative phase of $\pi/2$ is observed, and this is constant when the gain is increased further. As can be seen from the eigenmodes, in this regime the gain will only effect the relative intensities between the two channels.

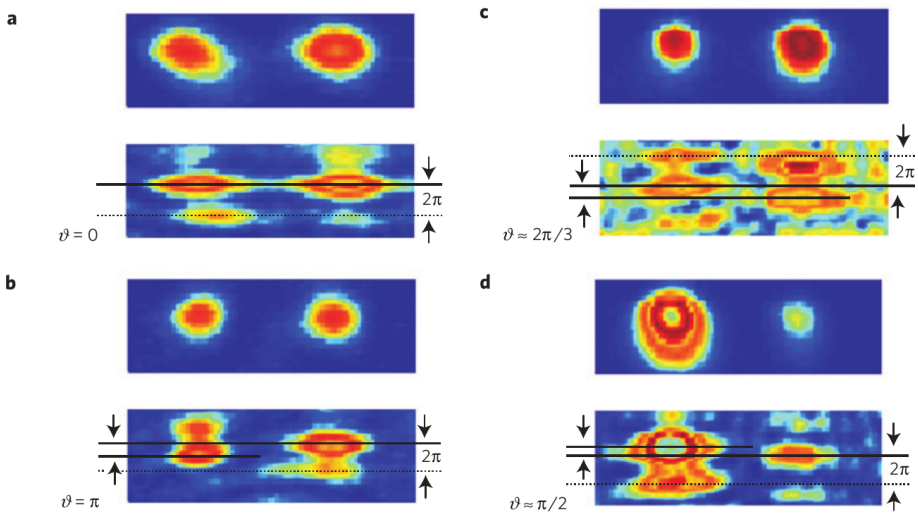

Figure 4.11: Measurements from [26], where ϑ is the phase difference between the modes and the gain is increased from **a** to **d**. Upper panels show intensity, lower panels show relative phase. Conventional states ($\gamma_G = 0$) are shown in **a** (even mode) and **b** (odd mode). $\mathcal{PT}$ symmetric states are shown on the right. The case $\gamma < 2\kappa$ (unbroken $\mathcal{PT}$ symmetry) is shown in **c** and $\gamma > 2\kappa$ (broken symmetry) is shown in **d**.

$\mathcal{PT}$ symmetric differential systems

As the above experiment already touched upon many experimental aspects of $\mathcal{PT}$, let us now look at more theoretical applications in the form of differential equations. We list a few examples from [27]. This starts with some small examples from earlier papers, including also non-linear $\mathcal{PT}$ symmetric systems. For non-linear differential systems the $\mathcal{PT}$ phase is defined to be broken if the solutions blow up or approach a limit point. In the remaining cases with oscillatory-like motion the phase is defined to be unbroken (this is discussed in more detail in [28]). The main subject of the paper concerns a predator-prey system modelling immune-response.

An elementary example of a non-linear $\mathcal{PT}$ symmetric system is a model of a self-catalyzing chemical reaction given by

$$\begin{aligned} \dot{x} &= -kxy \\ \dot{y} &= kxy. \end{aligned} \tag{4.11}$$

Defining $\mathcal{P}$ to swap $x \leftrightarrow y$ and $\mathcal{T}$ to replace $t \mapsto -t$, indeed this system is $\mathcal{PT}$ symmetric. For any $k \neq 0$ this system will not yield an equilibrium, hence the $\mathcal{PT}$ phase is always the broken one.

We now turn to the main problem treated in [27]. At the basis are the predator-prey equations as given by

$$\begin{aligned} \dot{x} &= ax - bxy \\ \dot{y} &= -ay + bxy \end{aligned} \tag{4.12}$$

which is $\mathcal{PT}$ symmetric for any chosen value of a and b. If we view x and y as complex variables, a generic solution is oscillatory, hence the system is in unbroken $\mathcal{PT}$ phase. By adding a cx^2 term to the equation for $\dot{x}$ this can be turned into an inward or outward spiral depending on the sign of c.

The next step is to couple such a system to its $\mathcal{PT}$ symmetric partner, where also the coupling obeys $\mathcal{PT}$ symmetry. The resulting system is

$$\begin{aligned} \dot{x}_1 &= x_1 - x_1 y_1 - c x_1^2 + g x_1 x_2 \\ \dot{y}_1 &= -y_1 + x_1 y_1 + f y_1 y_2 \\ \dot{x}_2 &= -x_2 + x_2 y_2 + c x_2^2 - g x_1 x_2 \\ \dot{y}_2 &= y_2 - x_2 y_2 - f y_1 y_2. \end{aligned} \tag{4.13}$$

Here $\mathcal{P}$ changes the label $1 \leftrightarrow 2$ and as usual $\mathcal{T}$ inverts time. It is reported that in unbroken symmetry regions the dynamics is either chaotic or almost periodic, depending on the initial conditions.

Such a system is then used to model a threat posed by two antigens (concentration y_1 and y_2) with corresponding antibodies (concentration x_1 resp. x_2). The second system is introduced as the $\mathcal{PT}$ symmetric partner, but it has interesting consequences; it turns out that the combined effect of the antigens could help the recovery of the patient. After some modifications in the system, the model's two (real) parameters f and g were varied and the behavior of the solutions was classified according to the disease being lethal, chronic or curable. The resulting plot is given in fig. 4.12. We see that the unbroken regime has only chronic behavior. The broken regime is split in the extreme cases; either the antigens grow out of bound or decay away.

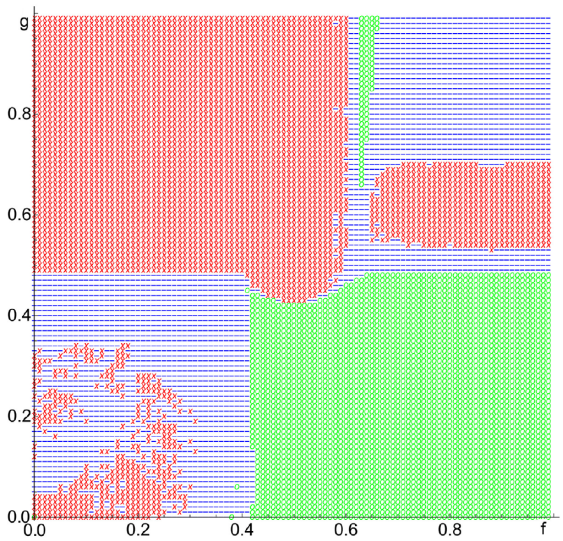

Figure 4.12: Indication of (un)broken $\mathcal{PT}$ symmetry in [27]. The blue hyphens (top right and bottom left) indicate unbroken regime; here the concentrations are oscillatory, meaning that the lethal decease is now chronic. The broken regime is divided in two parts; the red x's (mainly top left) indicate unbounded lethal solutions while the green o's (mainly bottom right) indicate decaying cured solutions.

Exploiting a genuine quantum system

Until now most $\mathcal{PT}$ experiments in literature did not use genuine quantum mechanics in their set-up; often optical techniques, microwave cavities or other systems were used (e.g. electric circuits in [29, 30]). The relevance of quantum mechanical treatment, appropriate when the system is of hamiltonian type, hinges on the formal equivalence of the modelling equations with a Schrödinger type equation. Fairly recently a real quantum experiment has been proposed in [31]. Although the $\mathcal{PT}$ symmetry is emphasized, the setup allows for more general non-hermitian systems.

The used architecture is that of circuit-QED; a superconducting circuit for which the quantum limit is appropriate. The setup is illustrated in fig. 4.13. Two qubits are individually coupled to two resonators, which in turn are coupled in the center. The cubits have tunable gap $\epsilon_j(t)$ while the superconductors have a tunable coupling $J(t)$. It is this tunability that allows one to pick certain non-hermitian (4×4) matrix hamiltonians, which for certain choices will be $\mathcal{PT}$ symmetric.

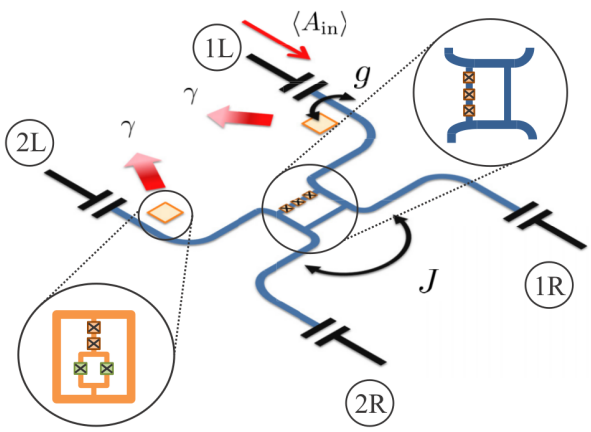

Figure 4.13: Setup as proposed in [31]. Two qubits (orange) and two resonators (blue) are coupled and are time tunable. Usually the input signal with strength $\langle A_{\text{in}} \rangle$ enters at leg 1L

The measurement then consists of measuring the transmission from one of the legs 1L, 1R, 2L, 2R to another. For instance, one can send a signal with amplitude $\langle A_{\text{in}} \rangle$ to 1L and measure at leg j, λ. This yields an average amplitude $\left\langle A_{\text{out}}^{j,\lambda} \right\rangle$ and so one finds the transmission coefficient

$$T_{1\text{L},j\lambda} = \frac{\left\langle A_{\text{out}}^{j,\lambda} \right\rangle}{\langle A_{\text{in}} \rangle}.$$

The result of a simulated measurement with $j, \lambda =$2R is shown in fig. 4.14; theoretically the plot corresponds to the real part of the eigenvalues of the system. The $\mathcal{PT}$ symmetry could be checked and exploited in this system like it was done in the previously discussed two-channel waveguide.

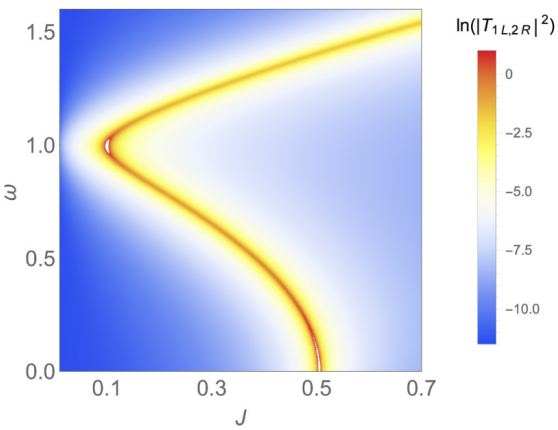

Figure 4.14: Simulated transmissions for varying input frequency ω and coupling J (also in frequency units), taken from [31]. Measuring transmissions allows to check $\mathcal{PT}$ theory in circuit-QED and so a quantum setting.

5 Three-channel waveguide system

In this section we explore a three-channel $\mathcal{PT}$ symmetry inspired waveguide system that provides an explicit setting for EP theory and could potentially be experimentally realized [32, 33]. This will motivate also later theory in section 6. However, some theory is already needed here we deal with that first. Most results of this chapter are published in [34].

The theoretical questions we need to address concern the mixing of EP permutations and the non-abelian properties that arise in this. Indeed, in case one encircles multiple EPs one has to properly compose the effects of the individual EPs. This was thought to be ambiguous [35]. One can solve this problem by considering based loops and their deformations. The proofs of mathematical statements are postponed until we look deeper into them in section 6. The theory of fundamental groups allows to generalize this technique to arbitrary degeneracy structures like exceptional lines in a three-dimensional parameter space.

We continue with a closer look a the three-channel waveguide. Concrete regions and examples can be found inside the system where one could verify the mathematical claims experimentally. We mimic this using numerical simulations and find that the result agree with the found theory.

5.1 Theoretical analysis

We start by addressing the issue of encircling multiple EPs and the induced composing of the individual effects. Let us first phrase this problem in a more precise and simple fashion. Consider two EPs encircled by two oriented loops γ_1 and γ_2, respectively, as depicted in fig. 5.1. Suppose one has measured the permutations obtained from the loops γ_1 and γ_2; which permutation should one obtain for a loop γ_3 encircling both EPs?

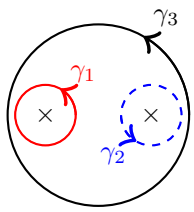

Figure 5.1: Two EPs (crosses) encircled individually by loops γ_1 and γ_2, respectively, and a loop γ_3 which encircles both EPs.

The essential insight is that one first needs to fix a common base point for the paths γ_1, γ_2 and γ_3; the permutations should be compared for the same initial system parameters. Let us denote by Δ the discriminant set of the family of operators, i.e. Δ is the set of parameters for which two or more eigenvalues coincide, and by X the complement of Δ in parameter space P. Fixing a basepoint $x_0 \in X$ we can consider the measurement paths that start and end at x_0, that is, the loops based at x_0. Let us denote by $\mathrm{Loop}(x_0)$ the set of oriented loops in X that are based at x_0 following appendix A. As each loop in $\mathrm{Loop}(x_0)$ is contained in X the operators have distinct eigenvalues at any point on such a loop. Tracing a loop $\gamma \in \mathrm{Loop}(x_0)$ induces a fixed change of eigenstates, in particular it induces a permutation p_γ of the eigenvalues. Denote by

$$\Lambda(x_0) = \{p_\gamma \mid \gamma \in \mathrm{Loop}(x_0)\} \tag{5.1}$$

the group of permutations that can be achieved in such a way. This is a subgroup of the symmetric group of the n distinct eigenvalues, and by using a labeling is isomorphic to a subgroup of S_n.

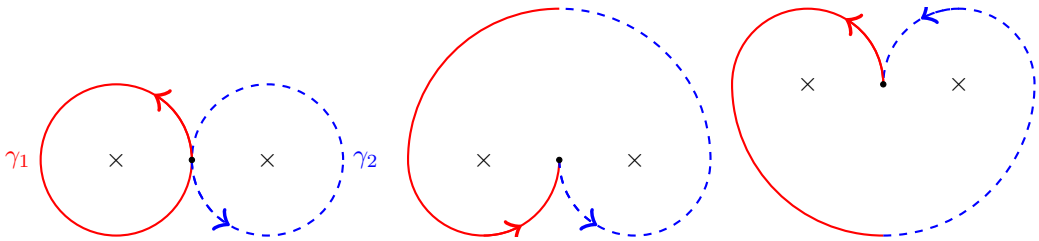

(a) Two paths around two EPs. (b) Deformed $\gamma_1\gamma_2$. (c) Deformed $\gamma_2\gamma_1$.

Figure 5.2: Example of loops based at the bold dot that enclose two EPs marked as crosses. The deformed $\gamma_1\gamma_2$ and $\gamma_2\gamma_1$ resemble each other, but are not homotopic relative to the base point.

A group like $\Lambda(x_0)$ was already mentioned in the book by Kato [1] where the term exceptional point was used for the first time, and the group was called the λ-group. The λ-group there consists of the permutations that arise from analytically continuing the eigenvalues back to some initial point. The group $\Lambda(x_0)$ is a generalization by allowing for more general adiabatic connections. The next section will investigate this, but already the connection in [8] suffices for our needs here.

The concatenation of two loops in $\mathrm{Loop}(x_0)$ defines a 'product' in $\mathrm{Loop}(x_0)$ that is in general non-abelian. By the holonomy interpretation, the assignment $\gamma \mapsto p_\gamma$ preserves this product in the sense that

$$p_{\gamma_2\gamma_1} = p_{\gamma_2} \circ p_{\gamma_1} \tag{5.2}$$

where in $\gamma_2\gamma_1$ we first track γ_1 and then γ_2.

It is at this point that the distinction between $\gamma_2\gamma_1$ and $\gamma_1\gamma_2$ becomes interesting. This is because we are mapping the loops to a permutation group that in general is non-commutative. In fact, as (based) loops the two products $\gamma_2\gamma_1$ and $\gamma_1\gamma_2$ may be different in the sense that they are not homotopic relative to the basepoint. The loops γ_1 and γ_2 both start and end at the basepoint x_0. The concatenation $\gamma_2\gamma_1$ is a loop that starts at x_0 and following γ_1 intermediately comes back to x_0, after which γ_2 is traversed which again ends at x_0. A homotopic deformation of $\gamma_2\gamma_1$ as a loop in $\mathrm{Loop}(x_0)$ is a continuous deformation of the concatenation $\gamma_2\gamma_1$ within X that keeps the starting point of γ_1 and the end point of γ_2 fixed; the intermediate visit of x_0 becomes irrelevant. This applies analogously to the product $\gamma_1\gamma_2$. In fig. 5.2 we show continuous deformations of $\gamma_1\gamma_2$ and $\gamma_2\gamma_1$. We in particular see that one cannot deform $\gamma_2\gamma_1$ to $\gamma_1\gamma_2$ within X if one needs to keep the basepoint fixed.

The continuous deformation of the based loops $\gamma \in \mathrm{Loop}(x_0)$ and their concatenation leads to the definition of the fundamental group $\pi_1(X, x_0)$ whose elements are the equivalence classes $[\gamma]$ of loops that are homotopic to a representative γ and where the group operation is defined by the product given by the concatenation of loops. The situation depicted in fig. 5.2 is then general. By the theory of fundamental groups, once fundamental paths are chosen, any loop can be written in terms of these. So far we used deformations to stress the non-commutativity of the product of two based loops. We want to come back to them later as they are also relevant for the concrete question of calculating permutations.

Let us now come back to the situation of fig. 5.1. First, we choose basepoints x_1, x_2 for the small loops γ_1 and γ_2, respectively, and x_3 for the big loop γ_3. The basepoints x_1 and x_2 are likely to be different. In this case we choose an oriented path b from x_1 to x_2 as shown in fig. 5.3a which allows us relate the based loops γ_1 and γ_2 in the sense that a loop $\gamma_2 \in \mathrm{Loop}(x_2)$ can be associated with a loop $b^{-1}\gamma_2 b \in \mathrm{Loop}(x_1)$. For convenience, we will refer to this operation as pull-back via b, and call b a bridge from x_1 to x_2.

As shown in fig. 5.3b, a bridge induces a fixed labelling of eigenvalues, and permutations

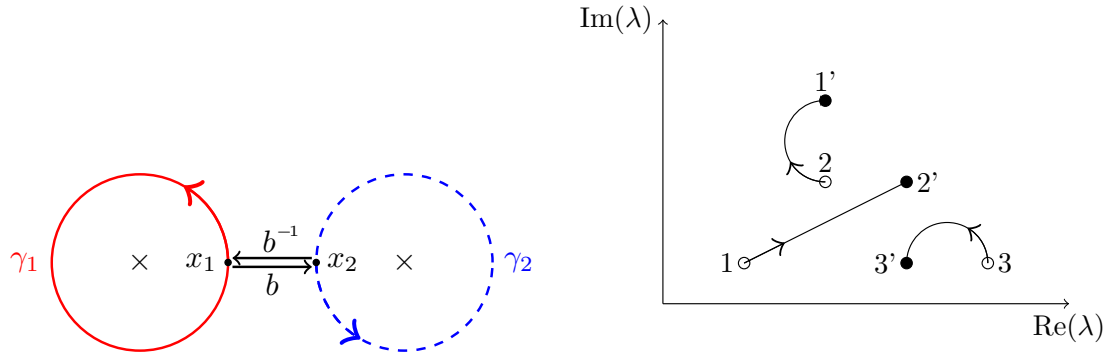

(a) Two loops with different basepoints. A bridge is needed to pull-back information from one point to the other. This requires that the bridge is traversed twice and in opposite directions.

(b) Example of eigenvalue paths induced from a bridge. Open circles mark the eigenvalues at x_1 and have unprimed labels, filled circles mark eigenvalues at x_2 and have primed labels. The bridge induces the relabelling $1 \mapsto 2'$, $2 \mapsto 1'$, $3 \mapsto 3'$.

Figure 5.3: Aspects of a connecting path or bridge, both in parameter and eigenvalue space.

must be rewritten accordingly. This means, if one wants to talk about the permutation 'first γ_1, then γ_2' one has to pick basepoints, and if these do not coincide also bridge(s). For the relabelling illustrated in fig. 5.3b, suppose, e.g., that γ_2 induces the permutation $(1'2'3')$ (where we use the cycle notation). Then pulling-back via b one obtains $1 \mapsto 2' \mapsto 3' \mapsto 3$, $2 \mapsto 1' \mapsto 2' \mapsto 1$ and $3 \mapsto 3' \mapsto 1' \mapsto 2$, that is, $b^{-1}\gamma_2 b$ induces (132).

Using a bridge from x_1 to x_3, the pull-back allows us to continue as if $x_3 = x_1$, a choice that would be convenient in experiment as well. By the previous discussion, the big loop can be decomposed into the smaller loops, and composing permutations accordingly yields a unique permutation for the big loop, given the labeling and bridges used. Observe that this technique may also be used to keep track of the occurring geometric phases. The various dependencies that occur we discuss together at the end of this subsection.

Permutations are topological

We now turn to the fact that permutations induced by loops around EPs are topological in nature, as opposed to geometric. This means that based loops that are homotopic induce the same permutation of eigenvalues. This does not assume anything on the nature of the degeneracies, i.e. whether they are EPs, DPs or yet another type. Note that this fact also allows one to pick the most convenient loop in a homotopy class, without any theoretical requirements on the quantum system. The proof is given in the next section and uses that $\Lambda(x_0)$ is a discrete group.

Lemma 5.1. If $\gamma, \tilde{\gamma} \in \mathrm{Loop}(x_0)$ are homotopic relative to x_0, then the induced permutations are equal, i.e. $p_\gamma = p_{\tilde{\gamma}}$. In other words, the assignment $\gamma \mapsto p_\gamma$ factors as

$$\begin{aligned} \mathrm{Loop}(x_0) \to\ & \pi_1(X, x_0) \to \Lambda(x_0) \\ \gamma \mapsto & [\gamma] \mapsto p_\gamma \end{aligned} \tag{5.3}$$

where each map preserves products.

Let us propose a procedure for checking the composition rule in the situation of a planar parameter space, where we consider a loop that encircles k EPs, each with winding number 1 which intuitively means that each EP is encircled exactly once. Homotopy theory allows to extend such a procedure to higher dimensional parameter spaces where

the degeneracies are of codimension 2 like the exceptional lines in the three-level system that we consider in section 5.2. A measurement could proceed according to the following steps

1. fix a loop γ encircling all EPs once, and choose a base point x_0 on this loop,
2. write $[\gamma] = [\gamma_k] \cdots [\gamma_1]$ where each $\gamma_i \in \mathrm{Loop}(x_0)$ encircles a single EP with winding number 1,
3. measure the permutations $p_i := p_{\gamma_i}$ and $p := p_\gamma$,
4. check p and $p_k \cdots p_1$ for equality.

Non-abelian behavior occurs if there are two loops γ_1, γ_2 such that $p_{\gamma_2} \circ p_{\gamma_1} \neq p_{\gamma_1} \circ p_{\gamma_2}$. As S_n is commutative for $n < 3$, a system in which this is possible should have $n \geq 3$ many levels. Note that EP3s are not required to see non-abelian behaviour. Instead it is sufficient to have a system with three levels and two EP2s with permutations (12) and (23), respectively.

Another observable property is orientation dependence, e.g. by comparing a loop encircling two EPs with a figure 8 shaped partner loop, or more precisely, compare the permutation along the loop $\gamma_2\gamma_1$ shown in fig. 5.2 with, e.g., ${\gamma_2}^{-1}\gamma_1$. As opposed to the previous construction the present one requires EPNs with $N \geq 3$. This is due to the fact that for an EP2 the permutation is always a transposition and hence equals its own inverse.

Examples

Let us determine the Λ-group for some well-known cases. Encircling a single EPN once yields an N-cycle, and one has $\Lambda(x_0) \cong \mathbb{Z}/N\mathbb{Z}$. This identification does not depend on x_0 if the parameter space is path-connected, which we assume for simplicity, but the precise eigenvalues permuted do depend on x_0. Consider now 2 EP2s, then there are a number of different possibilities depending on how the eigenvalue sheets are connected and whether the EPs are not located at the same point in parameter space, that is, if they can be circumscribed individually.

Suppose the EP2s share no sheet. Then the system must have at least 4 distinct eigenvalues, and we may take a 4-dimensional (sub)system. Fixing a basepoint and a labelling, we may assume that the EPs have permutations (12) resp. (34). If the EPs are at different locations, we can permute independently and one has $\Lambda(x_0) \cong S_2 \times S_2$. In case the EPs are on top of each other, the only non-trivial permutation is (12)(34), so $\Lambda(x_0) \cong S_2$.

Suppose the EP2s share one sheet. Then the system can be taken 3-dimensional, and the permutations as (12) and (23). These two transpositions generate S_3, and hence $\Lambda(x_0) \cong S_3$ as this is the largest group that can be obtained with a 3 dimensional system. We note that encircling both EP2s in the right order yields (12)(23) = (123), and as [35] showed, doing this 3 times yields the identity. For another loop, one may have the opposite order and measure (23)(12) = (132), again a 3-cycle. However, we stress that using the theory treated here we can calculate the outcome after encircling just once. This is crucial in showing non-abelian behavior as this manifests itself in the difference between (123) and (132), which are both 3-cycles. To conclude this case, if the EP2s would lie on top of each other the resulting structure would look like an EP3, which we treated above.

Finally, suppose the EP2s share both sheets, as happens in the standard case (e.g. [2]). Now the system can be taken 2-dimensional with both permutations equal to (12). Hence $\Lambda(x_0) \cong S_2$, similar to taking just 1 EP, and note that the EPs cannot be on top of each other without becoming equal.

We see that the Λ-group detects the differences in sheet structure. If we include more EPs or allow higher order EPNs one can reason similarly, be it with more involved permutations.

Remarks

Let us inspect how the exposition above depends on choices such as basepoints and bridges. We remark that this is similar to the discussion that two fundamental groups $\pi_1(X, x_0)$ and $\pi_1(X, x_1)$ with different base points x_0 and x_1 are isomorphic by a conjugation-like construction, the conjugacy provided by a bridge between x_0 and x_1.

Concerning the basepoint, choosing one fixes a path-connected component of X. Within this component, bridges can be used to connect different basepoints, relating Loop-spaces by conjugation (for the eigenvalues, standard bookkeeping of the labels appears). We disregard the case where X is not path-connected as it is in general not meaningful to compare levels associated with parameters in different connected components of X because of the absence of a continuous dependence of the levels on the parameters.

Given two bridges $b, \tilde{b}$ between the same basepoints, the results of pull-back of a loop may very well differ. Key is the loop $\tilde{b}^{-1}b \in \mathrm{Loop}(x_0)$, which may yield a non-trivial permutation. Indeed, b and $\tilde{b}$ may pass an EP on different sides, such that we approach the final point using different sheets, where the loop will indeed reveal this EP permutation. Again, there is uniqueness up to conjugation, as made precise in the next lemma.

Lemma 5.2. Let x_0 and x_1 be basepoints, let $b, \tilde{b}$ be bridges from x_0 to x_1. The two pull-back operations are related by conjugation with the permutation of $b^{-1}\tilde{b}$.

Proof. For $\gamma \in \mathrm{Loop}(x_1)$ arbitrary, one has $\tilde{b}^{-1}\gamma\tilde{b}$ homotopic to $(b^{-1}\tilde{b})^{-1}(b^{-1}\gamma b)(b^{-1}\tilde{b})$, where all factors are in $\mathrm{Loop}(x_0)$. The claim now follows. □

Note that conjugation in S_n leaves the cycle structure invariant, so one may think that a permutation depends only on the loop (and by the above, only the homotopy class). This holds true for the cycle structure, but one should still be careful when using concrete labeling, which varies even per basepoint.

Let us also discuss coordinate dependence. When reparametrizing parameter space, we assume that the reparametrization establishes a homeomorphism of the original parameter space. This induces a homeomorphism of the non-degeneracy space X, and so loops in one parametrization correspond to loops in the other. Also here a conjugation-like correspondence appears. It does supply another reason that deformations, even of the degeneracies themselves, do not change the physical aspects.

We emphasize that the exposition does not include any assumptions on the operators. However, it is well-known that hermitian systems do not allow for EPs. This is usually proven by the non-existence of a complete set of orthonormal eigenstates *at* an EP. Using the techniques above, we may provide a more topological proof, where we only need to look *around* the EP. More concretely, one may show non-existence of EPs by showing that $\Lambda(x_0)$ is trivial, as done in the next proposition. The premise is satisfied for any hermitian family and also includes exact $\mathcal{PT}$-symmetric systems [14].

Proposition 5.1. Let $T(x)$ be a family of $n \times n$ matrix operators. If $T(x)$ has real eigenvalues for any $x \in X$, then $\Lambda(x_0) = 0$ for all $x_0 \in X$.

Proof. Let $\gamma \in \mathrm{Loop}(x_0)$ be any loop in X, denote by $\lambda_i(t)$ the induced path of the ith eigenvalue. By assumption, each $\lambda_i(t)$ moves on the real axis, and we may label eigenvalues such that $\lambda_i(0) < \lambda_j(0)$ whenever $i < j$, where being in X allows for the strict inequalities.

Assume a non-trivial permutation is achieved, so we may consider the smallest eigenvalue (label i) that gets permuted. Observe that a bigger eigenvalue (label j) must take

its place; that is $\lambda_i(0) < \lambda_j(0)$, yet $\lambda_i(1) > \lambda_j(1)$. By the Intermediate Value Theorem, one must have $\lambda_i(t^*) = \lambda_j(t^*)$ for some $t^* \in (0,1)$. However, this implies a degeneracy which contradicts γ being in X. $\square$

In conclusion, we have found that encircling two or more EPs requires based oriented loops to answer the question of how the resulting permutation is composed from the permutations associated with the individual EPs. We also described how to relate the results for different base points. In the next subsection we will describe a very concrete example using an experimental setup that could be used to test the results.

5.2 Proposed experiment

In [26], two coupled waveguide channels are used, see also the treatment in section 4. They are subjected to laser pumping giving rise to a $\mathcal{PT}$ symmetric system in which $\mathcal{PT}$ phase transitions could be observed. We now investigate a three-channel waveguide system like in [32], see also the schematic picture in fig. 5.4. Laser pumping induces complex refractive indices, which translates to a complex potential $V_k = N_k + iP_k$ in the kth channel, where $N_k = k_0 n_k$ is the real refractive index part and $P_k = k_0\gamma_k/2$ the effective pumping part.

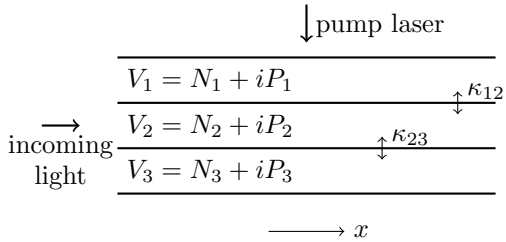

Figure 5.4: Schematic view of the experimental set-up (see the text).

By placing channels next to each other (real) couplings κ_{12}, κ_{23} are induced, which depend on the coupling lengths between the channels. The electric field amplitudes E_k change along the propagation direction x as (see [32] for experimental details)

$$i\frac{\mathrm{d}}{\mathrm{d}\,x}\begin{pmatrix}E_1\\E_2\\E_3\end{pmatrix} = \begin{pmatrix}V_1+iP_1 & -\kappa_{12} & 0\\ -\kappa_{12} & V_2+iP_2 & -\kappa_{23}\\ 0 & -\kappa_{23} & V_3+iP_3\end{pmatrix}\begin{pmatrix}E_1\\E_2\\E_3\end{pmatrix} \tag{5.4}$$

Let us redefine fields and measure relative to the central channel 2. Setting $v_k = V_k - V_2$, $p_k = P_k - P_2$, and taking equal couplings $\kappa_{12} = \kappa_{23} = \kappa$, the scaled fields $\widetilde{E}_k(x) = e^{i(V_2+iP_2)x}E_k(x)$ satisfy $i\frac{d}{dx}\tilde{\mathbf{E}} = H\,\tilde{\mathbf{E}}$, where $\tilde{\mathbf{E}} = (\widetilde{E}_1, \widetilde{E}_2, \widetilde{E}_3)^T$ and H is the operator

$$H = \begin{pmatrix}v_1+ip_1 & -\kappa & 0\\ -\kappa & 0 & -\kappa\\ 0 & -\kappa & v_3+ip_3\end{pmatrix} \tag{5.5}$$

which is similar to the idealized expression found in [33]. The electric field components hence satisfy a Schrödinger type equation with a non-hermitian operator where the role of time t is played by the spatial direction x.

We will restrict ourselves to the subspace of operators that are of the form

$$T(z,c) = \begin{pmatrix}z+2i & -\sqrt{2} & 0\\ -\sqrt{2} & 0 & -\sqrt{2}\\ 0 & -\sqrt{2} & cz-2i\end{pmatrix}, \tag{5.6}$$

where z is a complex and c a real parameter. This matches the desired family from eq. (5.5) after we identify.

$$\begin{aligned} v_1 &= \mathrm{Re}(z) \\ p_1 &= \mathrm{Im}(z) + 2 \\ v_3 &= c\mathrm{Re}(z) \\ p_3 &= c\mathrm{Im}(z) - 2 \\ \kappa &= \sqrt{2}. \end{aligned} \tag{5.7}$$

We note that c appears as the ratio of differences in refractive index;

$$c = \frac{v_3}{v_1} = \frac{n_3 - n_2}{n_1 - n_2}$$

and can thus vary of a large range, likely not excluding $c = \pm 1$. Concerning z, its real part may be limited in experiment as it needs a large difference in refractive indices. However, already interesting behaviour can be found around the $\mathrm{Re}(z) = 0$ plane. We note that $\mathrm{Im}(z)$ is bounded on one side by the loss in the channel and on the other side by maximum gain from the pump laser. The cases $c = \pm 1$ were investigated in [6], where it was shown that these are normal forms for EPs appearing in 3 dimensional systems. It was found that for $c = 1$ the system has an EP3 at $z = 0$, while for $c = -1$ the system has an EP2 at $z = 0$.

The decomposition of the parameter space

The parameter space of the system is the space $\mathbb{C} \times \mathbb{R}$ with coordinates (z, c). The EPs of the system are given by the parameters (z, c) for which the eigenvalues of $T(z, c)$ coalesce in a branch point singularity. One can find candidates for EPs by finding higher order zeros of the characteristic polynomial $p_{z,c}(\lambda) = \det(\lambda I - T(z, c))$. The parameter space thus decomposes into a degeneracy space Δ and a non-degeneracy space X. Δ is then given by the discriminant set

$$\Delta = \{(z, c) \in \mathbb{C} \times \mathbb{R} \mid \mathrm{discrim}(p_{z,c}(\lambda), \lambda) = 0\},$$

which forms lines in the three-dimensional parameter space. EPs can only be found on these lines, e.g. by finding higher order zeros of $p_{z,c}(\lambda)$ or by numerically tracking the eigenvalues along a closed loop. For the latter technique, we remark that deformation invariance of permutations allows one to check large pieces of Δ by just a single loop.

The parameterization $T(z, c)$ of the operator family is injective up to line the $z = 0$. The operator $T(0, c)$ is indeed independent of c, meaning that the entire $z = 0$ axis defines only 1 operator. This explains why the $z = 0$ line appears often in calculations. We will frequently use the characteristic polynomial of the system given by

$$p_{z,c}(x) = x^3 - (c + 1)zx^2 + [cz^2 - (1 - c)2iz]x + 2(c + 1)z. \tag{5.8}$$

Let us first identity the regions of $\mathcal{PT}$ symmetry. One can define the parity operator $\mathcal{P}$ to swap the outer channels of the waveguide, and define the time operator $\mathcal{T}$ to be complex conjugation. Checking the commutation relation one finds that the system is $\mathcal{PT}$ symmetric if and only if

$$\begin{aligned} \mathrm{Re}(z) &= c\mathrm{Re}(z) \\ \mathrm{Im}(z) + 2\gamma &= -(c\mathrm{Im}(z) - 2\gamma) \end{aligned}$$

or written differently

$$(1-c)\mathrm{Re}(z) = 0$$
$$(1+c)\mathrm{Im}(z) = 0.$$

Hence, if $|c| \neq 1$, the only solution is $z = 0$. For $c = 1$, any z real is enough, while for $c = -1$ one needs imaginary z. We conclude that the $\mathcal{PT}$ symmetric region consists of three lines, or where points are of the form $(0, a), (a, 1), (ai, -1)$ for a real. Let us investigate where the $\mathcal{PT}$ symmetry is exact/broken so that we know if, and so where, spontaneous breaking occurs.

At $z = 0$, the c-axis, the operator $T(0, c)$ is constant and given by

$$\begin{pmatrix} 2i & \sqrt{2} & 0 \\ \sqrt{2} & 0 & \sqrt{2} \\ 0 & \sqrt{2} & -2i \end{pmatrix}.$$

The characteristic polynomial reduces to $p_{0,c}(x) = x^3$, meaning we have $x = 0$ as triple zero. The eigenspace has dimension 1, and the eigenvector can be chosen as

$$\begin{pmatrix} i \\ \sqrt{2} \\ -i \end{pmatrix}.$$

We see $\mathcal{PT}v = v$, and by definition the $\mathcal{PT}$ symmetry is exact here (as we did not demand to have a complete set of eigenstates). Observe the alternating $\pi/2$ phase difference of the outer levels with respect to the central level.

For $c = 1$ and z real, the operator is

$$\begin{pmatrix} z+2i & \sqrt{2} & 0 \\ \sqrt{2} & 0 & \sqrt{2} \\ 0 & \sqrt{2} & z-2i \end{pmatrix}$$

and the characteristic polynomial reduces to $p(x) = x^3 - 2zx^2 + z^2x + 4z$. We note that $z = 0$ reduces the case to the above, so let us look at non-zero real z. The discriminant is $-z^2(432 + 16z^2)$, which does not change sign if we do not pass $z = 0$. The roots thus have the same structure everywhere; one real root and a non-trivial complex pair as one can check numerically. We conclude that the line, up to the point with $z = 0$, lies in the broken $\mathcal{PT}$ symmetry region.

For $c = -1$ and z imaginary (write $z = ai$ with $a \in \mathbb{R}$), the operator is

$$\begin{pmatrix} (a+2)i & \sqrt{2} & 0 \\ \sqrt{2} & 0 & \sqrt{2} \\ 0 & \sqrt{2} & -(a+2)i \end{pmatrix}$$

and the characteristic polynomial reduces to $p_{ai,c}(x) = x^3 + (4a + a^2)x$. The roots are thus

$$x_1 = 0, \quad x_2 = \sqrt{-a(a+4)}, \quad x_3 = -x_2.$$

So if $a \notin [-4, 0]$, the roots produce imaginary numbers, and thus the system is in broken $\mathcal{PT}$ phase. For $a \in [-4, 0]$ the symmetry is again exact; the eigenvectors can be put in the form

$$v_1 = \begin{pmatrix} i \\ (a+2)/\sqrt{2} \\ -i \end{pmatrix} \quad \text{and the conjugate ones as} \quad v_\pm = \begin{pmatrix} e^{\pm i\alpha} \\ \sqrt{2} \\ e^{\mp i\alpha} \end{pmatrix}$$

where

$$e^{i\alpha} = \frac{\sqrt{-a(a+4)} + (a+2)i}{2}$$

and α is real for $a \in [-4, 0]$. In fact, setting $u = (a+2)/2$, this interval translates into $u \in [-1, 1]$ and one has

$$\alpha = \tan^{-1}\left(\frac{u}{\sqrt{1-u^2}}\right).$$

As α is real for $a \in [-4, 0]$, one concludes exact symmetry by checking the eigenvectors directly.

To summarize, the system is $\mathcal{PT}$ symmetric on three lines in parameter space. Both phases occur, and the lay-out is as in fig. 5.5. Recall that the system has real eigenvalues at the blue parts and non-trivial complex conjugate pairs on the red.

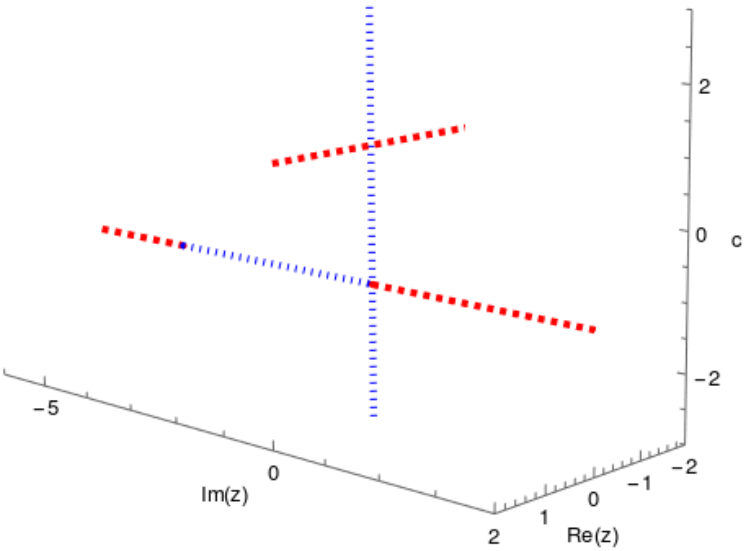

Figure 5.5: Illustrating the $\mathcal{PT}$ regions; blue dashed lines mark exact symmetry, whereas red blocks lines mark broken symmetry. The real lines extend to infinity.

Let us start the EP search with a search for EP3 candidates. To do this, one can compare coefficients; $x^3 - a_2x^2 + a_1x - a_0$ has a triple zero if and only if $a_0 = a_2^3/27$ and $a_1 = a_2^2/3$. The first equation tells us

$$-\frac{(c+1)^3z^3}{27} = 2(c+1)z$$

yielding

$$z = 0 \vee c = -1 \vee z^2 = \frac{-54}{(c+1)^2}.$$

The second condition yields

$$(c+1)^2z^2/3 = cz^2 - (1-c)2iz$$

which we can check for each separate case given by the first equation;

- if $z = 0$, any $c \in \mathbb{R}$ will do. Here the $z = 0$ line appears.
- if $c = -1$, one has $0 = -z^2 - 4iz = -z(z+4i)$, which gives $z = -4i$ as new solution.
- the other solution gives only complex c solutions which we discard.

This yields the conclusion that the EP3s are confined to the $z = 0$ axis and the point $(z, c) = (-4i, -1)$. Finding of the EP2s can be done numerically by obtaining Δ and checking its components for swaps after encirclement, i.e. using the merging path method as discussed in section 4. This method can also be used to check whether the found EP3 candidates are truly EP3s. Note that the phases of the eigenstates need not be considered.

The lines in Δ contained in the plane $\mathrm{Re}(z) = 0$ are shown in fig. 5.6. Here all points in Δ are EP2s, except for points on the c-axis which are EP3s. Two main features appear: a tangent intersection of two lines at $(0, -1)$ and a cusp at $(-4i, -1)$. Observe that both points appear in the EP3 calculations and are $\mathcal{PT}$ phase transitions.

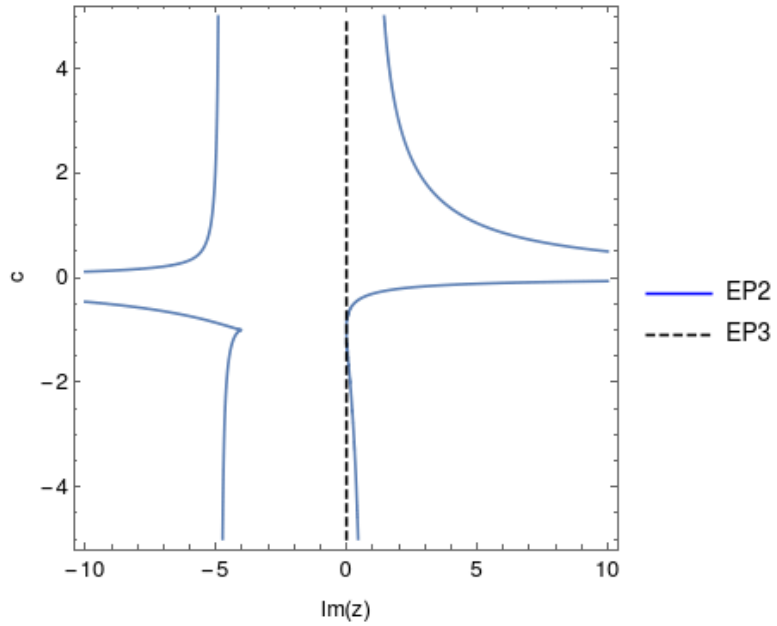

Figure 5.6: EP structure in the $\mathrm{Re}(z) = 0$ plane.

Figure 5.7 shows both degeneracies and $\mathcal{PT}$ symmetry lines in the three-dimensional (z, c)-space. All new degeneracy lines consist of EP2s as can be checked numerically. We see that the cusp in the plane in fig. 5.6 is in fact part of a more complex structure in the three-dimensional space. Here four lines move out of the plane of which two have $\mathrm{Re}(z) > 0$ and the other two have $\mathrm{Re}(z) < 0$. Also two additional lines of EPs appear top-right in the picture close to the central line that is already present in fig. 5.6.

The measurement

To measure an EP, two methods stand out; directly tracking the eigenstates and the merging path method were only the eigenvalues are tracked. Both were treated in section 4. Tracking eigenvalues only has clear experimental advantages; one does not need to track eigenstates adiabatically, dynamical phases are irrelevant, and slight deformation of the path yields the same permutation. The disadvantage is that the phase information may go unrecorded.

In this system, one could for fixed system parameters measure the profile of the wave in each waveguide. That is, one obtains (complex) $\tilde{E}_k(x)$ for $k = 1, 2, 3$. Writing these in one vector $\tilde{\mathbf{E}}(x)$, the profiles should follow

$$\tilde{\mathbf{E}}(x) = e^{-iHx}\tilde{\mathbf{E}}(x = 0) \tag{5.9}$$

in analogy to quantum mechanics. An advantage with respect to genuine quantum systems

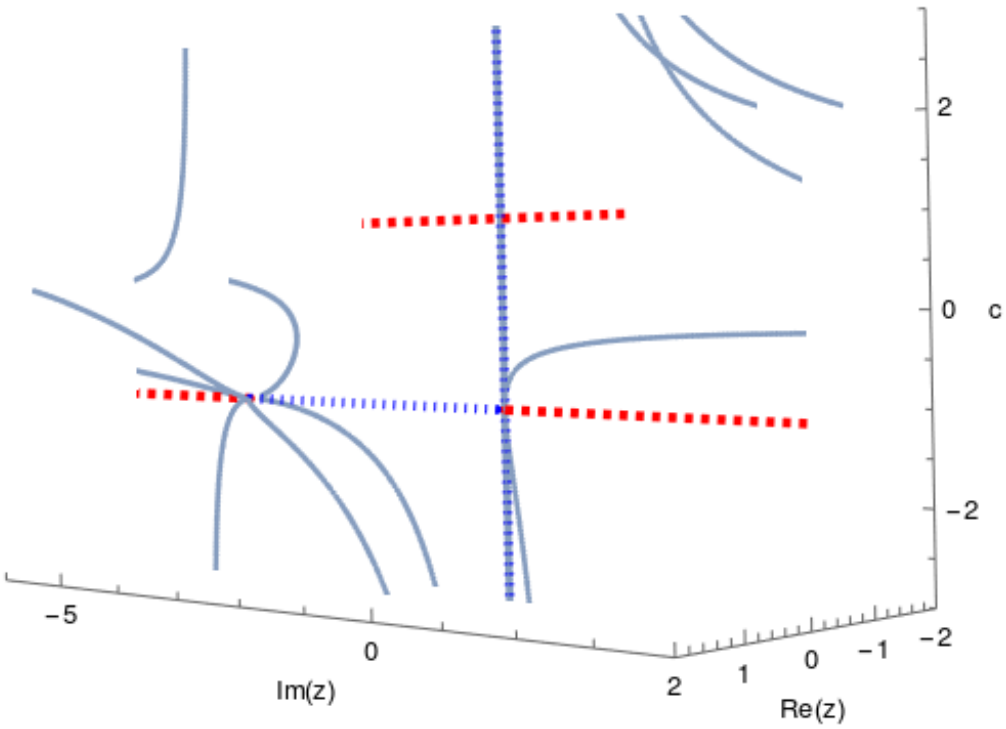

Figure 5.7: EP and $\mathcal{PT}$ structure in parameter space; the solid lines are EPs, the red blocks and blue stripes mark broken resp. exact $\mathcal{PT}$ symmetry. The picture is symmetric in $\mathrm{Re}(z) \mapsto -\mathrm{Re}(z)$.

is that now gain and loss happen in space (along the x-axis) and not in time. By deducing the eigenstates $\hat{E}_k(x)$ (again $k = 1, 2, 3$) theoretically, one can change to eigenstate basis. In this basis one must have

$$\hat{E}_k(x) = e^{-i\lambda_k x}\hat{E}_k(x = 0). \tag{5.10}$$

In this way the eigenvalue(s) can be obtained.

Examples

Let us discuss suitable paths to check the mentioned phenomena. Although other regions shown in fig. 5.7 would suffice as well, we are particularly interested in the region near the tangent intersection that involves both EP2s and EP3s. The region is shown in fig. 5.8.

Let us first deal with the problem of concatenating loops. The relevant loops are shown in fig. 5.9. We deliberately take the basepoint equal in all cases, hence the slight variation on fig. 5.1. The upper EP is an EP2, the lower an EP3, taken in the plane $c = -0.9$. We note that the situation is similar for c close to this value, although the distance between the EPs varies. Hence, one can vary c if it is desirable for experiment, and the discussion below will still hold.

In figs. 5.9a and 5.9b we show the employed fundamental paths γ_1 resp. γ_2 and find their induced permutations. As a reference, we investigate the paths $\gamma_2\gamma_1$ and $\gamma_1\gamma_2$ in resp. figs. 5.9c and 5.9d. Thus, the first four pictures show the resulting permutations of eigenvalues p_1, p_2, p_2p_1 and p_1p_2, respectively. The big loop in fig. 5.9e is base homotopic to $\gamma_2\gamma_1$, as can be seen by pulling the left side of the loop through the area between the EPs. We observe that the permutation induced by this loop indeed equals p_2p_1, and does not equal p_1p_2. This agrees with the problem discussed in fig. 5.2.

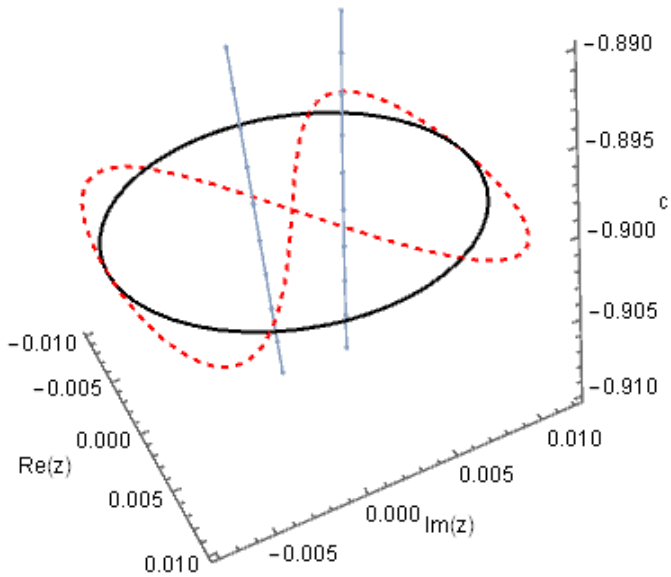

Figure 5.8: Paths near $(z, c) = (0, -1)$. The two blue lines are EP lines: the line $z = 0$ consists of EP3s and the other line consists of EP2s. The bold black circle and dashed red figure 8 are in the plane $c = -0.9$ and can be used to experimentally verify non-abelian behaviour (see the text).

Turning to the figure 8 loop in fig. 5.9f, we note that it can be deformed to ${\gamma_1}^{-1}\gamma_2$, so one would expect the permutation $(23)^{-1}(132) = (23)(132) = (12)$. Note that this is the same permutation as the one from $\gamma_1\gamma_2$ as γ_1 induces a transposition, yet $\gamma_1\gamma_2$ and ${\gamma_1}^{-1}\gamma_2$ are not homotopic. This does not contradict our claims; depending on the system, non-homotopic paths may induce the same permutation. One can still measure orientation dependence by traversing the figure 8 in opposite direction. This loop is homotopic to $({\gamma_1}^{-1}\gamma_2)^{-1} = {\gamma_2}^{-1}\gamma_1$, so yields the permutation $(132)^{-1}(23) = (123)(23) = (12)$. Hence this loop differs from $\gamma_2\gamma_1$ (which yields a (13)) only by orientation of the second part, and gives a different permutation.

One can include phases in the above theory in a natural way; the path γ_i can be associated with holonomy matrix $\tilde{p}_i$, which extends the permutation p_i. These holonomy matrices were already provided in [6] and are given for the EP2 resp. EP3 by

$$\tilde{p}_1 = \begin{pmatrix} -1 & 0 & 0 \\ 0 & 0 & 1 \\ 0 & 1 & 0 \end{pmatrix}, \quad \tilde{p}_2 = \begin{pmatrix} 0 & 1 & 0 \\ 0 & 0 & 1 \\ 1 & 0 & 0 \end{pmatrix}.$$

As the permutations induced by these matrices do not commute, the matrices themselves do not commute. Indeed, a direct check reveals

$$\tilde{p}_2\tilde{p}_1 = \begin{pmatrix} 0 & 0 & 1 \\ 0 & 1 & 0 \\ -1 & 0 & 0 \end{pmatrix}$$

$$\tilde{p}_1\tilde{p}_2 = \begin{pmatrix} 0 & -1 & 0 \\ 1 & 0 & 0 \\ 0 & 0 & 1 \end{pmatrix}$$

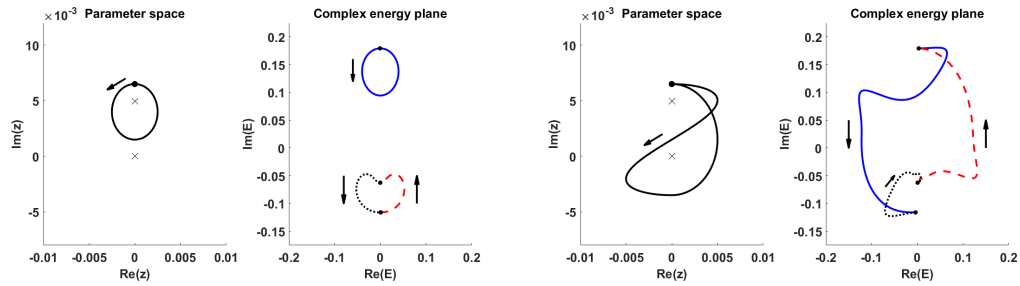

(a) Permutation (23).

(b) Permutation (132).

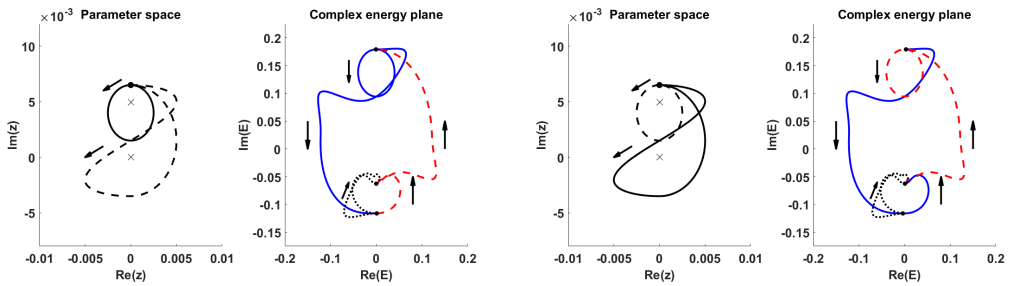

(c) Permutation (13) = (132)(23).

(d) Permutation (12) = (23)(132).

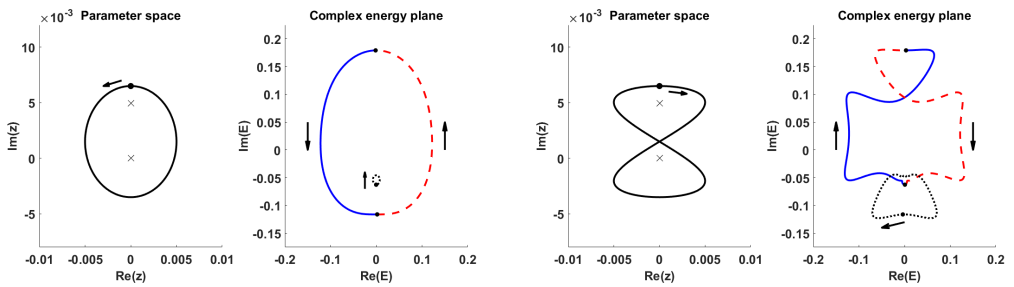

(e) Permutation (13).

(f) Permutation (12).

Figure 5.9: Loops in the plane plane $c = -0.9$ of the parameter space (left panels). All loops have the same basepoint, marked by a circle. The solid part of the loop is always traversed first, so before the dashed part of the loop. The orientations of the loops are indicated by arrows. The EPs are marked by crosses, where the upper one is an EP2 and the lower one is an EP3. The complex energy planes (right panels) show the resulting paths of the three eigenvalues, each drawn with its own color and style. Labelling eigenvalues top to bottom, we can read off the induced permutation given in the individual captions.

which projected to permutation yields the observed compositions

$$p_2 p_1 = (132)(23) = (13)$$
$$p_1 p_2 = (23)(132) = (12).$$

Note that the permutations (132) and (12) generate S_3, hence $\Lambda(x_0) \cong S_3$ for any non-degeneracy x_0.

The holonomy matrices allow to calculate the holonomy group at a point, in other words the group of adiabatic changes to the eigenstates of $T(x_0)$ with $x_0 \in X$. This group we call $\mathrm{Adia}(x_0)$ in the next section where we investigate its properties in greater detail. Assuming that no extra geometric phases occur, all phases are given by the minus signs in the products of $\tilde{p}_1$ and $\tilde{p}_2$. One can check that all diagonal matrices with any order of ± 1 can be achieved. Indeed, taking squares of the products above yields

$$(\tilde{p}_2\tilde{p}_1)^2 = \begin{pmatrix} -1 & 0 & 0 \\ 0 & 1 & 0 \\ 0 & 0 & -1 \end{pmatrix}$$
$$(\tilde{p}_1\tilde{p}_2)^2 = \begin{pmatrix} -1 & 0 & 0 \\ 0 & -1 & 0 \\ 0 & 0 & 1 \end{pmatrix}$$

and in addition

$$\tilde{p}_1(\tilde{p}_2\tilde{p}_1)^2 = \begin{pmatrix} 1 & 0 & 0 \\ 0 & -1 & 0 \\ 0 & 0 & 1 \end{pmatrix}.$$

With these matrices any order of $+1$ and -1 on the diagonal can be achieved. Hence the holonomy group $\mathrm{Adia}(x_0)$ is faithfully represented by generalized permutations matrices with entries in $\{\pm 1\}$, see also appendix B. It follows that $\mathrm{Adia}(x_0) \cong \{\pm 1\} \wr S_3$, where we use the so-called wreath product as explained in the same appendix. One can show that this is the full or achiral octahedral group, i.e. the symmetry group of the octahedron allowing reflections. As can be deduced from the matrices, it has a presentation given by $\langle a, b | a^3 = b^2 = (ab)^4 = e \rangle$, and is isomorphic to $S_4 \times S_2$. In particular, we see that any combination of permutation and phase changes (allowing only ± 1) can be achieved by traversing an appropriate based loop.

The degree of an exceptional point in systems with more than two parameters

Taking a closer look at the tangent intersection, one may ask the question what its degree should be. As reported in [6], the tangent intersection may behave as an EP2. This means that traversing a circle in the $c = -1$ plane which encircles this EP (and only this EP) yields the standard EP2 signature of swapping 2 eigenstates, as shown in fig. 5.10a, and as expected resembles the result of fig. 5.9e (using the obvious relabeling). However, the four lines arrive in a topological cross, and one may take a circle that goes through the other two quadrants. In this case, one can take a plane given by $\mathrm{Im}(z) = \epsilon i$ with $\epsilon > 0$ small, and take a large circle. Interestingly, this yields the standard EP3 signature, as seen in fig. 5.10b.

One can now do a similar construction with the point at $(-4i, -1)$ and conclude that its degree depends on the plane. In a general parameter space of dimension $d > 2$, any point where at least 3 EP lines meet has a variable degree (note that the degree of an EP is unambiguous on the lines).

Again fundamental groups provide an explanation. In case of a planar parameter space with an isolated EP, the fundamental group is $\mathbb{Z}$ and one has a map $\mathbb{Z} \to \Lambda(x_0)$. This has kernel $N\mathbb{Z}$, and N is the degree of the EP. Now, imagine 2 distinct EP structures/lines,

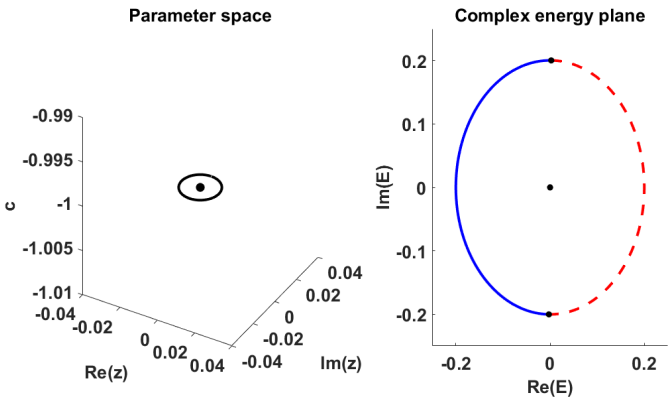

(a) The tangent intersection as EP2.

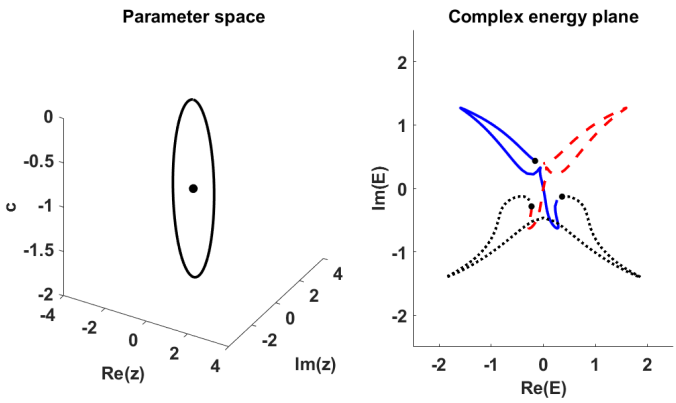

(b) The tangent intersection as EP3.

Figure 5.10: The tangent intersection as EPs of different orders.

as we want an intersection point necessarily for $d \geq 3$. The fundamental group is then the free product $\mathbb{Z} * \mathbb{Z}$, i.e. generated by 2 fundamental paths γ_1 and γ_2. Hence each γ_i induces a map $\mathbb{Z} \to \Lambda(x_0)$, with kernel $N_1\mathbb{Z}$ resp. $N_2\mathbb{Z}$. In case $N_1 \neq N_2$ clearly an issue arises, but even if $N_1 = N_2$ we see that degree should be associated to a fundamental path, or equivalently some surface. At the intersection point there is simply no canonical choice.

Summary

We showed how one can compose the effects obtained from encircling multiple EPs, which in fact works for an arbitrary degeneracy structure. The problem of finding the correct calculation can be solved by using the theory of fundamental groups, which requires based oriented loops. A relevant result here is that permutations associated to the loops are of topological as opposed to geometric nature, hence deformation can be used for convenience in both theory and experiment.

Applications of these insights were explored in a waveguide system, of which we investigated the parameter space and identified a region where all tests could be performed. The presence of both EP2s and EP3s allows one to demonstrate the non-abelian nature of systems with multiple EPs by experimentally tracking the eigenvalues.

6 Adiabatic geometry

In this section we will investigate the geometry behind the adiabatic approximation in finite-dimensional quantum state spaces. We will first trace the steps necessary to arrive at the dynamics induced by adiabicity. The dynamics can be written as a parallel transport equation, and we continue with investigation of the associated connection. This brings us to a comparison of different principal fiber bundle (PFB) constructions which support the connection depending on the physical setting. None of the found PFBs will support swaps of eigenstates in a natural way. Given our interest in EP theory, this is a crucial requirement for a suitable framework. We thus continue with another PFB that does allow for the swaps in a canonical way. After formulating this PFB, we turn to the connection and its holonomy. The adiabatic approximation will allow us to define special groups, hence the title 'adiabatic geometry'. We show how these groups can be used to summarize possible adiabatic evolutions and their use in the classification of degeneracies. We finish with a new EP definition based on this theory.

6.1 Adiabatic dynamics in non-degenerate systems

In this section we trace the steps starting from the adiabatic approximation and leading towards a parallel transport equation. We do not assume any property of the time-dependent hamiltonian $H(t)$, except finite-dimensionality, unless this is explicitly stated.

To start, let us phrase the adiabatic approximation in an exact way.

Definition 6.1 (Adiabatic approximation)**.** If a quantum system $H(t)$ starts in an eigenstate of $H(t_0)$, it will be in an instantaneous eigenstate of $H(t)$ at each point in time.

To extract the time-evolution or dynamics induced by this approximation, we want to apply the general method of expanding in eigenstate basis. It is at this point that we need to make further assumptions; a priori $H(t)$ may be any matrix, and its set $\{|\psi_i(t)\rangle\}$ of eigenvectors need not form a basis of the state space for arbitrary t. If $H(t)$ is required to be self-adjoint, then it is normal and so has a basis of eigenvectors, also known as eigenframe (cf. definition C.2). We saw that EPs are not compatible with this assumption, even if we require this only *around* but not *at* the EP. Indeed, around the EP the $\mathrm{Im}(E)$ sheet structure then collapses to constant 0, and the sheets can not be connected ('form a staircase').

Instead we require $H(t)$ to be non-degenerate for all t, a natural assumption as we will see at various points in the argument. Already here, it implies by theorem C.1 that we have an eigenframe at each point in time. Looking directly at the adiabatic approximation, we see that non-degenerateness allows a different phrasing: *eigenstates do not mix in time*. The reason is that now no superposition of linearly independent eigenvectors is an eigenstate. Indeed, if $H(t_1)$ has eigenstates $|\psi_1\rangle$ and $|\psi_2\rangle$ with associated energies E_1 resp. E_2 with $E_1 \neq E_2$, then

$$a|\psi_1\rangle + b|\psi_2\rangle$$

is not an $H(t_1)$ eigenstate for any $a, b \in \mathbb{C}$. Hence the eigenstates are well separated by non-degenerateness.

Theorem C.1 also implies the existence of dual eigencoframes; a basis of the dual space consisting of left-eigenvectors of $H(t)$, which is the dual basis of the $|\psi_k\rangle$ cf. lemma C.2. These elements we will denote by $\langle\chi_l|$ and satisfy

$$\langle\chi_l|H = E_l\langle\chi_l|$$
$$\langle\chi_l|\psi_k\rangle = \delta_{lk}.$$

The use of bra-ket notation is to notationally mimic usual identities; note that no inner product is used. The $\langle\chi_l|$ should be thought of as functionals that can act on vectors like

$|\psi_k\rangle$ by the canonical pairing between a vector space and its dual. We see that this pairing replaces the inner product, but as the pairing is bilinear instead of sesquilinear it is not an inner product itself.

Let us now do the computation (compare [36]) including the non-degenerateness assumption. We can thus write a general state $|\Psi(t)\rangle$ as a linear combination of the eigenstates;

$$|\Psi(t)\rangle = \sum_{k=1}^{n} e^{i\theta_k(t)} c_k(t)|\psi_k(t)\rangle$$

with $\theta_k(t) = -\frac{1}{\hbar}\int_0^t E_k(t')\,\mathrm{d}\,t'$ the dynamical phase. Substitution in the time-dependent Schrödinger equation gives

$$i\hbar \sum_{k=1}^{n} e^{i\theta_k}\left(\dot{c}_k|\psi_k\rangle + c_k|\dot{\psi}_k\rangle + i\dot{\theta}_k c_k|\psi_k\rangle\right) = \sum_{k=1}^{n} e^{i\theta_k} c_k(H|\psi_k\rangle).$$

The $\dot{\theta}_k$ and $H|\psi_k\rangle$ terms cancel, and so one has

$$\sum_{k=1}^{n} e^{i\theta_k}\dot{c}_k|\psi_k\rangle = -\sum_{k=1}^{n} e^{i\theta_k} c_k|\dot{\psi}_k\rangle.$$

At this point we want to project to single coefficient on the lefthandside, and this can be done using the corresponding dual covector $\langle\chi_l|$. This is instead of a bra '$\langle\psi_l|$'; the concept of bra is not defined in our situation as we do not have an inner product. One nevertheless obtains the exact result

$$\dot{c}_l = -\sum_{k=1}^{n} e^{i(\theta_k-\theta_l)} c_k\langle\chi_l|\dot{\psi}_k\rangle. \tag{6.1}$$

We now want to rewrite the off-diagonal part, i.e. the terms that contain c_k with $k \neq l$. To this end, we differentiate $H(t)|\psi_k(t)\rangle = E_k(t)|\psi_k(t)\rangle$ with respect to t and obtain

$$\dot{H}|\psi_k\rangle + H|\dot{\psi}_k\rangle = \dot{E}_k|\psi_k\rangle + E_k|\dot{\psi}_k\rangle.$$

Projecting out with $\langle\chi_l|$ produces

$$\langle\chi_l|\dot{H}|\psi_k\rangle + \langle\chi_l|H|\dot{\psi}_k\rangle = \dot{E}_k\langle\chi_l|\psi_k\rangle + E_k\langle\chi_l|\dot{\psi}_k\rangle$$

so in case $l \neq k$ this produces by the orthonormality relations

$$\langle\chi_l|\dot{H}|\psi_k\rangle + E_l\langle\chi_l|\dot{\psi}_k\rangle = E_k\langle\chi_l|\dot{\psi}_k\rangle$$

and by the non-degeneracy assumption one may conclude

$$\langle\chi_l|\dot{\psi}_k\rangle = \frac{\langle\chi_l|\dot{H}|\psi_k\rangle}{E_k - E_l}.$$

Hence one obtains without any approximation, but with non-degeneracy assumption;

$$\dot{c}_k = -\langle\chi_k|\dot{\psi}_k\rangle c_k - \sum_{l\neq k}^{n} e^{i(\theta_k-\theta_l)} c_l \frac{\langle\chi_l|\dot{H}|\psi_k\rangle}{E_k - E_l}. \tag{6.2}$$

The righthandside consists now of two terms; the diagonal resp. off-diagonal contribution to the dynamics. In other words, after writing the above system in matrix-vector notation the first term will appear exclusively at the diagonal while the second appears exclusively off-diagonal.

At this step, the implementation of the adiabatic approximation can be seen clearly. As already argued, the approximation is equivalent to the non-mixing of eigenstates. In eq. (6.2), this amounts to imposing a diagonal evolution. Hence the off-diagonal terms need to be set to 0. One observes that the discarded terms are $O(\dot{H})$, so discarding these is also known as the 'infinitely slow limit'[3]. We conclude that the adiabatic dynamics is given by

$$\boxed{\dot{c}_k = -\langle \chi_k | \dot{\psi}_k \rangle c_k} \tag{6.3}$$

which agrees with the usual formula for hermitian systems. Indeed, then the dual left-eigenvector $\langle \chi_l |$ is given by the bra of $|\psi_l\rangle$, assuming $|\psi_l\rangle$ is normalized.

Let us now inspect the solutions of eq. (6.3). A local solution is found by exponentiation and reads

$$c_k(t) = c_k(0) \exp\left(- \int_0^t \langle \chi_k(t') | \dot{\psi}_k(t') \rangle \, \mathrm{d}\, t' \right) = c_k(0) \exp(i\gamma_k(t)) \tag{6.4}$$

where one recognizes the generalized geometric phase (after the original geometric phase as found in [38]) defined as

$$\gamma_k = i \int_0^t \langle \chi_k(t') | \dot{\psi}_k(t') \rangle \, \mathrm{d}\, t'. \tag{6.5}$$

An important question concerning the dynamics is whether or not the geometric phase is real, that is if the exponent yields a U(1) phase factor. In the hermitian case, so after agreeing on some inner product, one can show that the geometric phase is real. The argument is given together with the below lemma. We see that the conjugate symmetry of the inner product is used, so this result is quite specific for the hermitian case.

Lemma 6.1. If $H(t)$ is hermitian for all t, then the geometric phases are real and given by

$$\gamma_k = i \int_0^t \langle \psi_k(t') | \dot{\psi}_k(t') \rangle \, \mathrm{d}\, t'.$$

Proof. In the hermitian case indeed one can take $\langle \chi_l | = \langle \psi_l |$ where the latter really uses the inner product and we assume all states are normalized. That is, one has $\langle \psi_k | \psi_k \rangle = 1$ at all times, so differentiating with respect to t gives

$$\langle \dot{\psi}_k | \psi_k \rangle + \langle \psi_k | \dot{\psi}_k \rangle = 0.$$

However, by conjugate symmetry of the inner product this reads

$$2\mathrm{Re}\left(\langle \psi_k | \dot{\psi}_k \rangle \right) = 0.$$

Hence the integrand is purely imaginary, and the lemma follows.

□

In a non-hermitian setting the above need not be true, as an explicit example in [36] shows. The geometric phase may contain an imaginary contribution, which means that the solution does not obey unitarity. This comes on top of the dynamical phase; as it is an integral over complex energies it is in general complex. As in [36], dynamical phase directly takes the decay rate of an eigenstate into account, and the geometric phase may be viewed as a correction.

[3] It may seem as if the remaining terms must then be neglected as well, but this is not the case as shown in [37].

The adiabatic dynamics can also yield a swap of the eigenstates, in addition to the complex scaling from the geometric phase. The key observation is that the exponent solution is local. One is not able to turn this into a global solution if the eigenvectors are multi-valued and different patches are needed. For example, if the eigenvectors follow complex root branch structure one can not preserve the labelling after walking around the branch point. In this case one needs to stitch different local solutions together, where this stitching may create a swap in the process.

It follows that the natural setting to consider the dynamics is given by a connection whose parallel transport gives eq. (6.3). Writing this equation as

$$\dot{c}_k + \langle \chi_k | \dot{\psi}_k \rangle c_k = 0 \tag{6.6}$$

shows that the equation is indeed of parallel transport form. The local connection matrix is given by

$$\omega = \begin{pmatrix} \langle \chi_1 | \mathrm{d} \, | \psi_1 \rangle & & & \\ & \langle \chi_2 | \mathrm{d} \, | \psi_2 \rangle & & \\ & & \ddots & \\ & & & \langle \chi_n | \mathrm{d} \, | \psi_n \rangle \end{pmatrix} \tag{6.7}$$

where the diagonal shape reflects the non-mixing of eigenstates.

This is the most general form of adiabatic parallel transport. In the next subsection we will investigate implementations of this theory in various settings with the associated PFBs.

6.2 Review of adiabatic connections

In this subsection we go over three different versions of connections inspired by the adiabatic approximation. That is, the adiabatic change of eigenstates is viewed as the holonomy given by a certain connection on a principal fiber bundle (PFB), see also appendix A. We will see different structure groups appearing depending on the setting in which the theory can be applied.

Although EPs do not appear in hermitian systems, we do want to consider such systems as well to obtain a broad picture. Some constructions only work in such a setting, and these are relevant to our discussion. When evaluating these, the following result will play a key role and so we state it here already (similar to a result in [34]).

Proposition 6.1. Let $H(x)$ be an operator family, depending smoothly on $x \in P$ where P denotes the parameter manifold. If $H(x)$ has real eigenvalues for every $x \in P$, then the eigenvalues and the eigenvectors are single-valued functions on the non-degeneracy space $X \subset P$.

Proof. It suffices to treat the eigenvalues as we work on X. Assuming they are multi-valued, there is a loop γ in P such that the eigenvalues are swapped. Indeed, for otherwise one has well-defined separated sheets and the eigenvalues are single-valued. Let us consider the paths of the eigenvalues. As all eigenvalues are real and there are finitely many of them, we can talk about the smallest permuted eigenvalue, call it λ_i. Thus, there is an eigenvalue $\lambda_j(0) > \lambda_i(0)$ that takes the place of $\lambda_i(0)$, that is $\lambda_j(1) = \lambda_i(0) < \lambda_i(1)$. By the Intermediate Value Theorem, we must have a crossing of λ_i and λ_j, which contradicts working in X. Hence every swap is trivial (the result in [34]), and the claim follows. □

The Berry-Simon connection

The first variant that appeared in literature is the connection now known as the Berry-Simon connection [39], introduced a little while after Berry's paper [38] on the geometric phase. It applies to hermitian systems, and is usually denoted by

$$A_k = i\langle\psi_k|d|\psi_k\rangle. \tag{6.8}$$

This expression is usually not used in matrix form and used to calculate the parallel transport of one selected eigenstate. The extra factor of i comes from the convention that A_k appears in an exponential factor. Indeed, using A_k one can rewrite the local solution in eq. (6.4) as

$$\psi_k(T) = \exp\left(i \oint_C A_k\right) \psi_k(0) \tag{6.9}$$

with T the return time and C the traversed curve in parameter space. In the usual convention one obtains the connection matrix as before, but without the factor i and with the usual bra-ket notation. As hermitian systems have real eigenvalues, by proposition 6.1 the eigenstates are single-valued meaning that the local solution is also global. Lemma 6.1 says that the geometric phase is real, hence the holonomy restrict to a U(1) action. Indeed, the exponent will be a pure phase, without further restrictions if no further assumptions are made.

The corresponding bundle is a hermitian line bundle. Explicitly, the setting is as follows. Let V be a finite-dimensional complex inner-product space (hence a finite-dimensional Hilbert space), let $T(x)$ be a family of hermitian operators acting on V where x may be taken from some parameter space P which is a smooth manifold. In [39], one considers a single fixed eigenvalue $\lambda_k(x)$, for which one assumes that the operators $T(x)$ all have an isolated non-degenerate spectrum. So, let us restrict P to the set of non-degeneracies X of the operator family $T(x)$. Then form the set

$$B_k = \{(x, v) \in X \times V \mid T(x)v = \lambda_k(x)v\} \tag{6.10}$$

of based eigenstates. One has a natural manifold structure on B_k, and a natural projection $\pi_k \colon B_k \to X$ given by $(x, v) \mapsto x$. By non-degeneracy, each fiber of π is in bijection with $\mathbb{C}^\times$. Equation (6.8) defines a connection on this PFB.

However, the group $\mathbb{C}^\times$ is much bigger than the biggest possible holonomy group U(1). To solve this, we remember that V is equipped with an inner product, and so one may shrink B_k down to normalized states and obtain

$$B'_k = \{(x, v) \in X \times V \mid T(x)v = \lambda_k(x)v, \|v\| = 1\} \tag{6.11}$$

with natural projection $\pi'_k = \pi_k|_{B'_k}$. Each fiber of π' is bijective to U(1). It follows that B'_k is the more natural candidate as the bundle corresponding to the Berry-Simon connection.

One may ask if it makes sense to consider all eigenvalues/eigenstates in one go. More precisely, what if we define a set B of elements (x, v) where v may be any eigenvector of $T(x)$? Looking at eq. (6.9), it follows that the holonomy group will be a subgroup of $U(1)^n$, meaning that the eigenstates do not feel each other. Hence this connection does not prompt us to consider all eigenstates at once. On the contrary, it hints at considering one eigenstate at a time.

Let D be a surface in parameter space such that $\partial D = C$, the traversed curve, one can rewrite eq. (6.9) as

$$\psi_k(T) = \exp\left(\int_D \mathrm{d}\, A_k\right) \psi_k(0). \tag{6.12}$$

This is related to the curvature of the connection defined (for the kth eigenstate) as

$$F_k = \mathrm{d}\, A_k. \tag{6.13}$$

Indeed, as U(1) is abelian no extra wedge term contributes to the curvature. We do note that in general the two-form that gives the phase is $\mathrm{d}\,\omega$, so that the curvature defined as $\mathrm{d}\,\omega + \omega \wedge \omega$ may be different.

The geometric phase as above turned out to pop up in various systems, also non-adiabatic ones for which physically it is not immediate clear why this is. The Aharonov-Bohm effect is a well-known example of a non-adiabatic setting for which the geometric phase calculation still works. An extension of the theory suitable for such cases is treated next.

Aharonov-Anandan connection

We want to discuss a generalization of the Berry connection known as the Aharonov-Anandan connection [40]. It is formulated in a hermitian setting, but its generality within this setting is striking. One can apply this formalism for any cyclic state, that is a state which returns to the same ray after some time. To formalize this, let us denote the state space by $\mathcal{P}$ (where we wish to exclude the 0 vector), and the projective state space by $\widehat{\mathcal{P}}$ whose elements we write as projection operators. So, a state $|\psi(t)\rangle$ moving in $\mathcal{P}$ is cyclic with period T if and only if

$$|\psi(T)\rangle = e^{i\phi}|\psi(0)\rangle \tag{6.14}$$

with ϕ real. Physical appearances of cyclic states are abundant, and the paper lists the three main classes. The first is the genuine cyclic state, the second is an adiabatic system by taking the adiabatic limit, and the third is a 'pseudo-cyclic case'. An example for the latter is a wave that is split and later recombined; although physically the system does not return, it may mathematically be treated a such.

The derivation of a generalized phase is done as follows. Given a cyclic state as in eq. (6.14), define

$$|\psi'(t)\rangle = e^{-if(t)}|\psi(t)\rangle$$

where f is any differentiable function such that $f(T) - f(0) = \phi$. This enables us to write

$$|\psi'(T)\rangle = |\psi'(0)\rangle.$$

Furthermore, using the TDSE one finds for f the equation

$$-\dot{f} = \langle\psi|H|\psi\rangle - i\langle\psi'|\dot{\psi}'\rangle. \tag{6.15}$$

The first term on the righthandside is the dynamical part, and one defines a new phase β where this is taken out, viz.

$$\beta := \phi + \int_0^T \langle\psi|H|\psi\rangle \,\mathrm{d}\,t. \tag{6.16}$$

One can deduce an alternative writing, almost identical to the geometric phase γ, as

$$\beta = \int_0^T \dot{f} + \langle\psi|H|\psi\rangle \,\mathrm{d}\,t = i\int_0^T \langle\psi'|\dot{\psi}'\rangle \,\mathrm{d}\,t. \tag{6.17}$$

One may check that this expression is independent of ϕ and the choices of f and the parameterization of the curve in $\widehat{\mathcal{P}}$. It is true that β does not depend on the used hamiltonian H. Hence β depends only on the traversed locus in $\widehat{\mathcal{P}}$.

Let us phrase this in a bundle framework. For this we need the projection $\pi\colon \mathcal{P} \to \widehat{\mathcal{P}}$ from state space to projective ray space. From eq. (6.14), we already see that an evolving state $|\psi(t)\rangle$ in $\mathcal{P}$ is cyclic if and only if its projection in $\widehat{\mathcal{P}}$ is a closed loop. Explicitly, using hermicity one can define a state $|\psi(t)\rangle$ to be cyclic with period T if and only if

$$|\psi(T)\rangle\langle\psi(T)| = |\psi(0)\rangle\langle\psi(0)|. \tag{6.18}$$

We note that one really needs the inner product on $\mathcal{P}$ to define this. The bundle defined by π has structure group $\mathbb{C}^\times$ by definition of projective space (we excluded the zero vector

in $\mathcal{P}$). Again, because one has an inner product available it is natural to work with $\mathcal{P}_1 = \{\psi \in \mathcal{P} \mid \|\psi\| = 1\}$ and the restricted bundle $\pi_1 \colon \mathcal{P}_1 \to \widehat{\mathcal{P}}$, which is a U(1) bundle. This matches the physical picture as the phase is real, resulting in U(1) actions on the states. Fixing $\mathcal{P}$ to be n-dimensional as usual, note that $\mathcal{P}_1 \cong S^{2n-1}$ and $\widehat{\mathcal{P}} \cong \mathbb{C}P^{n-1}$. Hence π is isomorphic to the standard projection $S^{2n-1} \to \mathbb{C}P^{n-1}$, independent of H and so the physical set-up that one wants to model. The norm-induced metric on $\mathcal{P}$ induces metrics on $\mathcal{P}_1$ and $\widehat{\mathcal{P}}$, and passing to $\mathbb{C}P^{n-1}$ one may show that the Fubini-Study metric appears in a natural way. In this observation one sees why the physical set-up matters so little; the problem is always phrased in the bundle $S^{2n-1} \to \mathbb{C}P^{n-1}$ endowed with the natural metric and so a natural parallel transport, independent of the hamiltonian H.

Let us connect this to the previous case of adiabatic dynamics. As can be guessed from eq. (6.17), if one chooses $|\psi'\rangle = |\psi_k\rangle$, the kth eigenstate of some hermitian hamiltonian, then β reduces to the usual geometric phase γ. The connection that is used is thus

$$A_\psi = i\langle\psi|d|\psi\rangle. \tag{6.19}$$

Mathematically, the bundle $\pi_1 \colon \mathcal{P}_1 \to \widehat{\mathcal{P}}$ is pulled back to parameter space P. The key object is a map $P \to \widehat{\mathcal{P}}$, i.e. a map sending given parameter values to some ray in a smooth way (compare [41]). We claim that the map

$$f_k \colon P \to \widehat{\mathcal{P}}, \quad x \mapsto |\psi_k(x)\rangle\langle\psi_k(x)| \tag{6.20}$$

is well-defined and provides the desired pull-back. That f_k is well-defined hinges on proposition 6.1; as H is hermitian, eigenstates are defined up to a phase (assuming fixed norm 1), so the projection to $\widehat{\mathcal{P}}$ yields an unambiguous answer. The relevant diagram is depicted in fig. 6.1; note that a similar story/diagram exists with $\pi \colon \mathcal{P} \to \widehat{\mathcal{P}}$, but as seen previously it is more natural to consider $\mathcal{P}_1$ and π_1. This yields a U(1)-bundle over P, similar to the Berry-Simon picture. The difference is that now one can pass through a degeneracy if one (manually) agrees on the specific eigenstate on this point by tuning f_k.

$$\begin{tikzcd}
 & \mathcal{P}_1 \arrow[r, "\cong"] \arrow[d, "\pi_1"] \arrow[dl, "f_k^*(\pi_1)"'] & S^{2n-1} \arrow[d] \\
P \arrow[r, "f_k"] & \widehat{\mathcal{P}} \arrow[r, "\cong"] & \mathbb{C}P^{n-1}
\end{tikzcd}$$

Figure 6.1: The AA-phase associated to π_1 yields the geometric phase after pull-back to parameter space P using eigenstate map f_k. The phase does not depend on the chosen hamiltonian, as is reflected in the canonical identification of π_1 with the projection $S^{2n-1} \to \mathbb{C}P^{n-1}$ and the flexibility of choosing f_k.

Let us discuss the physical applications of the theory in some more detail. In [40], it is shown that the Aharonov-Bohm (AB) effect can also be explained using the new phase β. This provided more insight in the question why a phase obtained in an adiabatic setting appears also in a non-adiabatic setting. It is also shown that β is gauge-invariant, and this is again applied to the AB effect where the gauged object is the electro-magnetic 4-potential A^μ.

The generality of the AA-connection also has its problems. As mentioned, the Fubini-Study metric appears naturally in the problem, and as can be deduced from fig. 6.1, the projection π_1 and so the AA-connection follow the induced parallel transport from this metric [40]. This means that the relevance of β in a physical setting is given by f_k only, where we can replace f by any smooth map from $P \to \widehat{\mathcal{P}}$. A hamiltonian H need not

appear, and in this way also non-degeneracy space X is irrelevant. Hence, the parameter space P will always be viewed as a pullback of $\mathbb{C}P^{n-1}$, where the geometry is fixed by the induced metric (see also [41]).

We conclude that the AA-connection is not an appropriate tool to study EPs. Not only does it depend heavily on hermitian theory, already in the hermitian setting the properties of the hamiltionian have no impact on the geometry and so the dynamics. The absence of a special role for degeneracies is also gone, and as can be found in [41] one can even generalize to $\mathcal{N}$-fold degenerate states leading to $\mathrm{U}(\mathcal{N})$-PFBs. We thus shift our attention to a generalization of the Berry-Simon picture suitable for non-hermitian systems.

Generalized Berry-connection

The previous connection was in a hermitian setting and so does not allow for the swaps that are so crucial for EP theory. Therefore, we now treat [8] in which the swaps are explicitly built into the formalism.

Unique to the approach in [8] is that the parameter space itself is extended, even before the state spaces are attached. The motivation is that this mediates the multi-valuedness of the eigenvalues. The parameter space of non-degeneracies X is first enlarged to an S_n-bundle $\widetilde{\mathfrak{M}}$ over X. However, it may be that the needed transition functions do not cover all permutations of S_n, and so one finds an irreducible subgroup $\mathfrak{h}$ of S_n. One may thus restrict the principal S_n-bundle $\widetilde{\mathfrak{M}}$ to a principal $\mathfrak{h}$-bundle $\mathfrak{M}$. It is this $\mathfrak{M}$ that is argued to be the correct parameter space for adiabatic evolution.

The final bundle is achieved by adding the state spaces. This is done similarly to the Berry-Simon procedure; one attaches a line (i.e. a copy of $\mathbb{C}$) to each point of $\mathfrak{M}$ and makes the proper identifications to stitch different patches together. The geometry is induced by imposing the non-hermitian form as seen in eq. (6.7) given by

$$A_k = i\langle\chi_k|d|\psi_k\rangle. \tag{6.21}$$

Let us review the obtained framework and its construction. First, this connection is more general than the Berry-Simon picture as in the hermitian case $\mathfrak{M} = X$ by single-valuedness (proposition 6.1). It allows one to perform parallel transport to any eigenstate and any non-hermitian setting as long as the parameter path lies in non-degenerate space. Another remarkable fact is the bottom-up approach used to construct the bundles, in contrast to the top-down approach that was very convenient in the previous cases. Also, the final result is not a PFB over X, the original and physical parameter space. If we do not reduce the S_n group to the irreducible subgroup $\mathfrak{h}$, the total bundle B is a $\mathbb{C}^\times$ bundle over $\widetilde{\mathfrak{M}}$, which is in turn an S_n bundle over X. In a diagram the situation is as indicated below.

$$\begin{tikzcd} B \arrow[d, "\mathbb{C}^\times"] \\ \widetilde{\mathfrak{M}} \arrow[d, "S_n"] \\ X \end{tikzcd}$$

In a way, we would like to collapse to diagram to a single arrow. Hence the structure group should involve both the S_n part from the multi-valuedness and a $\mathbb{C}^\times$ from the state space. We will see in the next subsection that this can be done.

A final note we make on the curvature. Again the structure group is $\mathbb{C}^\times$, as now $\mathfrak{M}$ is taken as the base manifold, so the curvature form is given by $\mathrm{d}\,\omega$ and hence gives the geometric phase upon integration. The discussion reduces to that of the Berry-Simon

case, except for the significant fact that here the geometric phases may be complex and reduction to U(1) is impossible in general.

Conclusion

Let us review how one can use the discussed bundles in the context of EPs. As already indicated, the hermitian cases will not suffice. The simplest reason is that the structure groups of such PFBs are either U(1) or $\mathbb{C}^\times$, independent of state space dimension n, and so do not allow for swaps of the eigenstates. The last PFB that we discussed does allow for swaps, but only via a modification of the parameter space; its structure group is still $\mathbb{C}^\times$.

We thus want to have yet another PFB, one where the swaps of the eigenstates should be present in the structure group itself. As complex scaling should also be in the group, we can look for the simplest group that can mix complex scalings and permute n objects. This group is $\mathbb{C}^\times \wr S_n$, where we use the wreath product as treated in appendix B. We note that this is the semi-direct product $\mathbb{C}^n \rtimes S_n$, where the first factor models the independent phase changes of n eigenstates and the second factor models the swaps. We note that the lay-out of this group was already described in [42], but it was not formalized in the way we do now.

We will show in a moment that this group is the structure group of a canonical PFB, but let us first compare it with better known groups. The relations are depicted in fig. 6.2. As written in the caption, one can order the groups according to the setting in which they are relevant. The first column applies to quantum systems where an inner product and a (for this inner product) hermitian operator govern the resulting unitary dynamics. In the second column one has no relation to an inner product, and the dynamics may be non-unitary. The third and fourth column contain groups with S_n only, meaning that they are relevant only within the adiabatic approximation, i.e. when the eigenstates are permuted. From top to bottom, the rows allow for more transformations of rays, hence respecting less fixed directions at each step.

$$\begin{tikzcd}
\mathrm{U}(1) \arrow[r] \arrow[d] & \mathbb{C}^\times \arrow[d] \arrow[dr] & & \\
 & & \mathbb{C}^\times \wr S_n \arrow[dl] & S_n \arrow[l] \\
\mathrm{U}(n) \arrow[r] & \mathrm{GL}(n, \mathbb{C}) & &
\end{tikzcd}$$

Figure 6.2: Summary diagram of the relevant groups, all arrows are (canonical) inclusions. The upper row concerns single-state changes, the lower general basis changes and the middle row eigendirection/eigenray preserving changes. The columns from left to right correspond to dynamics from hermitian, general, adiabatic and 'projective adiabatic' systems.

6.3 Defining the eigenframe bundle

The previous material may be extended with a canonical PFB suited for general adiabatic quantum theory, including EP theory as a subfield. In this section we will show that the eigenframes of an operator family form a PFB, with structure group $\mathbb{C}^\times \wr S_n$.

We want to emphasize that the formalism does not require the complex analytic theory of Riemann sheets. It is sufficient that the eigenvalues vary smoothly with system parameters. This allows us to use operators that also involve complex conjugates which are excluded in the complex analytic case.

Let us start from scratch. Let $T(x)$ be a family of operators on a fixed n-dimensional complex vector space V, where $T(x)$ depends on system parameters $x \in P$ with P a smooth manifold. In practice, P would be an allowed region with k real and l complex parameters, so an open subset of $\mathbb{R}^k \times \mathbb{C}^l$. Let us formalize the non-degeneracy space X as well.

Definition 6.2. Given a finite-dimensional operator family $T(x)$ depending smoothly on $x \in P$. Define the associated *non-degeneracy space* to be

$$X = P \setminus \Delta \tag{6.22}$$

where Δ is the discriminant set of $T(x)$ defined by

$$\begin{aligned} \Delta &= \{x \in P \mid T(x) \text{ is degenerate}\} \\ &= \{x \in P \mid \operatorname{discrim}(\det(\lambda I - T(x)), \lambda) = 0\}\,. \end{aligned} \tag{6.23}$$

Two important properties of this set X are given below. These will be needed later on.

Proposition 6.2. Given a non-degeneracy space X in parameter space P;

- the set X is open in P
- the set X has (real) codimension 2 in P.

Proof. As $T(x)$ depends smoothly on x, one has smooth dependence on x of $\det(\lambda I - T(x))$ and so of $d(x) = \operatorname{discrim}(\det(\lambda I - T(x)), \lambda)$. It follows that $\Delta = d^{-1}(\{0\})$ is closed in P, hence the complement X is open in P. For the second item, we note that X is given by two real equations, namely $\operatorname{Re}(d(x)) = 0$ and $\operatorname{Im}(d(x)) = 0$. As $d(x)$ is a smooth function on P, these two equations are independent. Hence the codimension is 2 as desired. □

Denoting by $\operatorname{Fr}(V)$ the set of bases/frames in V, we have a set

$$\operatorname{Fr}(T) = \{(x, f) \in X \times \operatorname{Fr}(V) \mid f_i \text{ is eigenvector of } T(x) \text{ for } i = 1, \ldots, n\} \tag{6.24}$$

with natural projection map to X given by

$$\pi \colon \operatorname{Fr}(T) \to X, \quad (x, f) \mapsto x \tag{6.25}$$

which sends a based frame to its basepoint. As X is open in P by proposition 6.2, it inherits the structure of a smooth manifold. Hence there is a natural manifold structure on $\operatorname{Fr}(T)$ generalizing the manifold structure of $\operatorname{Fr}(V)$. We like to show that given these manifold structures π is of $\mathbb{C}^\times \wr S_n$-PFB type.

Our first step to this end it to formulate a smooth $\mathbb{C}^\times \wr S_n$-action on $\operatorname{Fr}(T)$. We show that the natural action suffices, as given in the following lemma.

Lemma 6.2. The function given by

$$\begin{aligned} \mathbb{C}^\times \wr S_n \times \operatorname{Fr}(T) &\to \operatorname{Fr}(T) \\ ((g_1, \ldots, g_n, \sigma), (x, f_1, \ldots, f_n)) &\mapsto (x, g_1 f_{\sigma^{-1}(1)}, \ldots, g_n f_{\sigma^{-1}(n)}) \end{aligned} \tag{6.26}$$

or written in compact form as

$$((g, \sigma), (x, f)) \mapsto (x, g\sigma(f)) \tag{6.27}$$

defines a smooth $\mathbb{C}^\times \wr S_n$-action on $\operatorname{Fr}(T)$.

Proof. The identity of $\mathbb{C}^\times \wr S_n$ trivially yields the identity operation on $\mathrm{Fr}(T)$. The group structure is respected, as can be seen in compact notation;

$$\begin{aligned}(h,\tau)\cdot[(g,\sigma)\cdot(x,f)] &= (h,\tau)\cdot(x,g\sigma(f)) = (x,h\tau(g\sigma(f))) = (x,h\tau(g)\tau(\sigma(f)))\\ &= (h\tau(g),\tau\sigma)\cdot(x,f) = [(h,\tau)\cdot(g,\sigma)]\cdot(x,f)\end{aligned}$$

The action is smooth as it decomposes into scalar multiplications and swaps. □

We then focus on the properties of π.

Lemma 6.3. The map $\pi\colon \mathrm{Fr}(T)\to X$ is smooth, surjective and $\mathbb{C}^\times \wr S_n$-invariant.

Proof. As π is the restriction of the smooth projection $X\times \mathrm{Fr}(V)\to X$ to a submanifold it is smooth. Surjectivity of π is equivalent to saying that $T(x)$ has an eigenframe for any $x\in X$, which is guaranteed by theorem C.1. Invariance is easily seen as

$$\pi((g,\sigma)\cdot(x,f)) = \pi(x,g\sigma(f)) = x = \pi(x,f).$$

□

It remains to check that the bundle is locally trivial, for which we need the below result. For the proof we use the technique of the Frobenius covariant, which is an operator that projects on a desired eigenspace.

Lemma 6.4. Given $T(x)$ a smooth family of matrix operators acting on n-dimensional space V. Then each point $x_0\in X$ has a neighborhood U open in non-degeneracy space X such that there is a smooth moving eigenframe $f(x)$ defined on U.

Proof. Consider for $i=1,\dots,n$ the operator

$$A_i(x) = \frac{\prod_{j\neq i} T(x)-\lambda_j(x)I}{\prod_{j\neq i}\lambda_j(x)-\lambda_i(x)}$$

which is smooth on X and well-defined as all operators in the numerator commute. Note that $A_i(x)$ equals identity on the eigenspace of $\lambda_i(x)$ and is 0 on all other eigenspace (thus the complement in V). It follows that $A_i(x)$ is a smoothly varying projection operator to $\ker(T(x)-\lambda_i(x))$. Fix $x_0\in X$, let $f(x_0)$ be an eigenframe of $T(x_0)$. Extend this frame to a moving frame given by $f_i(x) := A_i(x)f_i(x_0)$. As $A_i(x)$ is a projection to the eigenspace $\ker(T(x)-\lambda_i(x))$, $f_i(x)$ is an eigenvector of $T(x)$ with correct eigenvalue. Also, $f_i(x)$ is smooth as $A_i(x)$ is smooth. Hence there is a neighborhood U_i of x_0 such that $f_i(x)$ is non-zero on U_i. Hence the $f_i(x)$ form a smooth local frame $f(x)$ on the open neighborhood $U=\bigcap_{i=1}^n U_i$ of x_0. □

We can now state one of our main results in the below theorem.

Theorem 6.1. Let V be an n-dimensional complex vector space, let $T(x)\colon V\to V$ be an operator family depending smoothly on parameter $x\in P$, where P is a smooth manifold. Let $X\subset P$ be the set of non-degeneracies of T. Then T canonically induces a PFB

$$\mathbb{C}^\times \wr S_n \to \mathrm{Fr}(T)\to X \tag{6.28}$$

which we call the *eigenframe bundle* of T.

Proof. Fix a point $x\in X$, then there is a small open ball $U\subset X$ containing x. Note that on U both eigenvectors and eigenvalues are well-defined single-valued functions. Given lemmas 6.2 and 6.3, it suffices to show that the restricted bundle $\pi^{-1}(U)\to U$ is trivializable, which is equivalent to finding a local section σ of π defined on U. That is, we want for each point $x_0\in X$ a local smooth moving frame. This is exactly the result of lemma 6.4. □

Observe that no inner product structure on V was necessary for the argument. Less important but still interesting is that at this point no left-eigenvectors were used as well.

One may feel as if there is a subtle contradiction going on concerning the S_n theory. On one hand, when listing eigenvectors one is free to choose an ordering. On the other hand, as we explicitly assume non-degenerateness, exchange of eigenvectors seems wrong as the energies are different. It is interesting that this discussion is reflected in the global versus local aspects of the structure group $\mathbb{C}^\times \wr S_n$. Locally, around the identity, the group is $(\mathbb{C}^\times)^n$, and indeed swaps are absent. Globally, the story changes significantly and a physical explanation for the swaps comes naturally. Imagine 2 quantum eigenstates at parameter x_0, one of high and one of low real energy. Now, adiabatically change system parameters to get far away, call this new point x_1. The energies may have moved in the complex plane, and the high versus low energy comparison at x_0 has lost its meaning at x_1. If one moves back to x_0 along a different path then indeed the states do not need to come back to the original configuration.

Knowing this PFB, we want to show that the parallel transport from the adiabatic approximation is compatible with the group structure. This is done in the next subsection, where also the corresponding holonomy theory is explored.

6.4 Adiabatic connection on the eigenframe bundle

We continue with the parallel transport eq. (6.6) and show that it induces a connection of $\mathrm{Fr}(T)$. Again we want to formulate the steps, one at a time.

The first step is to check that the matrix-valued form ω actually takes its values in the Lie algebra of the structure group. The algebra of $\mathbb{C}^\times \wr S_n$ is the algebra of its connected component $(\mathbb{C}^\times)^n$, and this is the commutative algebra $\mathbb{C}^n$. We will identify the algebra $\mathbb{C}^n$ of $\mathbb{C}^\times \wr S_n$ with the algebra of diagonal matrices in $M_n(\mathbb{C})$ via the map $(g_1, \dots, g_n) \mapsto \mathrm{diag}(g_1, \dots, g_n)$, which is an injective lie algebra morphism.

Lemma 6.5. One has $\omega \in \Omega^1(\mathrm{Fr}(T), \mathbb{C}^n)$.

Proof. Using the identification above, this follows from the diagonal form of ω in eq. (6.7). □

The next step concerns the transformation law. Let us first check it in general, so not yet imposing adiabatic behavior.

Lemma 6.6. Let $\{v_i\}$ be a local frame with $\{\theta^j\}$ the corresponding dual frame, set $\omega_i^j = \theta^j \,\mathrm{d}\, v_i$. If one changes the local frame as $v_i \to v_i' = A_i^l v_l$ with A invertible at each point, then

$$\omega \to \omega' = A^{-1}\omega A + A^{-1}\,\mathrm{d}\, A. \tag{6.29}$$

Proof. The corresponding change in dual frame is $\theta^j \to \theta^k (A^{-1})_k^j$, hence

$$\begin{aligned}\omega_i^j \to & \theta^k (A^{-1})_k^j \,\mathrm{d}(A_i^l v_l) = \theta^k (A^{-1})_k^j (A_i^l \,\mathrm{d}\, v_l + (\mathrm{d}\, A_i^l) v_l) = \theta^k (A^{-1})_k^j (A_i^l \,\mathrm{d}\, v_l + (\mathrm{d}\, A_i^l) v_l) \\ &= (A^{-1})_k^j (\theta^k \,\mathrm{d}\, v_l) A_i^l + (A^{-1})_k^j (\mathrm{d}\, A_i^l) \theta^k v_l = (A^{-1}\omega A)_i^j + (A^{-1})_k^j (\mathrm{d}\, A_i^k) \\ &= (A^{-1}\omega A)_i^j + (A^{-1}\,\mathrm{d}\, A)_i^j.\end{aligned}$$

□

Checking that the transformation preserves the form of the diagonal adiabatic ω suffices to show the following.

Proposition 6.3. Given an eigenframe PFB $\mathrm{Fr}(T)$, there is a canonical connection ∇ specified by connection 1-form $\omega \in \Omega^1(\mathrm{Fr}(T), \mathbb{C}^n)$ on it, given in (local) connection matrices by

$$\omega_i^j = \begin{cases} \theta^j \,\mathrm{d}\, v_i & \text{if } i = j \\ 0 & \text{else} \end{cases}. \tag{6.30}$$

Proof. By lemmas 6.5 and 6.6 we only need to check that the transformed connection matrix is diagonal so that we may reduce the group to $\mathbb{C}^\times \wr S_n$. For this, we observe that then A has the form of a generalized permutation matrix at each point. In particular, A and A^{-1} contain inverse permutations. As ω is diagonal, A^{-1} and ωA have inverse permutations and so $A^{-1}\omega A$ is diagonal. Similarly d acts diagonally and $A^{-1}\,\mathrm{d}\,A$ is diagonal. Hence ω' is diagonal. To summarize, each matrix ω is a local $\mathbb{C}^n$-valued 1-form with correct transformation law, hence it defines a connection of $\mathrm{Fr}(T)$. □

Given a connection form ω, one has a associated curvature given by

$$K = \mathrm{d}\,\omega + \omega \wedge \omega.$$

Let us compute it for the connection ∇. Note that as ω is diagonal, so is K. So if we agree that $\wedge$ is the implicit product between 1-forms, one has

$$K_i^i = \mathrm{d}\,\theta^i \wedge \mathrm{d}\,v_i + \theta^i\,\mathrm{d}\,v_i \wedge \theta^i\,\mathrm{d}\,v_i = \mathrm{d}\,\theta^i\,\mathrm{d}\,v_i - \mathrm{d}\,\theta^i v_i \theta^i\,\mathrm{d}\,v_i = \mathrm{d}\,\theta^i (I - v_i\theta^i)\,\mathrm{d}\,v_i.$$

This expression need not vanish. In fact, $v_k\theta^k = I$ by dual basis properties, so that the above equals

$$K_i^i = \sum_{j:j\neq i} \mathrm{d}\,\theta^i (v_j\theta^j)\,\mathrm{d}\,v_i = \sum_{j:j\neq i} \mathrm{d}\,\theta^i P_j\,\mathrm{d}\,v_i$$

where $P_j = v_j\theta^j$ is the projection operator on the span of v_j. This seems to account for the imposed non-mixing of eigenstate i with other eigenstates j. For the characteristic class one takes the trace and finds

$$\mathrm{tr}(K) = \sum_{(i,j):i\neq j} \mathrm{d}\,\theta^i P_j\,\mathrm{d}\,v_i$$

which sums all the used terms, hence measures the 'total non-mixing' that occurs.

It is interesting to consider the dynamics when we do not perform the adiabatic approximation. Tracing the proofs, by a similar argument it follows that in this case one obtains a $\mathrm{GL}(n, \mathbb{C})$-PFB over X and that the unapproximated ω by lemma 6.6 defines a connection on this PFB. The curvature of this connection is

$$K_i^j = \mathrm{d}\,\theta^j \wedge \mathrm{d}\,v_i + \theta^j\,\mathrm{d}\,v_k \wedge \theta^k\,\mathrm{d}\,v_i = \mathrm{d}\,\theta^j\,\mathrm{d}\,v_i - \mathrm{d}\,\theta^j v_k\theta^k\,\mathrm{d}\,v_i = \mathrm{d}\,\theta^j (I - v_k\theta^k)\,\mathrm{d}\,v_i = 0.$$

Indeed, we do not need to twist anything for the standard dynamics. Does zero curvature mean that no phase can occur? We can say two things about this. First, as seen in previous cases, the phase is obtained by integrating $\mathrm{d}\,\omega$ and not from K. Second, given that the structure group is now $\mathrm{GL}(n, \mathbb{C})$, eigenstates need not be conserved, and obtaining a phase becomes a troublesome notion.

6.5 The adiabatic group and the Λ-group

We will now consider the holonomy of the connection ∇ of the previous subsection in more detail. We will use the theory and notation as in appendix A.

First, as the connection is adiabatic, the holonomy operations correspond to state changes that can be achieved adiabatically. Hence we call the induced holonomy group at a point the *adiabatic group* at the point.

Definition 6.3. Given a matrix family T and its associated eigenframe bundle $\mathrm{Fr}(T) \to X$ endowed with the canonical connection ∇. For any $U \subset X$ open, define the *adiabatic group* at a point x_0 restricted to U, denoted $\mathrm{Adia}_T(U, x_0)$, to be the holonomy group at x_0 from the restricted bundle $\mathrm{Fr}(T)|_U \to U$. Equivalently, $\mathrm{Adia}_T(U, x_0)$ is the image of $\mathrm{Loop}(U, x_0)$ under the holonomy map. Symbolically;

$$\mathrm{Adia}_T(U, x_0) = \mathrm{Hol}_{x_0}(U, \nabla|_U) \tag{6.31}$$

We abbreviate $\mathrm{Adia}_T(X, x_0)$ as $\mathrm{Adia}(x_0)$ whenever possible.

We can immediately state some properties of these groups.

Lemma 6.7. In the situation of definition 6.3:

- the adiabatic group $\mathrm{Adia}_T(U, x_0)$ is isomorphic to a subgroup of $\mathbb{C}^\times \wr S_n$.
- given $x_0 \in V$ and $V \subset U \subset X$ open inclusions, then $\mathrm{Adia}_T(V, x_0)$ is a subgroup of $\mathrm{Adia}_T(U, x_0)$. In particular, any such group is a subgroup of $\mathrm{Adia}(x_0)$.

Proof. The adiabatic group is the holonomy of a connection with structure group $\mathbb{C}^\times \wr S_n$, hence the first follows. The second follows from $\mathrm{Loop}(V, x_0) \subset \mathrm{Loop}(U, x_0)$. □

We see that any element in $\mathrm{Adia}_T(U, x_0)$ preserves the set of eigenstates at x_0, and so there is an induced group of eigenstate/eigenvalue permutations. This group is similar to the λ-group as mentioned by Kato in [1], but the version we discuss now is more general as we allow more general connections, hence we call it the Λ-group. Let us make this precise. Let E_{x_0} be the set of eigenvalues of $T(x_0)$, and let us omit the U and T for brevity. As seen in the previous lemma, $\mathrm{Adia}(x_0)$ is isomorphic with a subgroup of $\mathbb{C}^\times \wr S_n$. As E_{x_0} has n elements, labelling the eigenvalues gives an isomorphism $\mathrm{Sym}(E_{x_0}) \cong S_n$. If we assume that the labels of eigenvalues and eigenstates match the below diagram of continuous group maps commutes

$$\begin{tikzcd} \mathrm{Adia}(x_0) \arrow[r] \arrow[d, hook] & \mathrm{Sym}(E_{x_0}) \arrow[d, "\cong"] \\ \mathbb{C}^\times \wr S_n \arrow[r, two heads] & S_n \end{tikzcd} \tag{6.32}$$

where the bottom map is the usual projection. The image of the top map is thus of special importance. It is a topological subgroup of $\mathrm{Sym}(E_{x_0}) \cong S_n$ with a (surjective) group map from $\mathrm{Adia}(x_0)$ to it.

Definition 6.4. Fixing $x_0 \in X$, define the group $\Lambda_T(U, x_0)$ as the subgroup of $\mathrm{Sym}(E_{x_0})$ of elements that can be achieved by an element of $\mathrm{Adia}_T(U, x_0)$. Equivalently, it is the image of the map $\mathrm{Adia}(x_0) \to \mathrm{Sym}(E_{x_0})$.

This finishes the definition of $\Lambda(x_0)$, and the following result is immediate.

Lemma 6.8. The group $\Lambda(x_0)$ is discrete.

This property of $\Lambda(x_0)$, which could still stand in some infinite-dimensional cases, allows for some strong results. We consider the induced map $\mathrm{Loop}(x_0) \to \Lambda(x_0)$ going via $\mathrm{Adia}(x_0)$, that is, the map that sends a loop to its induced permutation. It is interesting to note that this construction is the theoretical counterpart of the 'merging path method'. Indeed, in this method one measures for various loops if a permutation occurs. The discreteness of $\Lambda(x_0)$ implies that permutations are invariant under deformations of the based loop, as made precise below.

Proposition 6.4. The induced map from $\mathrm{Loop}(x_0)$ to $\Lambda(x_0)$ is a surjective group morphism. It factors through the fundamental group $\pi_1(X, x_0)$ as indicated in the below diagram.

$$\begin{tikzcd}
\mathrm{Loop}(x_0) \arrow[r, two heads, dotted] \arrow[d, two heads] \arrow[dr, two heads] & \pi_1(X, x_0) \arrow[d, two heads, dotted] \\
\mathrm{Adia}(x_0) \arrow[r, two heads] & \Lambda(x_0)
\end{tikzcd}$$

In other words, the group element of $\Lambda(x_0)$ induced by a path γ depends only on the based homotopy class $[\gamma]$.

Proof. The map $\mathrm{Loop}(x_0) \to \Lambda(x_0)$ is a composition of surjective group maps, hence one itself. By the discreteness of $\Lambda(x_0)$, intermediate loops from a based homotopy $H\colon \mathrm{Loop}(x_0) \times [0,1] \to \Lambda(x_0)$ are all constant and sent to the same element, in particular the initial and final ones. It follows that the obtained permutation is path deformation invariant. □

This result says that permutations are always of topological as opposed to geometrical nature, and this has strong consequences. For instance, one can deform a measurement path and still obtain the same permutation. This was already known, but the above also tells us how to compose the effects from multiple EPs. Indeed, any loop γ encircling an arbitrary EP structure gives a class $[\gamma] \in \pi_1(X, x_0)$, which can then be decomposed into a fixed product of fundamental classes $[\gamma_i]$ where each γ_i encloses a single EP structure (an EP, an exceptional line, exceptional surface, etc.). As we saw in the previous chapter this allows for non-abelian effects to occur.

We will now turn our attention to the kernel of the map $\mathrm{Adia}(x_0) \to \Lambda(x_0)$. This will tell us about the pure phase changes that occur in a system. At the end of this section we return to the Λ-group on its own as the key object with which to define an EP.

6.6 Phase group and SES theory

A surjective map of groups canonically induces a short exact sequence (SES) of groups via its kernel. In the previous subsection we saw that the map $\mathrm{Adia}(x_0) \to \Lambda(x_0)$ fits this requirement. The kernel of this map consists of those holonomy operations that do not permute the eigenvectors. That is, it is the group of solely (complex) phase changing actions; let us call it the *phase group*.

Definition 6.5. In the context of the adiabatic group, define the *phase group* at $x_0 \in X$, denoted $\mathrm{Phase}(x_0)$, as the kernel of $\mathrm{Adia}(x_0) \twoheadrightarrow \Lambda(x_0)$, in particular it is a normal/invariant subgroup of $\mathrm{Adia}(x_0)$. In other words, it is the group such that one has a short exact sequence of groups

$$0 \longrightarrow \mathrm{Phase}(x_0) \longrightarrow \mathrm{Adia}(x_0) \longrightarrow \Lambda(x_0) \longrightarrow 0. \tag{6.33}$$

We will refer to this SES as the adiabatic SES.

We note that this reflects the SES of the wreath product as found in appendix B. In fact, the following is true.

Corollary 6.1. One has the commuting diagram

$$\begin{tikzcd}
0 \arrow[r] & \mathrm{Phase}(x_0) \arrow[r] \arrow[d] & \mathrm{Adia}(x_0) \arrow[r] \arrow[d] & \Lambda(x_0) \arrow[r] \arrow[d] & 0 \\
0 \arrow[r] & (\mathbb{C}^\times)^n \arrow[r] & \mathbb{C}^\times \wr S_n \arrow[r] & S_n \arrow[r] & 0
\end{tikzcd} \tag{6.34}$$

where all vertical maps are injections.

Proof. The right square was already treated in diagram (6.32). Exactness of both sequences finishes the proof. □

This allows us to still use the general theory from the wreath product. Some immediate properties of the phase group are listed below, easily deduced from the above diagram.

Corollary 6.2. It holds that

- the $\mathrm{Phase}(x_0)$ is a subgroup of $(\mathbb{C}^\times)^n$, in particular it is commutative.
- for any permutation of eigenvalues at x_0, there are is a fixed amount/cardinality of adiabatic operations that induce this permutation. These differ by phases only, and their number equals $\#\mathrm{Phase}(x_0)$.
- the group $\mathrm{Adia}(x_0)$ is finite/discrete $\iff$ the group $\mathrm{Phase}(x_0)$ is finite/discrete.

The SES (6.33) resembles the SES (A.7) of the monodromy group as the groups in the middle coincide. However, they need not be isomorphic, a fact that can be checked by inspecting if the groups on the left are isomorphic. That is, one checks if $\mathrm{Phase}(x_0) \cong \mathrm{Hol}^0(x_0)$. One can deduce that is already violated for the standard EP2 as seen in the below example. The key observation is that phase changes may require non-contractible loops.

Example 6.1. Consider the standard EP2, where the holonomy group is generated by

$$\begin{pmatrix} 0 & -1 \\ 1 & 0 \end{pmatrix}$$

corresponding to a non-contractible fundamental loop. Squaring the above matrix yields $-I$, so that $\mathrm{Phase}(x_0) \cong \mathbb{Z}/2\mathbb{Z}$. Note that indeed $\Lambda(x_0) \cong \mathrm{Adia}(x_0)/\mathrm{Phase}(x_0) \cong \mathbb{Z}/2\mathbb{Z}$. Hence the associated adiabatic SES can be written as

$$0 \longrightarrow \mathbb{Z}/2\mathbb{Z} \longrightarrow \mathbb{Z}/4\mathbb{Z} \longrightarrow \mathbb{Z}/2\mathbb{Z} \longrightarrow 0. \tag{6.35}$$

However, any contractible loop yields no change at all so that $\mathrm{Hol}^0(x_0) = 0$. It follows that $\mathrm{Mon}(x_0) \cong \mathrm{Hol}(x_0) \cong \mathbb{Z}/4\mathbb{Z}$ and hence the holonomy SES is given by

$$0 \longrightarrow 0 \longrightarrow \mathbb{Z}/4\mathbb{Z} \longrightarrow \mathbb{Z}/4\mathbb{Z} \longrightarrow 0$$

which is indeed different.

Still, there is a strong connection between the two different SESs. As any contractible curve γ gives the identity permutation, the holonomy of γ lies in the phase group. In this way the following result comes up.

Lemma 6.9. The holonomy and adiabatic SESs are related via the below commutative diagram where exactness holds everywhere. In addition; one of the dashed arrows holds if and only if the other does.

$$\begin{tikzcd}
 & 0 \arrow[d] & 0 \arrow[d] & 0 \arrow[d, dashed] & \\
0 \arrow[r] & \mathrm{Hol}^0(x_0) \arrow[r] \arrow[d] & \mathrm{Hol}(x_0) \arrow[r] \arrow[d, "="] & \mathrm{Mon}(x_0) \arrow[r] \arrow[d] & 0 \\
0 \arrow[r] & \mathrm{Phase}(x_0) \arrow[r] \arrow[d, dashed] & \mathrm{Adia}(x_0) \arrow[r] \arrow[d] & \Lambda(x_0) \arrow[r] \arrow[d] & 0 \\
 & 0 & 0 & 0 &
\end{tikzcd}$$

Proof. First, there is a canonical map $\mathrm{Hol}^0(x_0) \to \mathrm{Phase}(x_0)$. It suffices to show that contractible loops can not induce a permutation. However, this follows from proposition 6.4. Injectivity is immediate.

In the fourth row we deal with quotients of the same group. As we just saw that there is an injection $\mathrm{Hol}^0(x_0) \to \mathrm{Phase}(x_0)$, by group theory there is a surjection $\mathrm{Mon}(x_0) \to \Lambda(x_0)$ given by enlarging the equivalence classes.

We note that the bottom left arrow is equivalent to $\mathrm{Hol}^0(x_0) = \mathrm{Phase}(x_0)$, which is equivalent to $\mathrm{Mon}(x_0) = \Lambda(x_0)$, which is equivalent to the top right arrow. □

Example 6.2. For the standard EP2 as just treated, this becomes the below diagram.

$$\begin{tikzcd}
 & 0 \arrow[d] & 0 \arrow[d] & & \\
0 \arrow[r] & 0 \arrow[r] \arrow[d] & \mathbb{Z}/4\mathbb{Z} \arrow[r] \arrow[d, "="] & \mathbb{Z}/4\mathbb{Z} \arrow[r] \arrow[d] & 0 \\
0 \arrow[r] & \mathbb{Z}/2\mathbb{Z} \arrow[r] & \mathbb{Z}/4\mathbb{Z} \arrow[r] \arrow[d] & \mathbb{Z}/2\mathbb{Z} \arrow[r] \arrow[d] & 0 \\
 & & 0 & 0 &
\end{tikzcd}$$

Observe that the 'phases are topological' assumption guarantees that $\mathrm{Hol}^0(x_0) = 0$ so that the upper line in the above diagram is trivial and the diagram basically reduces to the adiabatic SES. A difference between the lines indicates thus indicates that some phases may be reached only with non-contractible loops. Another quick result along this line of reasoning is the following.

Corollary 6.3. One has

- if $\mathrm{Phase}(x_0) = 0$, then $\mathrm{Hol}^0(x_0) = 0$ and $\Lambda(x_0) \cong \mathrm{Mon}(x_0) \cong \mathrm{Hol}(x_0)$
- if $\mathrm{Mon}(x_0) = 0$, then $\Lambda(x_0) = 0$ and $\mathrm{Phase}(x_0) \cong \mathrm{Hol}^0(x_0) \cong \mathrm{Hol}(x_0)$.

Splitting of the adiabatic SES

One may ask what it means if the adiabatic SES splits, either on the left or on the right. We will see that this question has physical relevance as well. We will use the Splitting Lemma as found in appendix B.

Let us start with the question of right splittings. As shown below, a corresponding physical question is 'given a feasible permutation of eigenstates, can it be realized without phase changes?'. Indeed, the image of this permutation under the right splitting would provide such a adiabatic operation. Formally, the following holds.

Lemma 6.10. The following are equivalent;

- there is a right splitting $\Lambda(x_0) \to \mathrm{Adia}(x_0)$
- one has $\mathrm{Adia}(x_0) = \mathrm{Phase}(x_0) \wr \Lambda(x_0)$
- for any $\sigma \in \Lambda(x_0)$, there is an operation $a \in \mathrm{Adia}(x_0)$ such that σ is achieved without extra phase factors.

Proof. The first two are equivalent by the Splitting Lemma. Assuming the third condition holds, one obtains a right splitting by sending σ to its corresponding a, the morphism property being immediate. Conversely, given $\mathrm{Adia}(x_0) = \mathrm{Phase}(x_0) \wr \Lambda(x_0)$, one has the map $\Lambda(x_0) \to \mathrm{Phase}(x_0) \wr \Lambda(x_0)$ given by inclusion into the second factor, also this being a morphism. □

Note that the adiabatic SES need not split. The standard EP2 provides a counterexample; the two eigenstates can be swapped, but precisely one of the states will carry an extra phase. The corresponding SES (eq. (6.35)) does not have a right splitting. Indeed, the induced semi-direct product would be $\mathbb{Z}/2\mathbb{Z} \times \mathbb{Z}/2\mathbb{Z}$ as all groups are commutative, but this has no element of order 4 as $\mathbb{Z}/4\mathbb{Z}$ has. On the other hand, observe that $\Lambda(x_0) = 0$ is a sufficient condition for the existence of a left-splitting

What about the left splittings? The Splitting Lemma says that a left splitting exists if and only if the middle group is the direct product of the outer two. That is, whether it holds that $\mathrm{Adia}(x_0) = \mathrm{Phase}(x_0) \times \Lambda(x_0)$. We can clearly see that this case has extraordinary experimental properties. Explicitly, phases and permutations can be achieved completely independently. Hence, there are paths along one can change phases, but none of these paths will permute states and vice versa. On the other hand, if phases and permutations can be reached individually, we have separate generators for $\mathrm{Phase}(x_0)$ and $\Lambda(x_0)$ and the direct product follows. We have thus shown the following.

Lemma 6.11. The following are equivalent;

- there is a left splitting $\mathrm{Adia}(x_0) \to \mathrm{Phase}(x_0)$
- one has $\mathrm{Adia}(x_0) = \mathrm{Phase}(x_0) \times \Lambda(x_0)$
- phase changes and permutations can be achieved independently

We observe that the same examples as for the right splitting can be used here to illustrate that the sequence may be left-split, but it also may not be.

Assuming topological effects only

Until now we discussed a framework that allows for geometric effects which are not topological per se. However, both EPs and DPs are famous for their topological robustness, that is invariance under continuous deformation of the path. Hence in this part we investigate what happens if all holonomy operations are topological in nature. Mathematically, we asumme there is a surjective morphism of groups $\pi_1(X, x_0) \twoheadrightarrow \mathrm{Adia}(x_0)$ such that the below diagram commutes, where all maps preserve products.

$$\begin{tikzcd}
 & & \mathrm{Loop}(x_0) \arrow[r, two heads] \arrow[d, two heads] & \pi_1(X, x_0) \arrow[d, two heads] \arrow[dl, dotted, two heads] & \\
0 \arrow[r] & \mathrm{Phase}(x_0) \arrow[r] & \mathrm{Adia}(x_0) \arrow[r] & \Lambda(x_0) \arrow[r] & 0
\end{tikzcd}$$

One may ask when there is also a map of groups $\pi_1(X, x_0) \to \mathrm{Phase}(x_0)$ making the diagram commute, that is when phases are of topological nature. The below lemma reveals that this happens in very special cases, namely if and only if no permutations are possible. That is, if and only if phase changes make up the entire holonomy. At this point we may recognize the setting of a DP, so one may argue there remains some interest in this speical case which is summarized below.

Lemma 6.12. The following are equivalent;

- the permutation group $\Lambda(x_0)$ is trivial
- $\mathrm{Phase}(x_0) = \mathrm{Adia}(x_0)$, that is, the adiabatic actions only change phases
- there exists a compatible group map $\pi_1(X, x_0) \to \mathrm{Phase}(x_0)$

Proof. The first two items are equivalent by group theory. Assume existence of a map $\pi_1(X, x_0) \to \mathrm{Phase}(x_0)$, then following an element via $\mathrm{Phase}(x_0)$ through the SES to $\Lambda(x_0)$ gives identity, implying the map $\pi_1(X, x_0) \to \Lambda(x_0)$ is trivial. As this map is a surjection, $\Lambda(x_0)$ must be trivial.

Assume the second item; as there is a map $\pi_1(X, x_0) \to \mathrm{Adia}(x_0)$, automatically have a compatible map $\pi_1(X, x_0) \to \mathrm{Phase}(x_0)$. □

Two cases where the assumption can be checked stand out. First, if $\mathrm{Adia}(x_0)$ is not discrete then the assumption does not hold. Indeed, the fundamental group is discrete, so by the above then also $\mathrm{Adia}(x_0)$ would be. On the other hand, if the operator family is complex analytic and the connection matches the connection from analytic continuation the assumption holds.

6.7 Applications in EP theory

We will now apply the theory from the previous section to EPs. We also use the representation theory discussed in appendix B. One idea is that the adiabatic SES (6.33) can be used to summarize the EP properties of achievable phases and permutations. We will first discuss well-known single EPs examples and after that inspect scenarios with two EPs.

Single EP case

Let us start with the isolated EPs in a complex analytic system. That is, let x be an EP, let U be an open set in $\mathbb{C}$ containing x, pick $x_0 \in U$ any point different from x. We assume that U contains no other EP. One finds $\pi_1(U, x_0) \cong \mathbb{Z}$, and so $\mathrm{Adia}(x_0)$ and all other groups in the adiabatic SES are discrete, commutative and cyclic.

In case of the standard EP2 the group $\mathrm{Adia}(x_0)$ has a representation generated by the matrix in eq. (2.3), so that

$$\tilde{p} = \begin{pmatrix} 0 & 1 \\ -1 & 0 \end{pmatrix}$$

from which it follows that $\mathrm{Adia}(x_0) \cong \mathbb{Z}/4\mathbb{Z}$. Going to $\Lambda(x_0)$, i.e. going to permutations we obtain the generator

$$p = \begin{pmatrix} 0 & 1 \\ 1 & 0 \end{pmatrix}$$

showing that $\Lambda(x_0) \cong \mathbb{Z}/2\mathbb{Z}$. From the matrices $\{p, p^2 = -I, p^3 = -p, p^4 = I\}$ only I and p^2 are diagonal. Hence $\mathrm{Phase}(x_0)$ is represented by these two matrices and is thus isomorphic to $\mathbb{Z}/2\mathbb{Z}$. The SES of the standard EP2 is then

$$0 \longrightarrow \mathbb{Z}/2\mathbb{Z} \longrightarrow \mathbb{Z}/4\mathbb{Z} \longrightarrow \mathbb{Z}/2\mathbb{Z} \longrightarrow 0$$

as found previously via the Λ-group. We observe that for 2D parameter space the (cyclic) Λ-group is either trivial or isomorphic to $\mathbb{Z}/2\mathbb{Z}$. These cases represent respectively a non-EP and an EP.

For the 3D case we can use the explicit results of [6], which reports both an EP2 and EP3 and the corresponding holonomy matrices. Indeed, after choosing a suitable basis, the EP3 has holonomy generator given by

$$\tilde{p} = \begin{pmatrix} 0 & 1 & 0 \\ 0 & 0 & 1 \\ 1 & 0 & 0 \end{pmatrix}$$

which has order 3, hence $\mathrm{Adia}(x_0) \cong \mathbb{Z}/3\mathbb{Z}$. As all non-zero entries already equal 1 no phases occur and $\mathrm{Phase}(x_0) = 0$. Equivalently, $p = \tilde{p}$ so that $\Lambda(x_0) \cong \mathrm{Adia}(x_0) \cong \mathbb{Z}/3\mathbb{Z}$. Hence the SES of this EP3 is

$$0 \longrightarrow 0 \longrightarrow \mathbb{Z}/3\mathbb{Z} \longrightarrow \mathbb{Z}/3\mathbb{Z} \longrightarrow 0.$$

The reported EP2 in 3D corresponds has generator

$$\tilde{p} = \begin{pmatrix} 0 & 1 & 0 \\ 1 & 0 & 0 \\ 0 & 0 & -1 \end{pmatrix}$$

so that $\mathrm{Adia}(x_0) \cong \mathbb{Z}/2\mathbb{Z}$. This is a serious difference with respect to the planar case. The phase change now occurs in a level that is not permuted, hence is unavailable to other levels. The SES reduces as well; the permutations are generated by

$$p = \begin{pmatrix} 0 & 1 & 0 \\ 1 & 0 & 0 \\ 0 & 0 & 1 \end{pmatrix}$$

so that $\Lambda(x_0) \cong \mathbb{Z}/2\mathbb{Z}$. In the set $\{p, p^2 = I\}$ only I is diagonal, so again $\mathrm{Phase}(x_0) = 0$. The SES is thus

$$0 \longrightarrow 0 \longrightarrow \mathbb{Z}/2\mathbb{Z} \longrightarrow \mathbb{Z}/2\mathbb{Z} \longrightarrow 0.$$

A clear indication of an EP is the non-triviality of $\Lambda(x_0)$, but as seen above the phase group may be trivial. For a DP the situation is opposite; now $\Lambda(x_0) = 0$ and $\mathrm{Phase}(x_0) \neq 0$. Considering the standard DP in 2D, the holonomy is generated by

$$\tilde{p} = \begin{pmatrix} -1 & 0 \\ 0 & -1 \end{pmatrix}$$

so that $\mathrm{Adia}(x_0) \cong \mathbb{Z}/2\mathbb{Z}$, and $\tilde{p}$ is already diagonal $\mathrm{Phase}(x_0) \cong \mathbb{Z}/2\mathbb{Z}$. This implies $\Lambda(x_0) = 0$, and indeed this is generated by

$$p = \begin{pmatrix} 1 & 0 \\ 0 & 1 \end{pmatrix} = I.$$

Multiple EP case

We can consider from a representation point of view what happens if more EPs are allowed to enter the picture. It implies that more generators are available, and the mixing may provide non-cyclic group structure, in particular the way to non-abelian groups is open. We consider only two EP cases as the general behavior is already illustrated there.

Let us start with a planar parameter space with two EPs. This already appears in standard EP2 examples as one obtains two EP2s, namely the plus and minus solution. However, these two EP2s are connected to the same branch structure, and the generator of the second EP2 equals

$$\begin{pmatrix} 0 & -1 \\ 1 & 0 \end{pmatrix} = \tilde{p}^3$$

where again $\tilde{p}$ is the generator of the first EP2. It follows that SES remains the same, and so the newly possible measurements will not find a change of states that was unavailable before.

Let us shift our attention away from EPs connected to exactly the same sheets. The other extreme of totally disconnected sheets is not that interesting as well as shown in below example.

Example 6.3. Consider s a complex parameter and, distinct complex constants c_1, c_2. Define

$$T(s) = \begin{pmatrix} ic_1 & s & & \\ s & -ic_1 & & \\ & & ic_2 & s \\ & & s & -ic_2 \end{pmatrix}$$

which has EP2s at $s = \pm c_1, \pm c_2$. The generators of the adiabatic group are essentially copies of the generator of the standard EP2, one for the two upper levels and one for the lower two levels. Hence they are represented by

$$p_1 = \begin{pmatrix} & -1 & & \\ 1 & & & \\ & & & 1 \\ & & 1 & \end{pmatrix}, p_2 = \begin{pmatrix} 1 & & & \\ & 1 & & \\ & & & -1 \\ & & 1 & \end{pmatrix}.$$

The SES is then

$$0 \longrightarrow \mathbb{Z}/2\mathbb{Z} \times \mathbb{Z}/2\mathbb{Z} \longrightarrow \mathbb{Z}/4\mathbb{Z} \times \mathbb{Z}/4\mathbb{Z} \longrightarrow \mathbb{Z}/2\mathbb{Z} \times \mathbb{Z}/2\mathbb{Z} \longrightarrow 0.$$

That is, it is given by products where now interconnection occurs.

It is interesting to look at the mathematical consequences of having two distincts EPs. As there is a surjective group morphism $\pi_1(X, x_0) \to \mathrm{Adia}(x_0)$ and so a surjective group morphism $\pi_1(X, x_0) \to \Lambda(x_0)$, the target groups can only be non-commutative if $\pi_1(X, x_0)$ is. The easiest example is the fundamental group of the figure '8', isomorphic to the free product $\mathbb{Z} * \mathbb{Z}$. This is indeed the fundamental group induces by 2 distinct EPs.

In order to have a non-commutative Λ-group, one needs to demand in addition that the 2 distinct EPs induce permutations that do not commute. As S_n is commutative for $n \leq 2$, one thus needs a 3 dimensional system. Furthermore, the EPs must connect different sheets. A system with an EP3 and an EP2 suffices, and the waveguide model of the previous chapter satisfies this requirement. In fact, the corresponding adiabatic SES was found to be

$$0 \longrightarrow \{\pm 1\}^3 \longrightarrow \{\pm 1\} \wr S_3 \longrightarrow S_3 \longrightarrow 0. \tag{6.36}$$

For the waveguide system we need non-planar parameter space, and the theory of this chapter was presented in such a way that it immediately generalizes. In general, the degeneracies are of codimension at least 2, so walking around is well-defined. In higher dimensions one would not consider loops around a point, but around a line, surface or hypersurface of degeneracies. However, as seen in the waveguide system, the degree of an EP becomes ill-defined.

6.8 A new definition of EP

We finish this section by discussing a new definition of EP based on the geometrical framework that we have been exploring.

As already argued in section 2, the coalescence definition 2.4 is the broadest serious EP definition available. As it can be used for any operator family that depends continuously on system parameters, only the trivial characterization 'non-hermitian degeneracy' is more general. Although coalescence in itself may be enough to describe some physical phenomena, e.g. two modes that suddenly coincide, for the EP picture it is not enough. The non-trivial sheets formed by eigenvalues and eigenvectors however are closely related to the behavior that is measured around the EP, as seen in section 4. This led us to

introduce definition 2.5 of an experimental EP, as indeed the swaps and the non-trivial sheet structure are equivalent viewpoints. We can now elaborate of this definition.

Let us formalize definition 2.5. The swaps of eigenvalues are given by the Λ-group, hence we should require this group to be non-trivial. As before, we write $\Lambda_T(U \cap X, x_0)$ for all the eigenvalue permutations at x_0 that can be achieved by x_0-based loops in $U \cap X$. Then the point x in parameter space P is an EP if and only if for any neighborhood U of x in P there is a point $x_0 \in U \cap X$ such that $\Lambda_T(U \cap X, x_0)$ is non-trivial, where we mimic definition 2.5. Indeed, within any neighborhood of x there lies a curve γ such that the eigenvalues get swapped by traversing γ. The definition is then as follows.

Definition 6.6. Given operator family $T(x)$ with parameter space P. A point $x \in P$ is called an (experimental) EP $\iff$ for any open set U in P containing x, there is an $x_0 \in U \cap X$ such that

$$\Lambda_T(U \cap X, x_0) \neq 0.$$

We did not include that x should be a degeneracy in the above definition as this is implicit; if x would not be a degeneracy one can take U small enough such that $U \cap X = U$ (using that X is open in P) and take U to be simply connected. For this choice one obtains $\Lambda_T(U \cap X, x_0) = 0$ for any $x_0 \in U \cap X$. The standard EPs from complex analytic theory satisfy the criterion; any neighborhood U that includes the branch point allows for a curve that traverses the branch cut. We do note that this definition does not need complex analytic branch cuts but allows for any smooth structure of connected eigenvalue sheets. In proposition 2.1 we already showed that this definition restricts the coalescence definition.

The construction above may remind one of the local holonomy group as discussed in appendix A. Indeed, the local holonomy group is non-trivial if and only if the restricted holonomy group is non-trivial for any open neighborhood. However, the construction above has a significant deviation from this setting. Observe that above we take a neighborhood U of the EP candidate x and fix a basepoint $x_0 \in U$ different from x. Hence for any basepoint x_0, there is a $U' \subset U$ such that $x_0 \notin U'$ and hence another basepoint needs to be found. For the local holonomy group one has $x = x_0$, hence the infinite intersection in eq. (A.8) is well-defined, whereas here one can not perform such a construction.

We thus claim that the physically intuitive definition above is a new definition for EP that does not suffer from non-triviality issues.

7 Conclusion

We investigated the theory of exceptional points and $\mathcal{PT}$ symmetric systems, both in the context of adiabatic quantum theory.

Although various characterizations of EPs are used in the literature, these are not equivalent and so a widely accepted precise EP definition is absent. Based on experiments, we claim that the swaps must be central in this definition.

The theory of $\mathcal{PT}$ symmetric systems aids in the study of EPs by providing explicit systems with EPs. However, it is not necessary to consider $\mathcal{PT}$ theory as not all systems with an EP are $\mathcal{PT}$ symmetric and $\mathcal{PT}$ symmetry needs to be broken explicitly in an experiment. The $\mathcal{PT}$ phase transitions thus give only a part of the EPs present in a parametrized system.

The explicit case of a three-channel waveguide system was treated, originating from $\mathcal{PT}$ theory and supporting various EPs. Both EP2s and EP3s were present, and we showed how their effects can be composed to generate a non-abelian group of adiabatic changes. The Λ-group was introduced to formalize the permutations of eigenvalues.

The needed geometry was treated as well, the basis formed by the adiabatic approximation from quantum mechanics. The adiabatic change as measured in experiment can be modelled on the principal $\mathbb{C}^\times \wr S_n$-bundle we called $\mathrm{Fr}(T)$ in a natural way, a PFB not found in the literature to date. The adiabatic approximation indeed allows to reduce the holonomy group at a non-degeneracy x_0, which we called $\mathrm{Adia}(x_0)$, to the group $\Lambda(x_0)$. The kernel of this map was identified with all solely phase changing operations and was called the phase group of the system at x_0, denoted $\mathrm{Phase}(x_0)$. These three groups fit together in a short exact sequence which can be used to describe and distinguish degeneracy structures.

The Λ-group also allows one to phrase a new definition of an exceptional point that specializes existing definitions. Indeed, one can define an EP by demanding that the Λ-group is non-trivial when restricted to any neighborhood of the EP, i.e. by demanding that swaps of eigenvalues occur arbitrarily close to the EP. This definition is physically intuitive and restricts the standard mathematical definition to non-trivial cases.

A Holonomy theory

We state some basics of holonomy theory; proofs are either a direct check or can be found in [43].

Given a connection on a principal G bundle $\pi\colon B \to M$ and a path $\gamma\colon [0,1] \to M$, one has a G-equivariant parallel transport operation $P_\gamma\colon \pi^{-1}(\{\gamma(0)\}) \to \pi^{-1}(\{\gamma(1)\})$, with inverse given by the operation obtained by tracing the path backwards. If the path is a loop based at x_0 then the parallel transport operations, also known as holonomies, are elements of $\mathrm{Aut}(\pi^{-1}(\{x_0\}))$ and form a group, called the holonomy group of the connection at x_0. To formalize this, given U a subset of M and $x_0 \in U$, we write the set of (piece-wise smooth) x_0-based loops in U as

$$\mathrm{Loop}(U, x_0) = \left\{\gamma\colon S^1 \to U \mid \gamma(0) = x_0\right\}. \tag{A.1}$$

For future use, we write

$$\mathrm{Loop}^0(U, x_0) = \{\gamma \in \mathrm{Loop}(U, x_0) \mid \gamma \text{ is contractible}\}. \tag{A.2}$$

Associating to a loop γ its parallel transport operation P_γ is given by a map

$$\begin{aligned} P\colon \mathrm{Loop}(U, x_0) &\to \mathrm{Hol}_{x_0}(U, \nabla) \\ \gamma &\mapsto P_\gamma \end{aligned} \tag{A.3}$$

where we already used that the image of the above map (in $\mathrm{Aut}(\pi^{-1}\{x_0\})$) is defined to be the holonomy group, that is

$$\mathrm{Hol}_{x_0}(U, \nabla) = \left\{A \in \mathrm{Aut}(\pi^{-1}\{x_0\}) \mid A = P_\gamma \text{ for some } \gamma \in \mathrm{Loop}(U, x_0)\right\}. \tag{A.4}$$

Also this set has a contractible path version given by

$$\mathrm{Hol}^0_{x_0}(U, \nabla) = \left\{A \in \mathrm{Hol}_{x_0}(U, \nabla) \mid A = P_\gamma \text{ for some } \gamma \in \mathrm{Loop}^0(U, x_0)\right\}. \tag{A.5}$$

On $\mathrm{Loop}(U, x_0)$ one has concatenation of loops which defines a product. This turns $\mathrm{Loop}(U, x_0)$ into a monoid, but not into a group as e.g. inverses are missing. Nevertheless, P does send a concatenation of two loops to the product of their holonomies, so P preserves the products (or, P is a morphism of monoids).

Another result that we use in the main text is the following; the holonomy group of a PFB is always contained in the structure group.

Lemma A.1. Let $\pi\colon B \to M$ be a G-PFB with some compatible connection ∇. Then for all $x \in M$ and open subsets U containing x_0 one has

$$\mathrm{Hol}_{x_0}(U, \nabla) \leq G.$$

It is also true that $\mathrm{Hol}^0_{x_0}(U, \nabla)$ is a normal subgroup of $\mathrm{Hol}_{x_0}(U, \nabla)$. Hence there is a quotient with the structure of a group, known as the monodromy group.

Definition A.1. The monodromy group of a connection ∇ restricted to open set U containing x_0 is the quotient

$$\mathrm{Mon}_{x_0}(U, \nabla) = \mathrm{Hol}_{x_0}(U, \nabla) / \mathrm{Hol}^0_{x_0}(U, \nabla). \tag{A.6}$$

Associated to it is the SES of groups

$$0 \longrightarrow \mathrm{Hol}^0_{x_0}(U, \nabla) \longrightarrow \mathrm{Hol}_{x_0}(U, \nabla) \longrightarrow \mathrm{Mon}_{x_0}(U, \nabla) \longrightarrow 0. \tag{A.7}$$

An interesting result involving all terms in the above SES is the following.

Lemma A.2. The group $\mathrm{Hol}^0_{x_0}(U,\nabla)$ is the connected subgroup of $\mathrm{Hol}_{x_0}(U,\nabla)$. In particular, the group $\mathrm{Mon}_{x_0}(U,\nabla)$ is discrete.

Observe that all groups are in fact Lie groups and the maps are all smooth.

The last notion we want to consider here is that of local holonomy group. For this, fix $x \in M$ and let U_k be a family of nested sets such that

$$\bigcap_{k=1}^{\infty} U_k = x$$

then the local holonomy group at x is defined as

$$\mathrm{Hol}^*(x,\nabla) = \bigcap_{k=1}^{\infty} \mathrm{Hol}^0(U_k,\nabla). \tag{A.8}$$

One can show that this does not depend on the chosen family U_k and so is a well-defined object.

B Wreath product

We introduce the concept of a wreath product between an arbitrary group G and a subgroup H of S_n. The following lemma from group theory is a convenient tool for this.

Lemma B.1 (Splitting Lemma)**.** Given a SES of groups

$$0 \longrightarrow A \xrightarrow{\ i\ } B \xrightarrow{\ \pi\ } C \longrightarrow 0$$

then B is the semi-direct product $A \rtimes C \iff$ there is a right splitting $s\colon C \to B$ (that is, $\pi \circ s = \mathrm{id}_C$). Also, a left splitting $r\colon B \to A$ (that is, $r \circ i = \mathrm{id}_A$) exists $\iff$ one has $B \cong A \times C$.

There exist general formulations of the wreath product, but for us the following definition suffices.

Definition B.1. Let G be any group, and let H be a subgroup of S_n for some n. The wreath product $G \wr H$ is defined as the semi-direct product $G^n \rtimes H$, where H acts on G^n by permutation action. Explicitly, $G \wr H$ is the set $G^n \times H$ with product

$$(h,\tau)\cdot(g,\sigma) = (h\tau(g),\tau\sigma).$$

The number n is referred to as the degree (of H or $G \wr H$).

One can also write this using a short exact sequence

$$0 \longrightarrow G^n \longrightarrow G \wr H \longrightarrow H \longrightarrow 0$$

where $G^n \to G \wr H$ is inclusion in $G^n \times \{1_H\}$, and $G \wr H \to H$ is projection on the last factor. The map $H \to G \wr H\colon h \mapsto (1_{G^n}, h)$ is a right-splitting of this sequence, implying that $G \wr H$ is indeed a semi-direct product of G^n and H.

In the context of Lie groups, the group H is always discrete. Hence the connected component of the identity of $G \wr H$ is diffeomorphic to that of G^n. This follows from the discreteness of H; one can't leave $G^n \times \{1_H\}$ as a path from identity to some point outside descends to a path in H, which must be constant.

In the text we consider PFBs with structure groups of the form $G \wr H$, in particular the holonomy group will be a subgroup of $G \wr H$. We note that the restricted holonomy group lies in the connected component of $G \wr H$, which by the above is the connected component of G. This means that actions of H (the swaps in the main text) will never be reached with contractible paths.

Induced representation of wreath product

A representation (V, π) of G naturally induces a representation of $G \wr H$ in the following way. First, one has a natural representation $(\bigoplus^n V, \bigoplus^n \pi)$ of G^n. For the wreath product one alters this representation using the permutations from H. That is, one introduces the matrices that permute the V's in $\bigoplus^n V$.

In the text we are interested in the case $G = \mathbb{C}^\times$ which has a canonical 1 dimensional representation on $\mathbb{C}$. The representation of $G \wr H$ then consists of permutation matrices where non-zero entries are replaced by non-zero complex numbers. These matrices are called generalized permutation matrices and are defined as follows.

Definition B.2. A generalized permutation matrix is a matrix $A \in \mathrm{GL}(n, \mathbb{C})$ of the form

$$A = DP$$

where D is diagonal and P a permutation matrix. The space of generalized permutation matrices with entries in $\mathbb{C}^\times$ we denote by $S_n(\mathbb{C})$.

It follows that the representation induces an isomorphism $\mathbb{C}^\times \wr S_n \cong S_n(\mathbb{C})$. The use of this induced representation can easily be illustrated.

Example B.1. The standard EP2 has holonomy generator

$$\begin{pmatrix} 0 & -1 \\ 1 & 0 \end{pmatrix}$$

which is indeed on the described form.

Another map that will be of interest in the main text is the canonical surjective morphism $\Pi\colon S_n(\mathbb{C}) \to S_n$ sending a matrix $A = DP$ to its unique underlying permutation matrix P (here we identify S_n with the permutation matrices in $\mathrm{GL}(n, \mathbb{C})$).

In the text one fixes a basis ψ_i of eigenstates and acts on these with holonomy operations that can change (complex) phases and labels but do not mix the eigenstates. More precisely, the groups $\mathrm{Adia}(x_0)$ are subgroups of $\mathbb{C}^\times \wr S_n$ and will follow the representation discussed here. An element of $\mathrm{Adia}(x_0)$ will send $\psi_i \mapsto \alpha_i \psi_j$, and this can be modeled with a matrix $\tilde{p}$ defined by

$$\tilde{p}_i^j = \begin{cases} \alpha_i & \text{if } \psi_i \text{ becomes } \alpha_i \psi_j \\ 0 & \text{else} \end{cases}$$

and indeed $\tilde{p} \in S_n(\mathbb{C})$. Hence we get a representation $\tilde{P}\colon \mathrm{Adia}(x_0) \to S_n(\mathbb{C})$.

We note that the map $\Pi\colon S_n(\mathbb{C}) \to S_n$ in terms of the representation matrices just sets all phase factors to 1. That is, the representing matrix is given by

$$p_i^j = \begin{cases} 1 & \text{if } \psi_i \text{ becomes } \psi_j \\ 0 & \text{else} \end{cases}$$

which gives a genuine permutation matrix. In the text we discuss the Λ-group which is isomorphic to a subgroup of S_n. The above matrices give a representation $P\colon \Lambda(x_0) \to S_n$. As $P = \Pi \circ \tilde{P}$, this representation is compatible with the one of $\mathrm{Adia}(x_0)$.

Example B.2. For the standard EP2, setting phases to 1 gives

$$\begin{pmatrix} 0 & 1 \\ 1 & 0 \end{pmatrix}$$

reflecting the swap of the eigenstates.

Finally, in the text we consider the group $\mathrm{Phase}(x_0)$ being the kernel of the map $\mathrm{Adia}(x_0) \to \Lambda(x_0)$. Hence, it inherits a representation from $\mathrm{Adia}(x_0)$ which is a restriction of $\tilde{P}$. Being the kernel, the matrices representing $\mathrm{Phase}(x_0)$ do not permute the basisvectors and are thus diagonal. Hence we get the following result on the decompostion of this representation.

Lemma B.2. The representation of $\mathrm{Phase}(x_0)$ is fully reducible, the irreducibles being representations of a subgroup of $\mathbb{C}^\times$.

Quite opposite is the representation of $\Lambda(x_0)$; this representation need not be a restriction of $\tilde{P}$. That is, the matrices corresponding to P may very well *not* be achieved in the representation $\tilde{P}$ of $\mathrm{Adia}(x_0)$. An example is the standard EP2; it is possible to permute the two eigenvalues, but it is impossible to do this without introducing a phase.

C Bi-orthogonality theory

In this section we collect properties of eigenvector normalization and existence theorems on system formed by them. We assume V is a vector space over F of finite dimension n, and A an $n \times n$ matrix. We assume no more properties unless stated otherwise. Also, one has the dual vector space $V^\vee = \mathrm{Hom}(V, F)$ of dimension n. By definition, one has a canonical pairing given by $\theta v = \theta(v)$, where $v \in V$ and $\theta \in V^\vee$. This pairing will not be denoted by extra symbols, similar to standard matrix-vector products, but primarily to distinguish it from inner products later on and to underline the canonical nature.

First, let us revise that given a right-eigenvector with eigenvalue λ, there is also a left-eigenvector with eigenvalue λ.

Lemma C.1. Let A be a finite-dimensional matrix, then λ has a right-eigenvector $\iff$ λ has a left-eigenvector.

Proof. This follows as left-eigenvectors of A correspond to right-eigenvectors of A^T, with the same eigenvalue, and $\det(\lambda I - A) = \det(\lambda I - A^T)$.

□

The following two definitions are of main interest.

Definition C.1 (Bi-orthogonal set)**.** Given a finite-dimensional operator A on V, a *bi-orthogonal* set for A is a set $\{(\theta^j, v_i)\} \subset V^\vee \times V$ where each θ^j, v_i is resp. a left- or right eigenvector of A for the same eigenvalue, satisfying

$$\theta^j v_i = \delta_i^j.$$

Definition C.2 (Eigenframe)**.** An *eigenframe* of A is a basis of V consisting of eigenvectors of A. This definition extends naturally to the case of frame bundles over M where $A = A(x)$ depends on $x \in M$.

Next, we want to have a sufficient condition for the existence of a bi-orthogonal set, that is, to have a guarantee that self-orthogonalities do not appear.

Given a basis $\{v_i\}$ of V, one can always find a dual basis $\{\theta^j\}$ of $V^\vee$ defined by the conditions $\theta^j v_i = \delta_i^j$. Hence, in case the v_i are eigenvectors of A, one would like the θ^j to be left-eigenvectors.

Lemma C.2. Let A have an eigenframe, then the dual frame is an eigencoframe.

Proof. Let the frame consist of vectors v_i, let θ^j be the dual vectors, i.e. $\theta^j v_i = \delta_i^j$. As the v_i form a basis, it is enough to check equality of $\theta^j A$ and $\lambda_j \theta^j$ (no sum for the latter) on each v_i. One obtains

$$\theta^j A v_i = \theta^j \lambda_i v_i = \lambda_i \delta_i^j = \lambda_j \delta_i^j = \lambda_j \theta^j v_i$$

for each v_i, hence $\theta^j A$ and $\lambda_j \theta^j$ are equal. This means that the θ^j are indeed left-eigenvectors. □

This result becomes particularly interesting once there is a sufficient condition for the existence of an eigenframe. Non-degeneracy of the operator is sufficient.

Theorem C.1. Let $A \in M_n(\mathbb{C})$ have a non-degenerate spectrum. Then

- there are n linearly dependent eigenvectors of A, hence A has an eigenframe
- the eigenframe and eigencoframe form a bi-orthogonal set for A.

Proof. By non-degenerateness, the n eigenvectors are not linearly dependent and the first follows. The second follows as the $\theta^j v_i = \delta_i^j$ identity follows from the dual basis identity. □

Given a basis $\{v_i\}$ of a finite dimensional vector space over $\mathbb{C}$, there is a unique inner product for which the basis is orthonormal. For this inner product, we note that

$$\langle \alpha v_i, v_j \rangle = \bar{\alpha} \delta_{ij}$$

so $\langle \alpha v_i, - \rangle = \bar{\alpha} \theta_i$, inducing a conjugate-linear map $V \to V^\vee$ given by $v_i \to \theta_i$ via the inner product. If V was already equipped with an inner product, there is no guarantee it is the same as the basis induced one. Also, if A has an eigenframe and one takes the inner product induced by this frame, then A need not be self-adjoint. Indeed, A acts diagonally on its eigenframe, so A is self-adjoint if and only if all the diagonal entries are real, which need not be the case.

We summarize the implications in a diagram, where each arrow is independent of the others. Fix an operator A on finite dimensional complex space V.

$$\begin{tikzcd}
\text{Non-degenerateness} \arrow[r] & \text{Eigenframe} \arrow[r] \arrow[d] & \text{Eigencoframe/Bi-orthogonal set} \\
& \text{Frame} \arrow[r] & \text{Orthonormalizing } \langle -, - \rangle
\end{tikzcd}$$

So far, we note that the inner product on V did not play an important role. We note that given the eigenvectors $\{v_i\}$ and duals $\{\theta^j\}$, the duality/orthonormality condition $\theta^j v_i = \delta_i^j$ fixes normalization of the θ_i. However, normalization of the v_i has not been done, and we may recognize some projective aspects of quantum state space.

We finish with a lemmas that treats the effect of a basis transformation.

Lemma C.3. Let $\{(\theta^j, v_i)\}$ be a bi-orthogonal system for an operator A. Let S be an invertible matrix. Then if $A = S^{-1} A' S$, one has a bi-orthogonal system for A' given by $\{(\theta^j S^{-1}, S v_i)\}$.

Proof. If $Av = \lambda v$, then $A'(Sv) = \lambda(Sv)$, so a right-eigenvector v is sent to eigenvector Sv. Likewise, if $wA = w\lambda$, then $(wS^{-1})A' = \lambda(wS^{-1})$. Hence the listed (co)vectors are eigen(co)vectors. The orthogonality follows as

$$(w^j S^{-1})(S v_i) = w^j v_i = \delta_i^j.$$

□

References

[1] T. Kato, *Perturbation theory for linear operators*, Vol. 132, Grundlehren der mathematischen Wissenschaften (Springer, 1966).

[2] W. D. Heiss, "The physics of exceptional points", Journal of Physics A: Mathematical and Theoretical **45**, 444016 (2012).

[3] F. Keck, H. Korsch, and S. Mossmann, "Unfolding a diabolic point: a generalized crossing scenario", Journal of Physics A: Mathematical and General **36**, 2125 (2003).

[4] H. Hodaei, A. U. Hassan, S. Wittek, H. Garcia-Gracia, R. El-Ganainy, D. N. Christodoulides, and M. Khajavikhan, "Enhanced sensitivity at higher-order exceptional points", Nature **548**, 187 (2017).

[5] W. Langbein, "No exceptional precision of exceptional point sensors", arXiv preprint arXiv:1801.05750 (2018).

[6] G. Demange and E.-M. Graefe, "Signatures of three coalescing eigenfunctions", Journal of Physics A: Mathematical and Theoretical **45**, 025303 (2012).

[7] A. Seyranian, O. Kirillov, and A. Mailybaev, "Coupling of eigenvalues of complex matrices at diabolic and exceptional points", Journal of Physics A: Mathematical and General **38**, 1723 (2005).

[8] H. Mehri-Dehnavi and A. Mostafazadeh, "Geometric phase for non-hermitian hamiltonians and its holonomy interpretation", Journal of Mathematical Physics **49**, 082105 (2008).

[9] N. Moiseyev, *Non-hermitian quantum mechanics* (Cambridge University Press, 2011).

[10] W. Heiss and H. Harney, "The chirality of exceptional points", The European Physical Journal D - Atomic, Molecular, Optical and Plasma Physics **17**, 149 (2001).

[11] W. Heiss and G. Wunner, "Chiral behaviour for three wave guides at an exceptional point of third order", arXiv preprint arXiv:1703.09455 (2017).

[12] C. M. Bender, D. C. Brody, H. F. Jones, and B. K. Meister, "Faster than hermitian quantum mechanics", Phys. Rev. Lett. **98**, 040403 (2007).

[13] C. M. Bender, P. N. Meisinger, and Q. Wang, "Finite-dimensional $\mathcal{PT}$-symmetric Hamiltonians", Journal of Physics A: Mathematical and General **36**, 6791 (2003).

[14] A. Mostafazadeh, "Exact $\mathcal{PT}$ -symmetry is equivalent to Hermiticity", Journal of Physics A: Mathematical and General **36**, 7081 (2003).

[15] C. M. Bender, "Introduction to $\mathcal{PT}$-symmetric quantum theory", Contemporary Physics **46**, 277 (2005).

[16] C. M. Bender and S. Boettcher, "Real Spectra in Non-Hermitian Hamiltonians Having $\mathcal{PT}$ Symmetry", Phys. Rev. Lett. **80**, 5243 (1998).

[17] P. Dorey, C. Dunning, and R. Tateo, "The ODE/IM correspondence", Journal of Physics A: Mathematical and Theoretical **40**, R205 (2007).

[18] A. Mostafazadeh, "Pseudo-Hermiticity versus $\mathcal{PT}$-symmetry III: Equivalence of pseudo-Hermiticity and the presence of antilinear symmetries", Journal of Mathematical Physics **43**, 3944 (2002).

[19] C. Zheng, L. Hao, and G. L. Long, "Observation of a fast evolution in a parity-time-symmetric system", Philosophical Transactions of the Royal Society of London A: Mathematical, Physical and Engineering Sciences **371** (2013) `10.1098/rsta.2012.0053`.

[20] C. Dembowski, H.-D. Gräf, H. L. Harney, A. Heine, W. D. Heiss, H. Rehfeld, and A. Richter, "Experimental observation of the topological structure of exceptional points", Phys. Rev. Lett. **86**, 787 (2001).

[21] R. Uzdin, A. Mailybaev, and N. Moiseyev, "On the observability and asymmetry of adiabatic state flips generated by exceptional points", Journal of Physics A: Mathematical and Theoretical **44**, 435302 (2011).

[22] J. Doppler, A. A. Mailybaev, J. Böhm, U. Kuhl, A. Girschik, F. Libisch, T. J. Milburn, P. Rabl, N. Moiseyev, and S. Rotter, "Dynamically encircling an exceptional point for asymmetric mode switching", Nature **537**, 76 (2016).

[23] W. Heiss, "Phases of wave functions and level repulsion", The European Physical Journal D-Atomic, Molecular, Optical and Plasma Physics **7**, 1 (1999).

[24] H. Xu, D. Mason, L. Jiang, and J. Harris, "Topological energy transfer in an optomechanical system with exceptional points", Nature **537**, 80 (2016).

[25] R. El-Ganainy, K. G. Makris, M. Khajavikhan, Z. H. Musslimani, S. Rotter, and D. N. Christodoulides, "Non-Hermitian physics and PT symmetry", Nature Physics **14**, 11 (2018).

[26] C. E. Rüter, K. G. Makris, R. El-Ganainy, D. N. Christodoulides, M. Segev, and D. Kip, "Observation of parity-time symmetry in optics", Nature physics **6**, 192 (2010).

[27] C. M. Bender, A. Ghatak, and M. Gianfreda, "$\mathcal{PT}$-symmetric model of immune response", Journal of Physics A: Mathematical and Theoretical **50**, 035601 (2016).

[28] C. M. Bender, D. D. Holm, and D. W. Hook, "Complexified dynamical systems", Journal of Physics A: Mathematical and Theoretical **40**, F793 (2007).

[29] J. Rubinstein, P. Sternberg, and Q. Ma, "Bifurcation diagram and pattern formation of phase slip centers in superconducting wires driven with electric currents", Phys. Rev. Lett. **99**, 167003 (2007).

[30] J. Schindler, A. Li, M. C. Zheng, F. M. Ellis, and T. Kottos, "Experimental study of active LRC circuits with $\mathcal{PT}$ symmetries", Phys. Rev. A **84**, 040101 (2011).

[31] F. Quijandría, U. Naether, Ş. K. Özdemir, F. Nori, and D. Zueco, "$\mathcal{PT}$-symmetric circuit QED", Phys. Rev. A **97**, 053846 (2018).

[32] J. Schnabel, H. Cartarius, J. Main, G. Wunner, and W. D. Heiss, "$\mathcal{PT}$-symmetric waveguide system with evidence of a third-order exceptional point", Phys. Rev. A **95**, 053868 (2017).

[33] J. Schnabel, H. Cartarius, J. Main, G. Wunner, and W. D. Heiss, "Simple models of three coupled $\mathcal{PT}$-symmetric wave guides allowing for third-order exceptional points", Acta Polytechnica **57**, 454 (2017).

[34] E. J. Pap, D. Boer, and H. Waalkens, "Non-abelian nature of systems with multiple exceptional points", Phys. Rev. A **98**, 023818 (2018).

[35] J.-W. Ryu, S.-Y. Lee, and S. W. Kim, "Analysis of multiple exceptional points related to three interacting eigenmodes in a non-hermitian hamiltonian", Physical Review A **85** (2012) `10.1103/PhysRevA.85.042101`.

[36] J. Garrison and E. Wright, "Complex geometrical phases for dissipative systems", Physics Letters A **128**, 177 (1988).

[37] A. Aguiar Pinto, M. Nemes, J. Peixoto de Faria, and M. Thomaz, "Comment on the adiabatic condition", American Journal of Physics **68**, 955 (2000).

[38] M. V. Berry, "Quantal phase factors accompanying adiabatic changes", Proc. R. Soc. Lond. A **392**, 45 (1984).

[39] B. Simon, "Holonomy, the Quantum Adiabatic Theorem, and Berry's Phase", Phys. Rev. Lett. **51**, 2167 (1983).

[40] Y. Aharonov and J. Anandan, "Phase change during a cyclic quantum evolution", Phys. Rev. Lett. **58**, 1593 (1987).

[41] A. Bohm, A. Mostafazadeh, H. Koizumi, Q. Niu, and J. Zwanziger, *The geometric phase in quantum systems: foundations, mathematical concepts, and applications in molecular and condensed matter physics* (Springer Science & Business Media, 2013).

[42] J. Anandan and L. Stodolsky, "Some geometrical considerations of Berry's phase", Physical Review D **35**, 2597 (1987).

[43] S. Kobayashi and K. Nomizu, *Foundations of differential geometry*, Vol. 1, 2 (Interscience publishers New York, 1963).

Acknowledgements

Let me finish the thesis with some words of thanks. I would like to thank my supervisors for their supervision and stimulating discussions. In addition I want to thank my room mates at the university for the pleasant working time together. Also, I would like to thank my family for continuous support. Foremost, I want to express my gratitude towards the Lord God who has given me all what was necessary, and more, to write this thesis and to complete a wonderful time as a student.